

WADD-TR-60-37

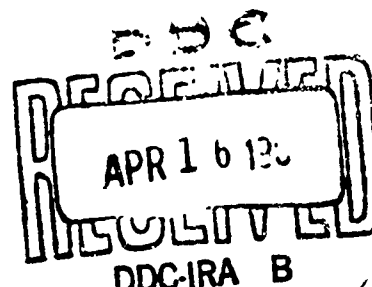
PART V

AD 613046

PHYSICAL METALLURGY OF TUNGSTEN AND TUNGSTEN BASE ALLOYS

TECHNICAL REPORT NO. WADD-TR-60-37, PART V
AUGUST 1964

AF Materials Laboratory
Research and Technology Division
Air Force Systems Command
Wright-Patterson Air Force Base, Ohio



COPY	2	OF	3	107P
HARD COPY			\$. 4.00	
MICROFICHE			\$. 0.75	

PROJECT NO. 7351, TASK NO. 735101

(Prepared under Contract No. AF 33(657)-2241
by Westinghouse Lamp Division, Bloomfield, New Jersey;
Heinz G. Soll, George W. King, Randolph H. Schnitzel and N. Francis Corulli, Authors)

ARCHIVE COPY

NOTICES

When Government drawings, specifications, or other data are used for any purpose other than in connection with a definitely related Government procurement operation, the United States Government thereby incurs no responsibility nor any obligation whatsoever; and the fact that the Government may have formulated furnished, or in any way supplied the said drawings, specifications, or other data, is not to be regarded by implication or otherwise as in any manner licensing the holder or any other person or corporation, or conveying any rights or permission to manufacture, use, or sell any patented invention that may in any way be related thereto.

Qualified requesters may obtain copies of this report from the Defense Documentation Center (DDC), (formerly ASTIA), Cameron Station, Bldg. 5, 5010 Duke Street, Alexandria, Virginia, 22314.

This report has been released to the Office of Technical Services, U.S. Department of Commerce, Washington 25, D. C., for sale to the general public.

Copies of this report should not be returned to the Research and Technology Division, Wright-Patterson Air Force Base, Ohio, unless return is required by security considerations, contractual obligations, or notice on a specific document.

CLEARINGHOUSE FOR FEDERAL SCIENTIFIC AND TECHNICAL INFORMATION, OFSTI
INPUT SECTION 410.11

LIMITATIONS IN REPRODUCTION QUALITY OF TECHNICAL ABSTRACT BULLETIN
DOCUMENTS, DEFENSE DOCUMENTATION CENTER (DDC)

AD 613046

- 1. AVAILABLE ONLY FOR REFERENCE USE AT DDC FIELD SERVICES.
COPY IS NOT AVAILABLE FOR PUBLIC SALE.
- 2. AVAILABLE COPY WILL NOT PERMIT FULLY LEGIBLE REPRODUCTION.
REPRODUCTION WILL BE MADE IF REQUESTED BY USERS OF DDC.
- A. COPY IS AVAILABLE FOR PUBLIC SALE.
- B. COPY IS NOT AVAILABLE FOR PUBLIC SALE.
- 3. LIMITED NUMBER OF COPIES CONTAINING COLOR OTHER THAN BLACK
AND WHITE ARE AVAILABLE UNTIL STOCK IS EXHAUSTED. REPRODUCTIONS
WILL BE MADE IN BLACK AND WHITE ONLY.

TSL-121-2/64

DATE PROCESSED: 7 Apr 65

PROCESSOR: dwiarchek

FOREWORD

This report was prepared by members of the scientific staff of the Metals Research Section of the Lamp Division of Westinghouse Electric Corporation, under USAF Contract No. 33(657)-8247. This contract was initiated under Project No. 7351, "Metallic Materials", Task No. 735101, "High Temperature Alloys." The project was administered under the direction of the AF Materials Lab., Research and Technology Division, Air Force Systems Command, with Mr. J. K. Elbaum as project engineer. This report presents the results of research and development conducted during the period from June 1, 1963, through April 30, 1964.

The authors of this report have shared in the execution of the various programs of the contract, as follows:

Project Manager	- H.G. Sell
The Effect of Thoria on the Elevated Temperature Tensile Properties of High-Purity Tungsten	- G.W. King
The Effect of Carbon on the Mechanical Properties of Tungsten and W-0.35% Ta	- R.H. Schnitzel
Screening Alloys: W-25% Re, W-25% Re-1% ThO ₂ W-25% Re-1% HfN, W-3.5% Ta-C	- G.W. King - R.H. Schnitzel
Thermochemistry of Dispersed Second Phases in Tungsten	- N.F. Cerulli

The authors wish to thank Messrs. W.R. Morcom and R.C. Koo for assistance and helpful suggestions. They acknowledge with gratitude the contributions of Dr. Lui Wei (X-ray analyses), Messrs. M.F. Quaely (C and gas analyses), T.A. Ellis (spectrographic analyses), J.J. Leek (single-crystal growth), and J.J. Corcoran, C.D. Johnson, R.K. Courtney and R.M. Byrnes (carburizing, heat-treating, specimen preparation, and tensile testing).

ABSTRACT

Tensile properties of high purity powder metallurgy tungsten and W-1% ThO₂ alloy were determined at various strain rates and temperatures (800-2400°C). 1% ThO₂ imparts a slight overall increase in strength properties, although above 0.5 T_m these properties are affected by void formation.

The tensile properties of pure W and W-0.35% Ta single crystals (worked, and worked and recrystallized) investigated from R.T. to 1200°C are shown to be affected by C, particularly in the quenched condition.

An alloy screening program was conducted with W-25% Re, and 1% ThO₂ and 1% HfN additions, and with single crystals of W-3.5% Ta-C. The W-Re alloys have superior strength up to 2400°C. A yield stress of 47 kpsi was found at 1600°C in the quenched W-3.5% Ta-C single crystal.

Reactions between ThO₂ and W, C, and several carbides were investigated as was the reaction W-TaC. A phase diagram of the W-Ta-C system resulted.

This technical documentary report has been reviewed and is approved.



I. Perlmutter
Chief, Physical Metallurgy Branch
Metals and Ceramics Division
AF Materials Laboratory

TABLE OF CONTENTS

	<u>Page</u>
I. INTRODUCTION	1
II. THE EFFECT OF THORIA ON THE ELEVATED TEMPERATURE TENSILE PROPERTIES OF HIGH PURITY TUNGSTEN	2
1. Materials	2
2. Experimental Procedures	2
3. Experimental Results	4
4. Discussion	21
III. EFFECT OF CARBON ON THE TENSILE PROPERTIES OF TUNGSTEN AND W-0.35%Ta	30
A. Pure Tungsten and W-0.35%Ta Single Crystals	30
1. Preparation of Single Crystals and Test Procedure	30
2. Impurity Analyses	31
3. Tensile Test Results	31
a) Tungsten Single Crystals	34
b) W-0.35%Ta Single Crystals	34
c) Effect of Quenching Temperature	44
d) Aging Effects in W-0.35%Ta Single Crystal . .	44
e) Strain Aging Effects in W-0.35%Ta Single Crystals	47
4. Optical and Electron Metallography	50
B. Worked and Recrystallized Pure Tungsten and W-0.35% Ta Single Crystals	50
1. Preparation of Specimens and Test Procedure . . .	52
2. Recrystallization Temperature of W-0.35%Ta . . .	52
3. Tensile Test Results	52

TABLE OF CONTENTS (cont'd)

	<u>Page</u>
a) As Worked Crystals	52
b) Worked and Recrystallized Crystals	55
c) Discussion	59
1. Strengthening Mechanism	59
2. Yield Points and Serrations	62
3. The Effect of Quenching Temperature ..	62
4. The Effect of Carbon in Recrystallized Tungsten and W-0.35%Ta Crystals	63
IV. SCREENING ALLOYS	66
A. The Effect of 1%ThO ₂ or 1%HfN on the High Tempera- ture Tensile Properties of W-25%Re	66
1. Tensile Test Results	66
2. Discussion of Results	69
B. The Effect of Carbon Precipitates on the High Temperature Strength Properties of W-3.5%Ta Single Crystals	69
1. Tensile Test Results	71
2. Discussion of Results	71
V. THERMOCHEMISTRY OF DISPERSED SECOND PHASE IN TUNGSTEN	73
1. Automatic Recording Balance	73
2. Decarburization of TaC	74
3. The W-Ta-C Liquidus Surface	76
4. ThO ₂ Reactions with W and Some Other Refractory Materials	80
a) Thoria + Tungsten Reaction	80
b) Thoria + WC Reaction	89
c) Reactions of Thoria and Some Other Carbides	89
VI. SUMMARY	93
VII. REFERENCES	95

ILLUSTRATIONS.

<u>Figure</u>		<u>Page</u>
1	Effect of Annealing on the Microstructure of Swaged High Purity Tungsten - 45X	5
2	Effect of Annealing on the Microstructure of W-1%ThO ₂ ..	6
3	Yield Strength of Recrystallized High Purity Tungsten and W-1%ThO ₂	8
4	Ultimate Strength of Recrystallized High Purity Tungsten and W-1%ThO ₂	9
5	Log Ultimate Strength vs Log Strain Rate of High Purity Tungsten at Various Temperatures	10
6	Log Ultimate Strength vs Log Strain Rate of W-1%ThO at Various Temperatures	11
7	Ductility of Recrystallized High Purity Tungsten and W-1%ThO ₂	12
8	Effect of Strain Rate and Temperature on Tensile Fractures of High Purity Tungsten - 45X	14-15
9	Effect of Strain Rate and Temperature on Tensile Fractures of W-1%ThO ₂ - 45X	16-17
10a	Effect of Strain Rate and Temperature on the Micro-structure of High Purity Tungsten and W-1%ThO ₂ - 1000X .	18
10b	Effect of Strain Rate and Temperature on the Micro-structure of High Purity Tungsten and W-1%ThO ₂ -1000X ..	19
10c	Effect of Strain Rate and Temperature on the Micro-structure of High Purity Tungsten and W-1%ThO ₂ -1000X ..	20
11	Ratio of the Ultimate Strengths of W-1%ThO ₂ and Pure Tungsten as a Function of Temperature and Strain Rate ..	24
12	Grain Boundary (Row of Etch Pits) Held up by Thoria Particles Indicated by Arrows - 5000X	25
13	Log Strain Rate vs 1/T of High Purity Tungsten at Various Levels	26
14	Log Strain Rate vs 1/T for W-1%ThO ₂ at Various Stress Levels	27

ILLUSTRATIONS (Cont'd)

<u>Figure</u>		<u>Page</u>
15	Apparent Activation Energy of High Purity Tungsten and W-1%ThO ₂ as a Function of Stress	29
16	Carbide Precipitates in W-0.35%Ta after Carburizing	32
17	0.2% Yield Stress of Variously Treated Tungsten Single Crystals	40
18	Ductility of Pure Single Crystal Tungsten for Various Conditions. (x---x Elong.; □---□ %R.A.)	41
19	0.2% Yield Stress of Variously Treated W-0.35%Ta Single Crystals	42
20	Ductility of the Variously Treated W-0.35%Ta Single Crystals (x---x% Elong.; □---□ %R.A.)	43
21	Effect of 2450°C Quench on Tensile Properties of Carburized Single Crystals of Pure W and W-0.35%Ta	45
22	Comparison of the 0.2% Yield Stress Peak of Carburized and Quenched Single Crystals of Tungsten Quenched from 2450°C and W-0.35%Ta Quenched from 2200°C	46
23	Effect of Isothermal Anneals on the Yield Stress of Carburized and Quenched W-0.35%Ta Single Crystals (Δ---Δ Annealed 400°C; ▨---▨ Annealed 700°C)	46
24	Strain Aging Effects in Variously Treated W-0.23%Ta Single Crystals Tested at 300°C and 600°C	48
25	Effect of Isochronal Annealing (80 min.) on ΔY and ΔG of Prestrained (1%) W-0.35%Ta Single Crystals in Various Conditions and Tested at 300°C	49
26a	Carburized plus Quenched Pure W Single Crystal, Tested 1200°C - 500X	51
26b	Carburized plus Quenched W-0.35%Ta Single Crystal, Tested 1000°C - 500X	51
27a	Transmission Electron-micrograph of a Carburized Single Crystal Tungsten-147,000X	51
27b	Transmission Electron-micrograph of a Carburized W-0.25%Ta Single Crystal - 147,000X	51

ILLUSTRATIONS (Cont'd)

<u>Figure</u>		<u>Page</u>
28	Recrystallization Response of Rolled W-0.35%Ta Alloy Single Crystals (~50% R.A.)	53
29	Effect of Carburizing and Quenching on the 0.2% Yield Stress of Rod Rolled (~50% R.A.) Tungsten and W-0.35%Ta Single Crystals	54
30	Comparison of a 2200°C Quench on the Tensile Properties of Single Crystal and Polycrystalline Tungsten	57
31	.2% Yield Stress of Alloy Single Crystal and Poly-Crystalline Alloy	58
32	Comparison of 0.2% Yield Stress and % Elongation of Carburized and Quenched Polycrystalline (G.S=0.36mm) and Single Crystal W-0.35%Ta (▲—▲ Single Crystal; □—□ Polycrystal)	60
33a	Precipitates in a Carburized Worked and Quenched W-0.35%Ta Tensile Specimen Tested at 1200°C - 500X	61
33b	Precipitates in Carburized Worked and Quenched W-0.35%Ta Tensile Specimen Tested at 800°C- 500X	61
34	Schematic of the Various Approximate Strengthening Contributions to the Yield Stress of Tungsten	65
35	Microstructure of Recrystallized (1/2 hr.; 2400°C) W-25%Re; - 50X	68
36	Ultimate Tensile Strength of Pure and Commercial Tungsten, and several Tungsten Rhenium Alloys	70
37a	Photomicrograph of Carburized and Quenched Single Crystal, Tested 1600°C - 500X	72
37b	Carbon Replica of W-3.5%Ta Carburized, + Quenched Single Crystal, Tested 1600°C - 5000X	72
37c	Photomicrograph of W-3.5%Ta Single Crystal Carburized and Quenched, Tested at 2250°C - 500X	72
38	Automatic Recording Balance Assembly. (A, Vacuum Pump Unit; B, Furnace; C, Balance; D, Program Controller; E, Temperature and DTA Recorder; F, TGA Recorder).....	74
39	Continuous Recording Balance with Vacuum Housing Raised and Case Open	75

ILLUSTRATIONS (Cont'd)

<u>Figure</u>		<u>Page</u>
40	View of Vacuum Furnace with Element Opened for Loading	77
41	Polished Section of a TaC Compact fired at 3325°C for 20 min. in the EB Furnace. Decarburized skin is light section at the right.	78
42	Joins along which Melting Points were made in the W-Ta-C System	79
43	An Early Stage in the Construction of a Plexiglas Model of the W-Ta-C Liquidus Surface. Grid Spacing Equals 100°C, and the Base of the Model Represents 24000°C	81
44	Contour Isotherms of the Suggested Liquidus Surface for the W-Ta-C System	82
45	Clay Model of W-Ta-C Liquidus Surface. "Peak" in Background is TaC.	83
46	Metallographic Section Taken near the W-Rich Corner of the W-Ta-C System	84
47	Weight Loss of W, ThO ₂ , and a W + ThO ₂ Mixture	85
48	Weight Loss of ThO ₂ + C Mixtures Heated to 2000 C. (Arrows indicate theoretical Loss Expected.)	87
49	Weight Loss of ThO ₂ + 5% C Mixtures Heated to 1700, 1850, and 2000°C. Arrow Indicates Theoretical Loss Expected.	88
50	Weight Loss of ThO ₂ + WC Mixtures Heated to 2000°C. Arrows Indicate Theoretical Loss Expected	90
51	Weight Loss of Various ThO ₂ + Carbide Mixtures	91

TABLES

<u>Table</u>		<u>Page</u>
1	Solid Source Mass Spectrometric Analysis of High Purity Tungsten and W-1%ThO ₂ (at.ppm).....	3
2	Effect of Annealing on Hardness (Vickers) of Tungsten and W-1%ThO ₂	7
3	Summary of Metallographic Observations on Preferential Sites of Void Formation and Stress Induced Grain Growth in Pure W and W-1%ThO ₂	22
4	Average Carbon and Vacuum Fusion Analyses of Fractured Tungsten Single Crystal Tensiles - ppm by weight	33
5	Residual Resistance Ratios (R298°K/R4.2°K) of as Melted and Carburized Tungsten Single Crystals as a Function of Heat Treatment	35
6	Tensile Properties of Tungsten Single Crystals	36
7	Tensile Properties of W-0.35%Ta Single Crystals	38
8	Tensile Properties of Carburized and Quenched Single Crystal Tungsten, Rolled at 700°C to 50% R.A.	55
9	Tensile Properties of Carburized and Quenched W-0.35%Ta Rolled at 900°C to 50% R.A.	55
10	Grain Size of Carburized and Quenched W and W-0.35%Ta Rolled to 50% R.A. and Recrystallized	55
11	Tensile Properties of Carburized Polycrystalline Tungsten Made from Single Crystal (quenched after rolling)..	56
12	Tensile Properties of Polycrystalline W-0.35%Ta made from Single Crystal (quenched after rolling)	56
13	Tensile Properties of Carburized Polycrystalline W-0.35%Ta made from Single Crystal (quenched after rolling)	59
14	Tensile Properties of W-25%Re, W-25%Re-1%ThO ₂ and W-25%Re-1%HfN	67
15	Tensile Properties of Carburized and Quenched W-3.5%Ta Single Crystals	71

I. INTRODUCTION

The problem of strengthening tungsten at high temperatures ($> 0.5 T_m$) by a dispersed second phase has been the subject of previous contract programs documented in WADD Technical Reports 60-37, Parts I, II, III and IV (1,2,3 and 4). Particularly relevant to this report is WADD Technical Report 60-37, Part IV. The work discussed in the following sections represents a continuation of programs which had yielded a certain measure of success in the understanding of factors that control the high temperature strength properties of tungsten. Four major programs were carried out with the following objectives:

1. To investigate the tensile properties of a W-1% ThO_2 alloy which was made by a powder metallurgy technique using thoria particles of submicron size and to elucidate further those metallurgical factors that affect its high temperature strength properties.
2. To determine the effect of heat treatment on the tensile properties of carburized pure W and W-0.35% Ta alloy single crystals as melted and after selected degrees of work.
3. To screen a few selected powder metallurgy tungsten base alloys as potential high temperature alloy candidates for further study.
4. To study the compatibility with tungsten of the dispersoids used in these investigations (1,2,3,4) and also the thermochemical reactions which may occur between the dispersoids.

The results are presented and discussed in four separate sections in the order presented above. The significance of the results and their implications on a dispersed second phase alloy development program are analyzed in the summary at the end of the report.

Manuscript released by the authors May 1964 for publication as a WADD Technical Report.

II. THE EFFECT OF THORIA ON THE ELEVATED TEMPERATURE TENSILE PROPERTIES OF HIGH PURITY TUNGSTEN

It has long been recognized that a second phase of hard particles has a strengthening effect on a pure metal. At low or intermediate temperatures ($< 0.5 T_m$), the strengthening effect is thought to arise mainly from the interaction of dislocations with dispersed particles. Above $0.5 T_m$, dynamic recovery processes greatly alter the deformation mechanisms from those simply involving glide, and grain boundaries may act as sources of weakness rather than strength because of grain boundary sliding. Grain boundary sliding at high temperatures has been postulated to be the primary factor giving rise to the formation of voids or cavities at grain boundaries (5,6,7) which in turn cause premature failure and poor ductility (8). Voids, once formed, can grow by the condensation of vacancies from the equilibrium concentration (5) or from the excess vacancies produced by the deformation (8,9).

The high temperature tensile properties of unalloyed tungsten have previously been investigated by Sikora and Hall (10) and also by Taylor and Boone (11). The purpose of the present work was to investigate the effect of a dispersed second phase of thoria (1% by weight) on the tensile properties of powder metallurgy tungsten at intermediate (0.3 to $0.5 T_m$) and high (0.5 to $0.7 T_m$) temperatures.

1. Materials

The unalloyed tungsten was produced by a powder metallurgy technique. The W-1% ThO_2 alloy was produced by dry blending of thoria powder of submicron size particles with high purity H_2WO_4 powder, followed by hydrogen reduction. The reduced powder blend was die pressed at room temperature and then resistance sintered in a hydrogen atmosphere. The ingots were reduced to rod size by swaging. The high purity tungsten was swaged to 78% R.A. and the W-1% ThO_2 alloy to 85% R.A. Buttonhead tensile specimens (gauge diameter 0.093 in., gauge length 1 in.) were made from the swaged rod by grinding. The analyses of the swaged materials are presented in Table 1.

2. Experimental Procedures

Tensile testing was carried out in a "hard" tensile machine equipped with a resistance type vacuum furnace. The pressure at all test temperatures was of the order of 10^{-5} mm Hg. Temperatures were read with a micro-optical pyrometer. The temperature was found to be constant during the test. A temperature gradient determination over the specimen gauge length was made with a chromel-alumel thermocouple at 1000°C . The temperature variation was not more than $\pm 5^\circ\text{C}$.

Table 1

Solid Source Mass Spectrometric Analysis of
High Purity Tungsten and W-14%Th02 (at. ppm)

Element	High Purity Tungsten	W-14%Th02	Element	High Purity Tungsten	W-14%Th02
H	*ND	1700	Zn	0.07	0.11
Li	0.4	4	Ga	*ND	0.9*M
B	0.1	0.5	As	*ND	1*M
C	30	3100	Br	*ND	0.3
N	10	29	Rb	*ND	0.7
O	100	12,000*NU	Sr	0.1	0.1
F	10	300*NU	Y	*ND	23
Na	*ND	0.8	Mo	*ND	0.06
Mg	10	9	Ag	0.1	0.04
Al	40	77	Tin	*ND	0.6
Si	30	380	Sn	0.1	0.3
P	10	55	Sb	*ND	0.4
S	2	7	Ca	0.4	*ND
Cl	1	7	Ba	*ND	0.2
K	1	4	La	*ND	0.06
Ca	10	76	Pr	*ND	0.4
Sc	1	0.5	Nd	*ND	0.1
Cr	4	70	Dy	*ND	0.5
Mn	1	70	Ta	*ND	0.1
Fe	0.1	450	Pb	*ND	0.4*M
Co	0.03	2	Bi	*ND	2300
Ni	5		Ta	0.1	
Cu	0.5				

*ND - Not Determined

*NU - Inhomogeneous impurity; may be from surface or segregated in bulk.
*M - All or part of this impurity is due to ion source memory.

3. Experimental Results

Recrystallization: The recrystallization response of the two materials was investigated by correlating hardness measurements with microstructural observations. The effect of annealing (30 min.) on their microstructure is shown in Fig. 1 for the high purity tungsten and in Fig. 2 for the alloy. It is apparent that the grain size and morphology of the recrystallized materials are markedly different. W-1% ThO₂ has an elongated grain structure after annealing at all temperatures up to 2400°C, whereas the high purity tungsten develops a fine grain equiaxed structure when annealed above 1500°C.

The hardness data (Table 2) indicate the recrystallization temperatures of the high purity tungsten to be about 1400°C. The microstructural observations, on the other hand, indicate a primary recrystallization temperature of about 1500°C. This confirms the earlier results by Koo (12) that two modes of recrystallization occur in unalloyed tungsten: (1) below 1500°C strain induced grain boundary migration, and (2) at or above 1500°C nucleation and growth. On the contrary, in the alloy there is only one mode of recrystallization, namely strain induced grain boundary migration (Fig. 2). The hardness values listed in Table 2 place the recrystallization temperature at about 1650°C.

Tensile Test Results: The yield strength of the two materials as a function of temperature and strain rates (8.4×10^{-5} and $3.3 \times 10^{-2} \text{ sec}^{-1}$) is shown in Fig. 3. A maximum in yield strength occurs in both the pure tungsten and the W-1% ThO₂ alloy. This maximum is shifted to higher temperature at the faster strain rate. It can also be noted that the yield strength of the alloy is greater than that of the pure tungsten throughout the test temperature range (800°C-2400°C). Increasing the strain rate increases the yield strength of both materials.

The ultimate strength decreases with increasing temperature over the entire temperature region, but the alloy has higher strength than pure tungsten at all temperatures; Fig. 4. The magnitude of the strength difference decreases from 10,000 psi at 1000°C to only 2,700 psi at 2400°C. The effect of strain rate on ultimate strength is summarized in Fig. 5 for the high purity tungsten and Fig. 6 for the alloy. The data presented in these figures reveal that the ultimate strength increases with increasing strain rate.

The ductility, as represented by the total elongation, is shown in Fig. 7. A maximum occurs in the temperature dependence of the ductility of each material which apparently is not related to the maximum in yield strength; Fig. 3. It is noted that pure tungsten has better ductility than W-1% ThO₂ below the maximum.

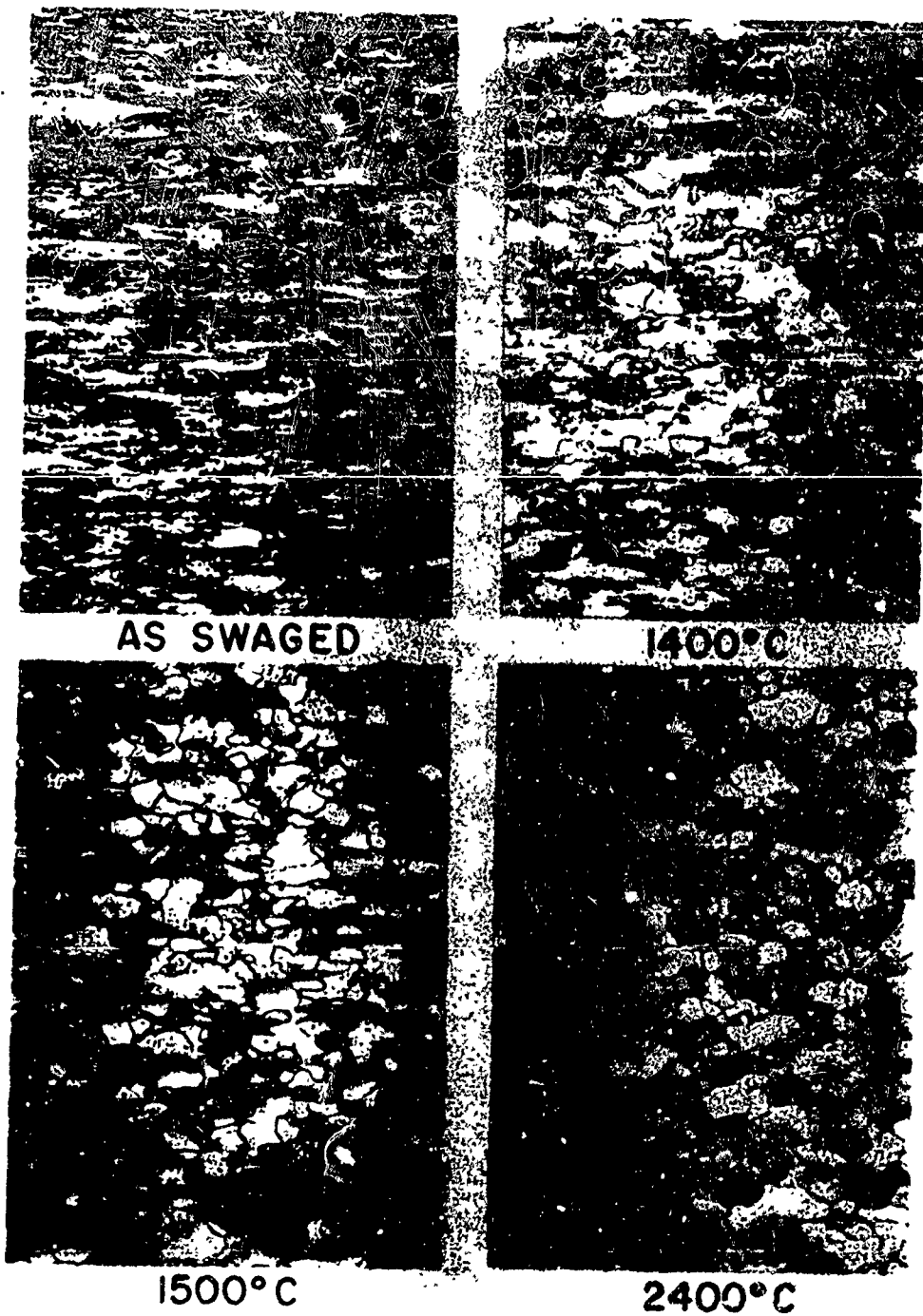


FIG. I EFFECT OF ANNEALING ON MICROSTRUCTURE OF SWAGED HIGH PURITY TUNGSTEN.

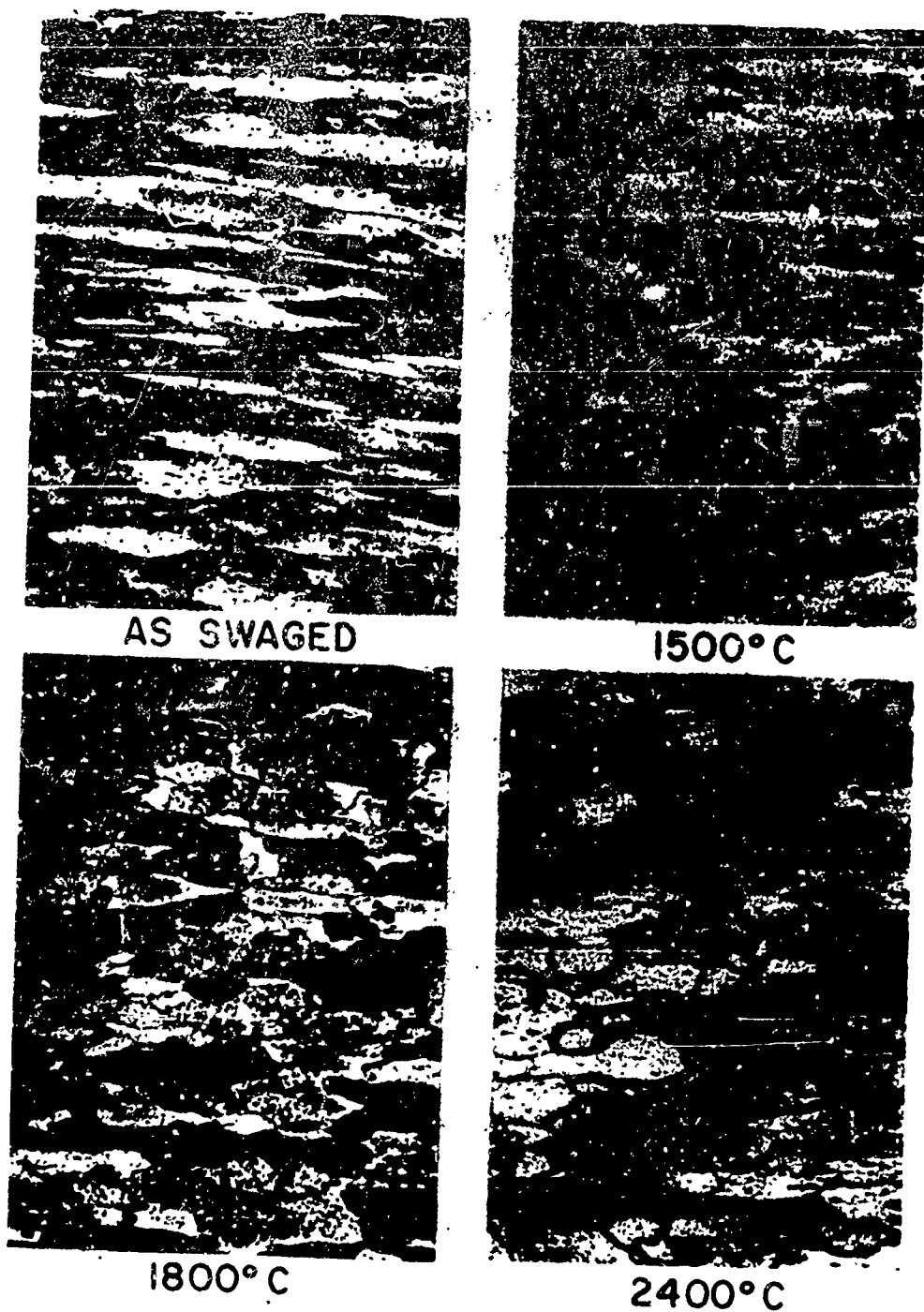


FIG. 2 EFFECT OF ANNEALING ON MICROSTRUCTURE OF
SWAGED W-1% ThO₂.

Table 2

Effect of Annealing on Hardness (Vickers) of Tungsten and W-1% ThO₂

<u>Annealing Temp. °C</u>	<u>Vickers Hardness</u>	
	<u>W-1% ThO₂</u>	<u>Tungsten</u>
As Swaged	459	450
1000	-	453
1200	-	438
1400	-	374
1500	427	374
1600	390	-
1800	379	-
2200	363	-
2400	376	371

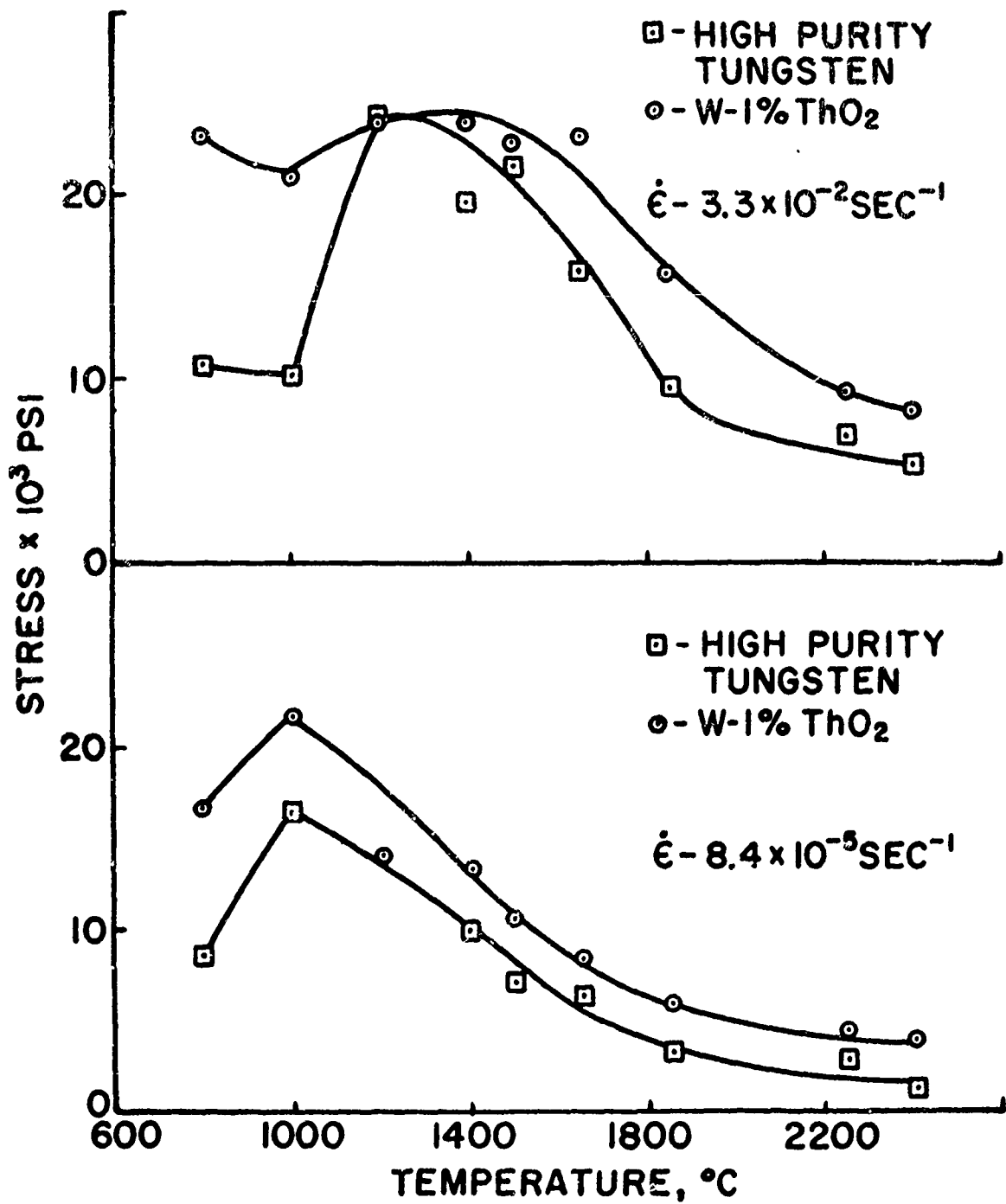


FIG. 3 YIELD STRENGTH OF RECRYSTALLIZED HIGH PURITY TUNGSTEN AND W-1% ThO_2 .

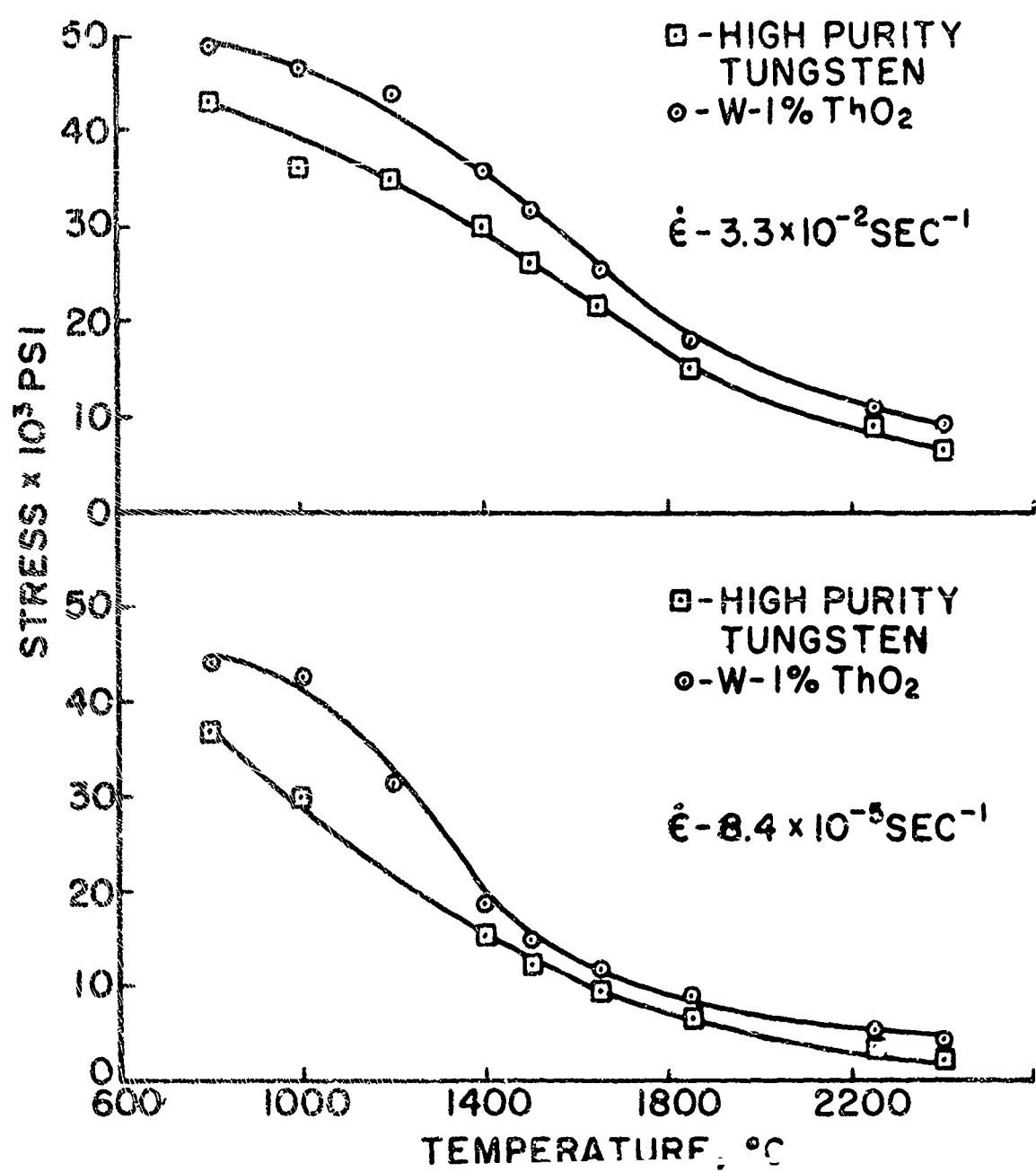
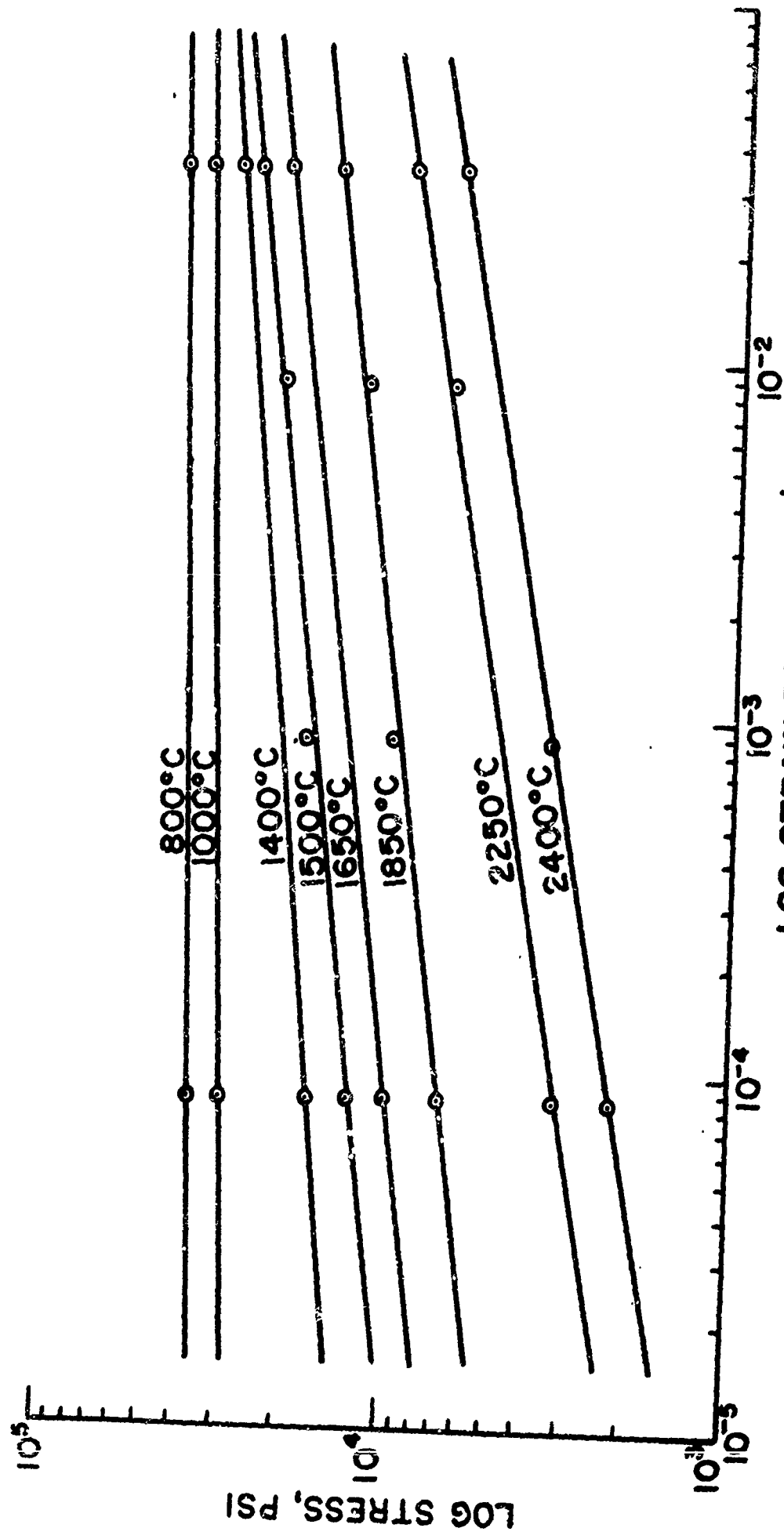
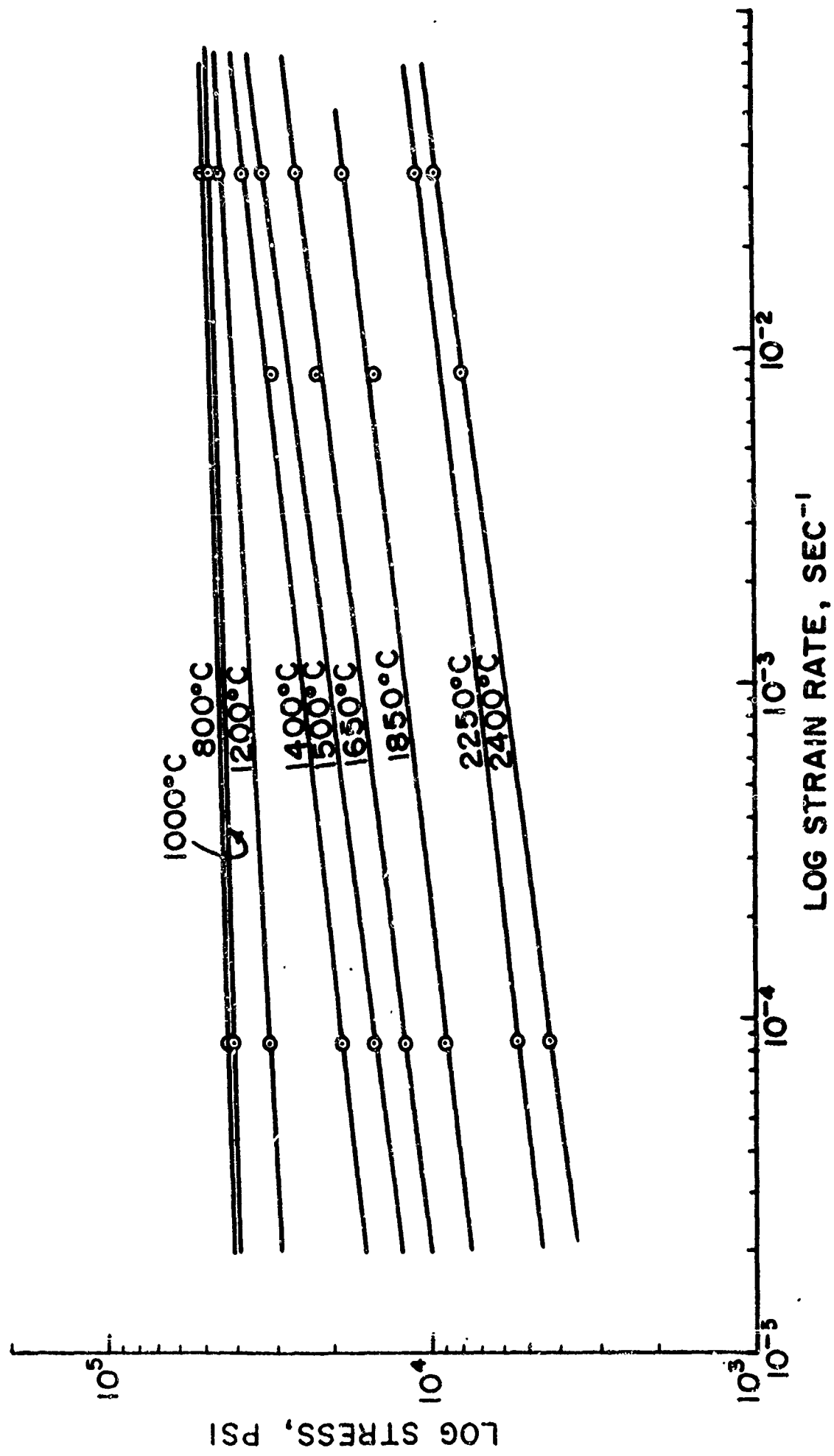


FIG. 4 ULTIMATE STRENGTH OF RECRYSTALLIZED HIGH PURITY TUNGSTEN AND W-1% ThO₂.





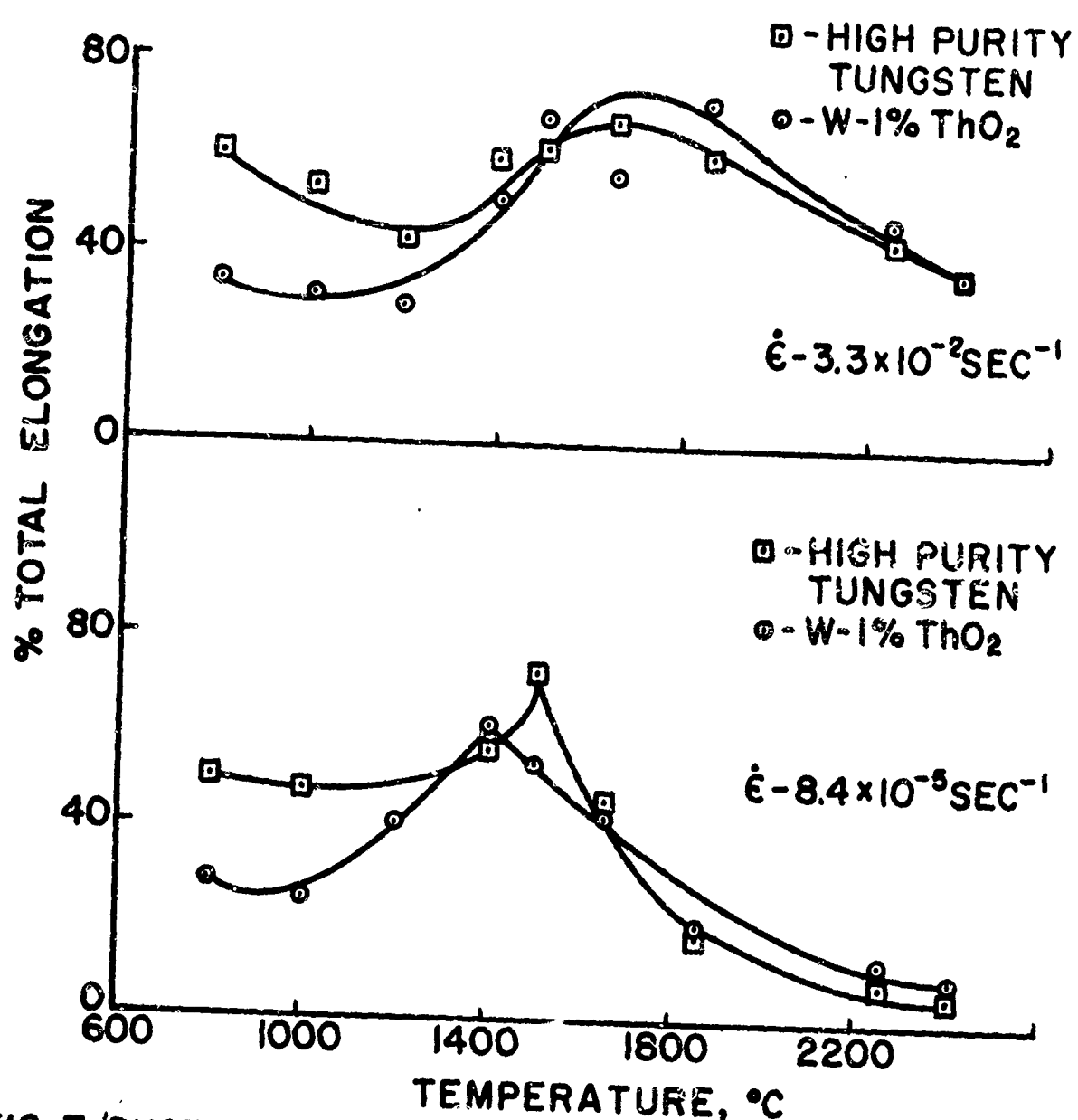


FIG. 7 DUCTILITY OF RECRYSTALLIZED HIGH PURITY TUNGSTEN AND W-1% ThO₂.

However, above the maximum, the reverse is true. The results also show, as has been generally found for deformation of unalloyed tungsten at high temperatures (10,11) that better ductility is realized at the higher strain rates.

Fracture Behavior: Metallographic specimens were polished in a 10% KOH solution and etched in an alkaline potassium ferricyanide solution. Photomicrographs of the fractures which occurred are shown in Fig. 8 for the high purity tungsten and in Fig. 9 for the alloy. A transition from a ductile to a brittle intergranular mode of fracture occurred at 1500°C for high purity tungsten (Fig. 8), and at 1650°C for W-1% ThO₂ (Fig. 9) tested at a strain rate of $8.4 \times 10^{-2} \text{ sec}^{-1}$. Increasing the strain rate by about three orders of magnitude to $3.3 \times 10^{-2} \text{ sec}^{-1}$ increases the transition temperature of the ductile to brittle intergranular mode of fracture by approximately 150°C.

It is also apparent that large voids or cavities are present in the fractured tensile specimens tested above 1500°C (pure tungsten) or 1650°C (W-1% ThO₂), and that increasing the strain rate decreases the apparent void density. No voids were observed in the unstressed tensile heads.

Microstructure of Uniformly Strained Gauge Sections: Microstructures of uniform gauge sections of the high purity tungsten and the alloy are shown in Fig. 10. Of particular interest is the effect of strain rate on the preferential sites for void formation and on the deformation substructure. At 1500°C and 1650°C, corresponding to the temperatures at which severe void formation occurs in high purity tungsten and the alloy respectively, voids are formed at boundaries parallel and transverse to the tensile axis, at triple points, and also at sub-boundaries, irrespective of strain rate. At these temperatures the subgrains produced by the deformation become smaller with increasing strain rate; Fig. 10A. At an intermediate temperature (1850°C) and slow strain rates, voids form preferentially at transverse boundaries and triple points. At the fast strain rates, which give rise to a much finer deformation substructure, voids are noted to form also at sub-boundaries; Fig. 10B. At the highest test temperature (2400°C) voids are formed almost exclusively at transverse boundaries and triple points in the high purity tungsten. However, a few voids form at low angle boundaries in W-1% ThO₂ tested under the same conditions. A substructure develops in both materials at the fast strain rate; Fig. 10C.

A comparison was made between the grain size in the uniform gauge section and the grain size in the unstressed heads of tensile specimens. In virtually all cases the grain size in the heads is equal to or greater than the grain size in the uniform

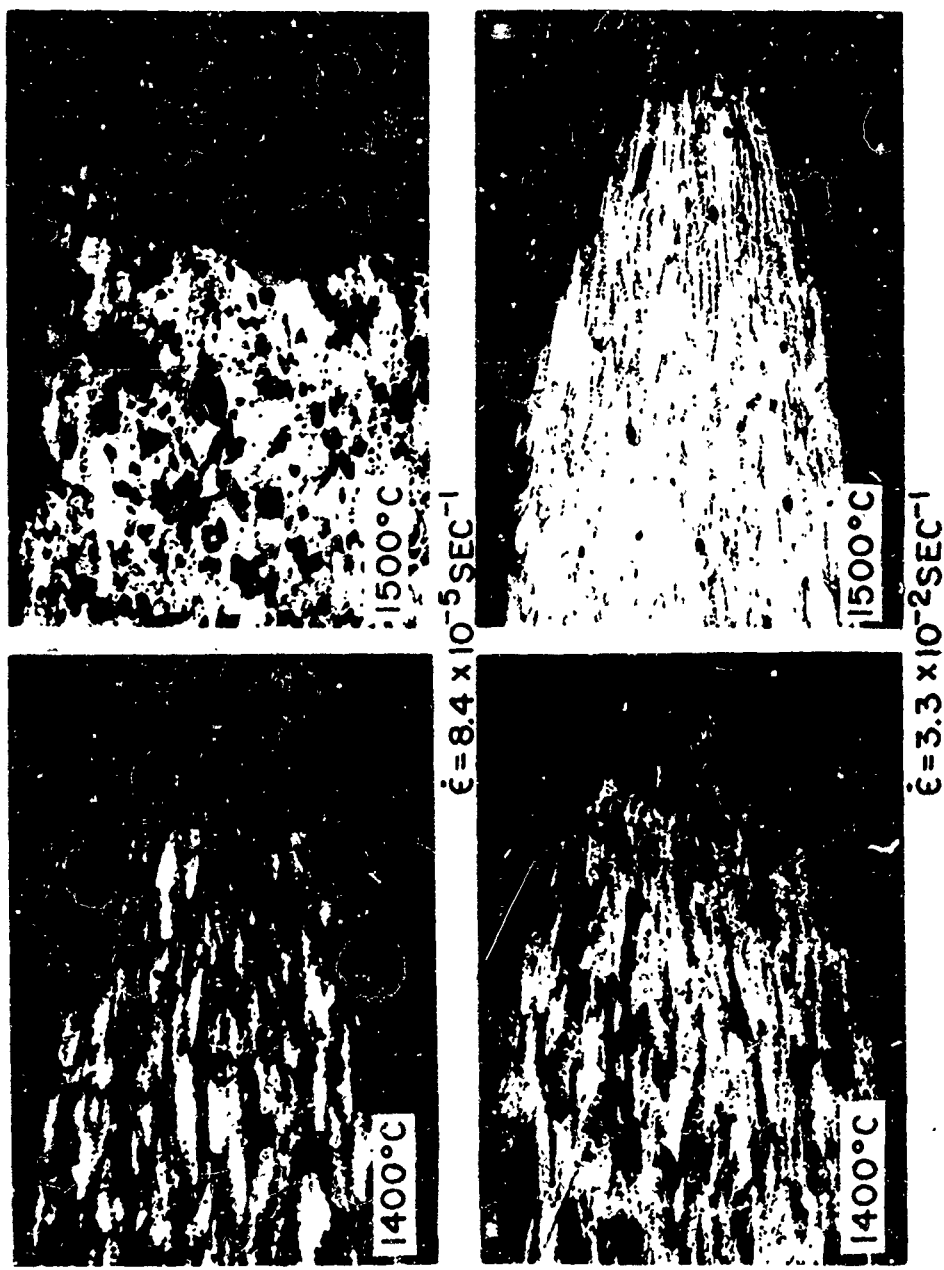


Fig. 8 Effect of Strain Rate and Temperature on Tensile
Fractures of High Purity Tungsten
45X

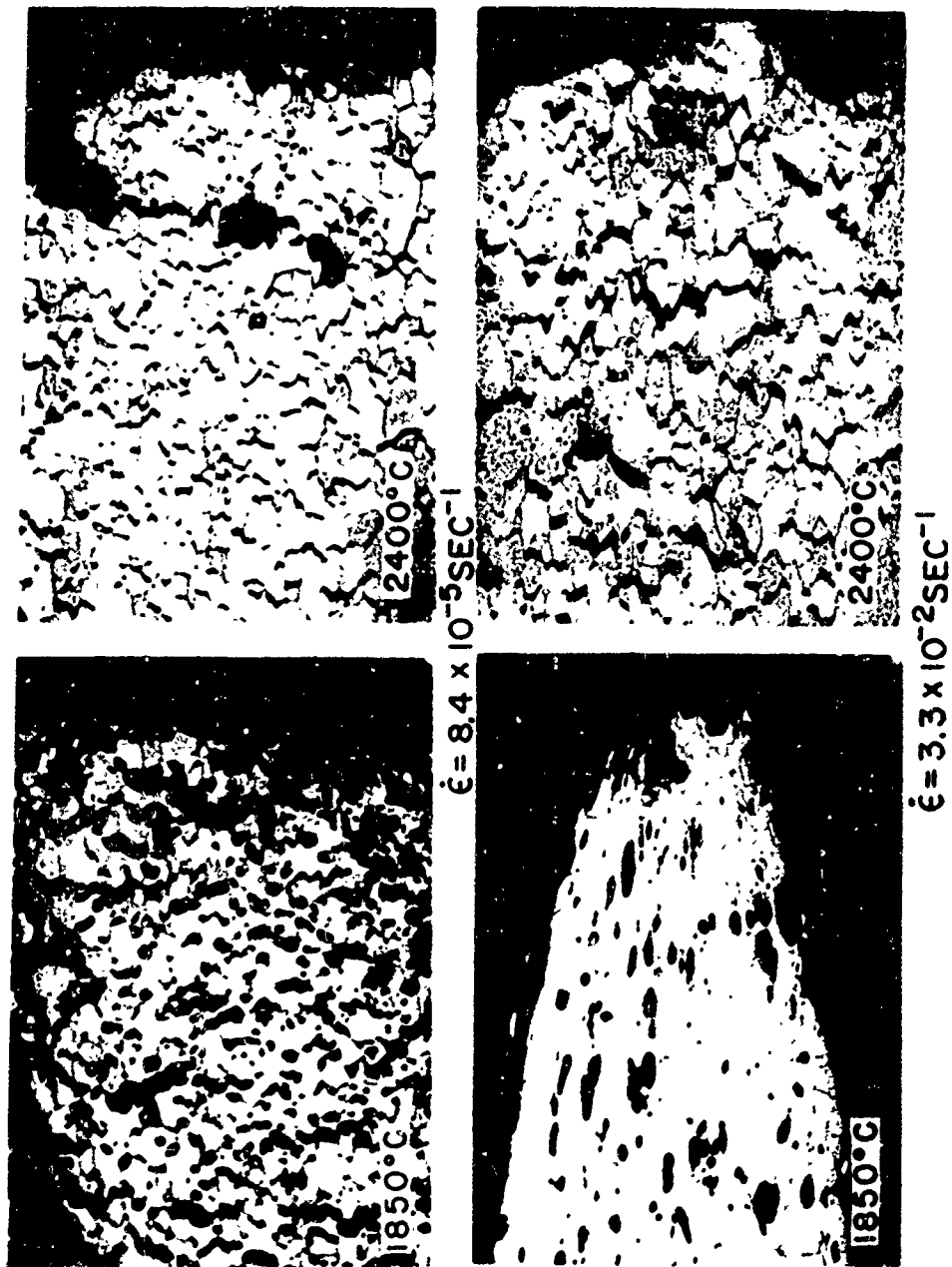


Fig. 8 continued - Effect of Strain Rate and Temperature on Tensile Fractures of High Purity Tungsten 45X

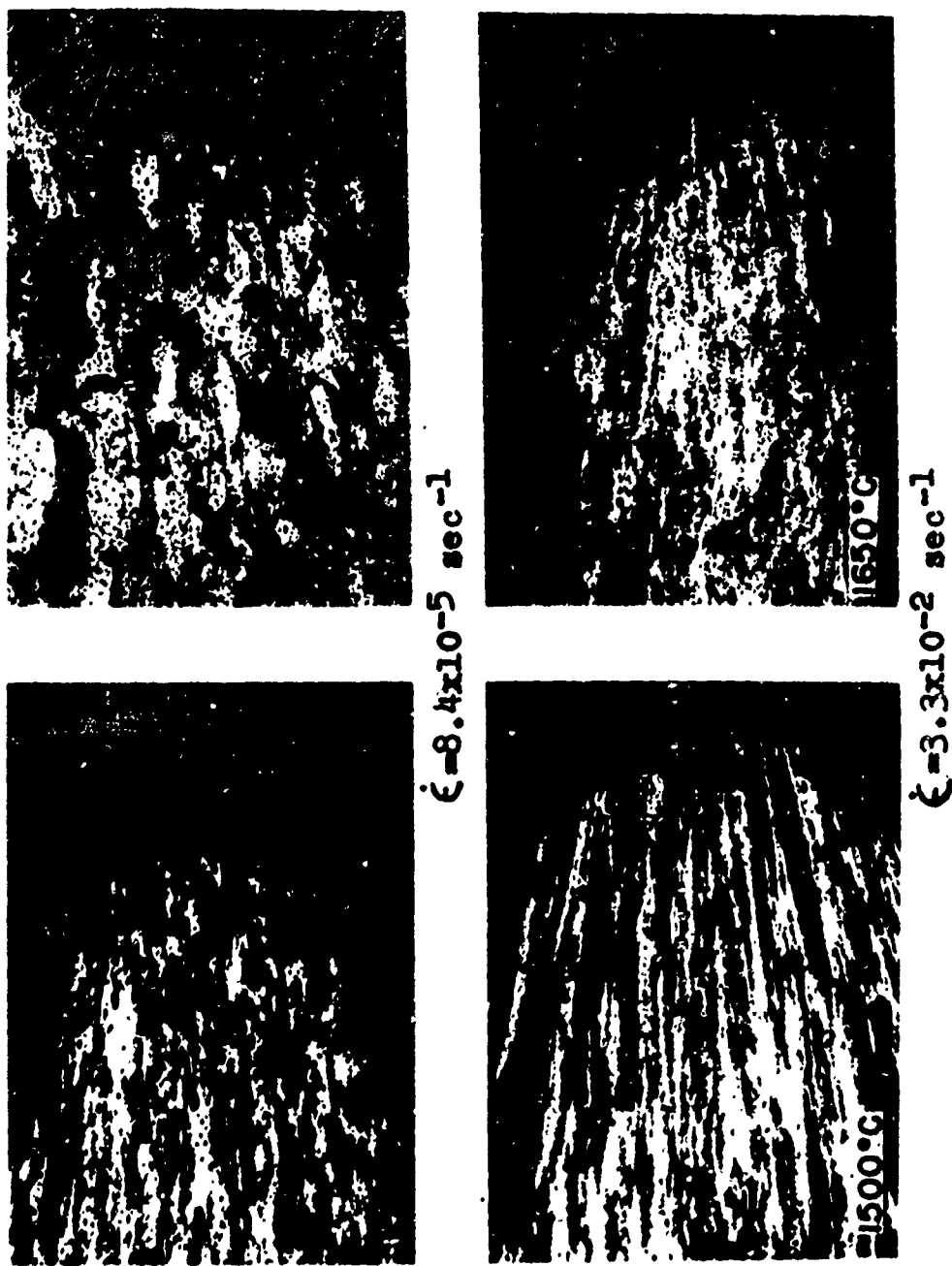


Fig. 9 Effect of Strain Rate and Temperature on Tensile Fractures of W-1% ThO₂; 45X



$8.4 \times 10^{-5} \text{ sec}^{-1}$

1850°C



$3.3 \times 10^{-2} \text{ sec}^{-1}$

1850°C



1850°C



2400°C

Fig. 9 (continued) - Effect of Strain Rate and Temperature on Tensile Fractures of W-1% ThO₂; 45X

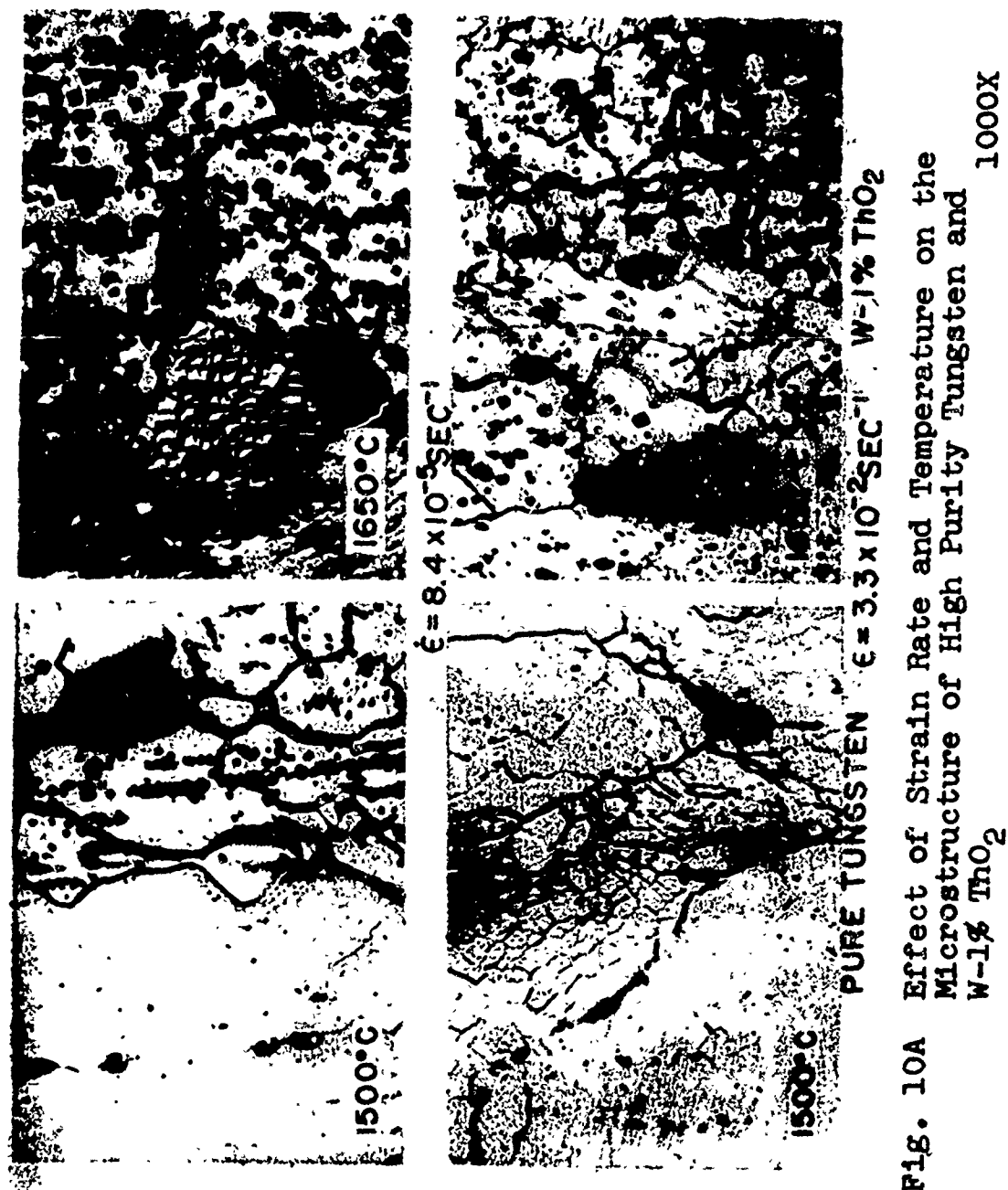


Fig. 10A Effect of Strain Rate and Temperature on the Microstructure of High Purity Tungsten and W-1% ThO_2 1000X

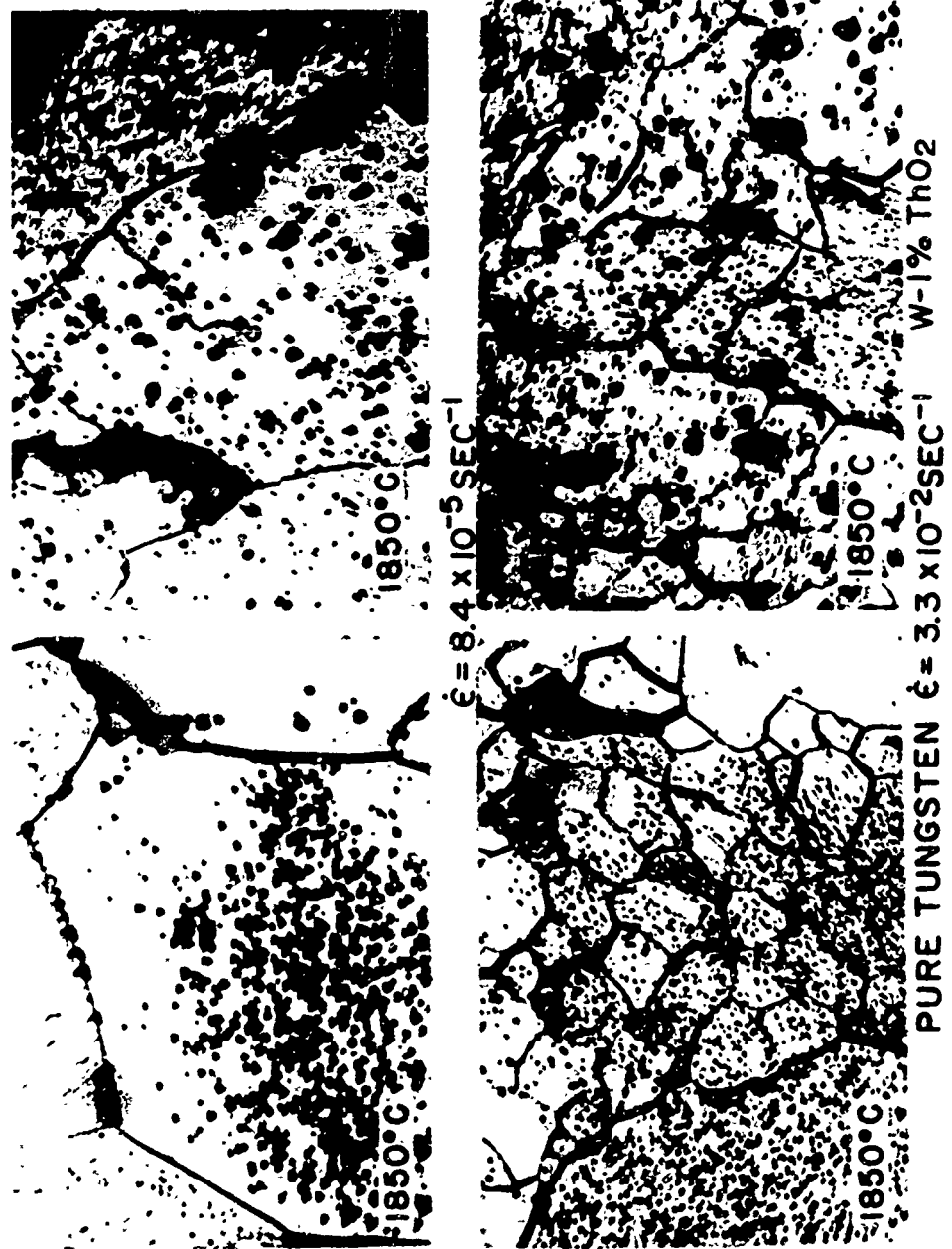


FIG. 10B Effect of Strain Rate and Temperature on the Microstructure of High Purity Tungsten and W-1% ThO₂ 1000X

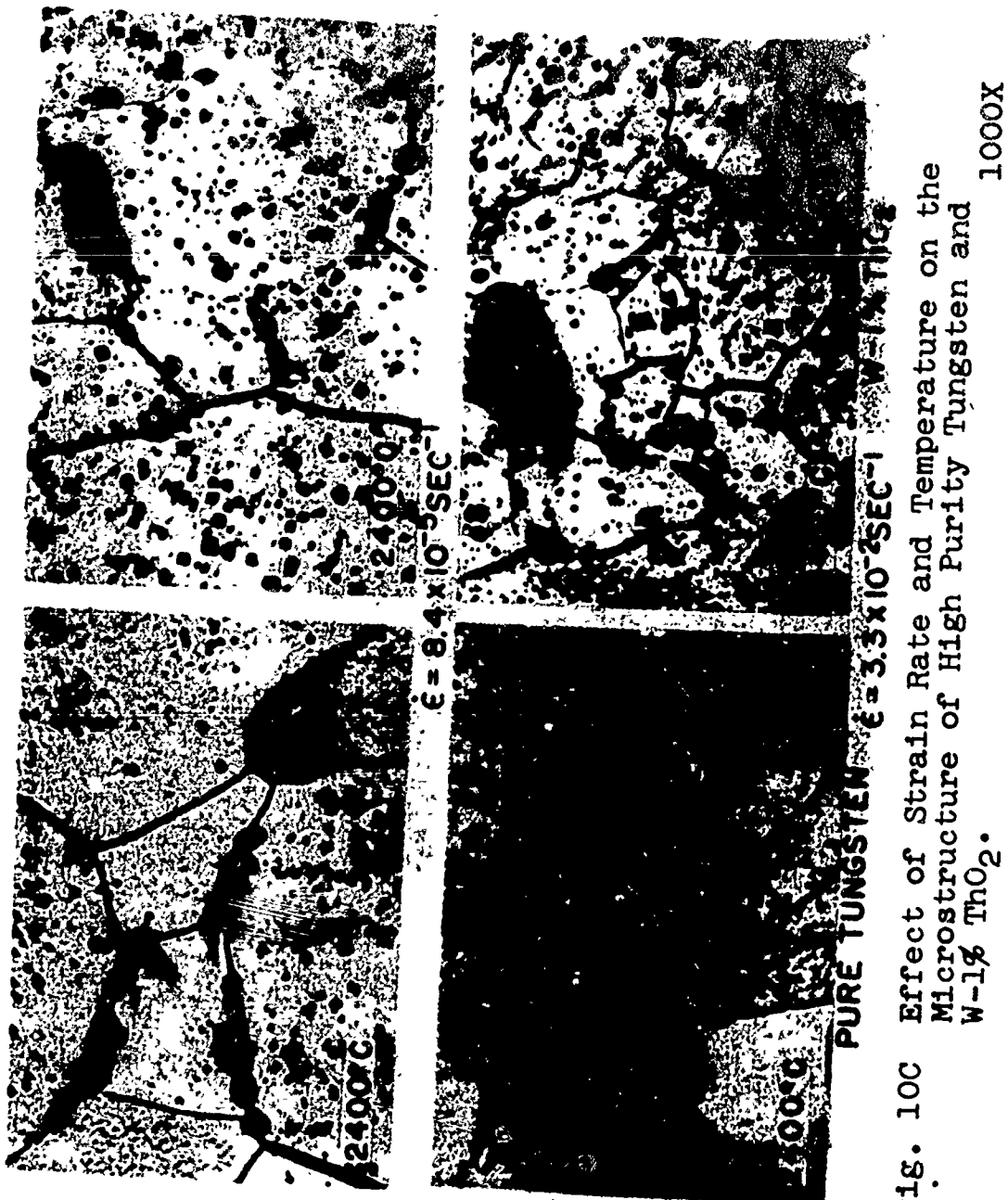


Fig. 10C Effect of Strain Rate and Temperature on the Microstructure of High Purity Tungsten and W-1% ThO₂. 1000X

gauge sections. However, the amount of reduction in grain size in the uniform gauge section tends to decrease with increasing temperature or decreasing strain rate (Table 3). This suggests that some degree of strain induced grain boundary migration did occur.

4. Discussion

The data presented show that the addition of 1% thoria by weight has a modest effect on the strength of tungsten over a wide temperature region (0.3 - 0.7 T_m). A comparison of the results on high purity tungsten with the data published by Sikora and Hall (10) and also Taylor and Beone (11) generally show good agreement. However, the magnitude of the strength and ductility of the various materials as a function of temperature, and also the temperatures at which maxima occur in the tensile properties differ somewhat. The differences in tensile properties are undoubtedly influenced by different amounts of trace impurities. The analyses reported in Table 1 suggest that the tungsten presently investigated is probably the purest tested to date.

The peak in the temperature dependence of the yield strength of the high purity tungsten as well as that of the alloy (Fig. 3) is suggestive of the type of effects which have been previously attributed to dislocation - interstitial impurity interactions. However, since it is unlikely that interstitial atoms can have much influence on dislocation motion at temperatures at which the peak is observed at the fast strain rate in pure tungsten (1200-1500°C), or in W-1% ThO₂ (1200-1658°C), the effect is considered to be caused by a dislocation interaction with substitutional impurities or possibly by microprecipitation.

Theories of strengthening by precipitates were found to be inapplicable to the results obtained on W-1% ThO₂. The interparticle spacing ($\sim 7\mu$) is too large to be of significance in the Orowan theory (13). The theory of Fisher, Hart and Pry (14), which considers the incremental strain hardening due to the formation of dislocation loops around dispersed second phase particles, is also unsatisfactory in explaining the observed strengthening. The yield strength of the alloy is more strongly enhanced by thoria than the ultimate strength, Fig. 3 and 4, a fact not supporting their theory.

A factor which necessarily influences the tensile properties is the effect of thoria on the microstructure of tungsten. The addition of 1% ThO₂ results in a large elongated grain structure in the recrystallized condition, as compared to a finer equiaxed

Table 3

Summary of Metallographic Observations on Preferential Sites of Void Formation and Stress-Induced Growth in Pure and Manganese

Pure Tungsten		Dg/Dh		Dg/Dh	
Test	Temp.	Void Location	$3 \cdot 3 \times 10^{-5} \text{ sec}^{-1}$	$8 \cdot 1 \times 10^{-5} \text{ sec}^{-1}$	$3 \cdot 3 \times 10^{-2} \text{ sec}^{-1}$
1500°C	T.P.; P.B.; T.B.; S.B.	T.P.; P.B.; T.B.; S.B.	-0.15	-0.314	-0.316
1650°C	T.P.; P.B.; T.B.; S.B.	T.P.; P.B.; T.B.; S.B.	-0.15	-0.133	-0.132
1850°C	T.P.; T.B.	T.P.; T.B.	-0.174	-0.212	+0.49
2400°C	T.P.	T.B.	-0.056	+0.040	-0.327

W-14Th02		Dg/Dh		Dg/Dh	
Test	Temp.	Void Location	$3 \cdot 3 \times 10^{-5} \text{ sec}^{-1}$	$8 \cdot 1 \times 10^{-5} \text{ sec}^{-1}$	$3 \cdot 3 \times 10^{-2} \text{ sec}^{-1}$
1500°C	P.B.; T.B.; S.B.	P.B.; P.B.	-0.072	-0.316	-0.316
1650°C	T.P.; T.B.; P.B.; S.B.	T.P.; T.B.; P.B.; S.B.	-0.074	-0.132	-0.132
1850°C	T.P.; T.B.	T.P.; T.B.	-0.061	-0.061	-0.061
2400°C	T.P.; T.B.	T.P.; T.B.	-0.020	-0.020	-0.020

Triple Points		Dg/Dh		Dg/Dh	
Test	Temp.	Void Location	$3 \cdot 3 \times 10^{-5} \text{ sec}^{-1}$	$8 \cdot 1 \times 10^{-5} \text{ sec}^{-1}$	$3 \cdot 3 \times 10^{-2} \text{ sec}^{-1}$
T.P.	-	Triple Points	-	-	-
T.B.	-	Parallel Boundaries	-	-	-
S.B.	-	Transverse Boundaries	-	-	-
T.B.	-	Sub-Boundaries	-	-	-
Dg	-	Grain diameter in uniform gauge section	-	-	-

structure in the high purity tungsten. Also, unalloyed re-crystallized tungsten is free of coarse sub-structure, whereas sub-structure is retained in W-1% ThO_2 after recrystallization. The present evidence suggests that the structural effect on the strength is not related to microscopic grain size, in that the small grained high purity tungsten has substantially lower strength at intermediate temperatures (0.3-0.5 T_m) than the W-1% ThO_2 alloy which has a coarse elongated grain structure. It is possible that the improved strength of the alloy is partially caused by the ability of the thoria dispersion to retard dynamic recovery during testing (14), and to prevent the complete removal of substructure during annealing (15). Previous investigations have shown a correlation between tensile strength and substructure. However, the effect of subgrain size on tensile strength was concluded to be significantly less than the effect of microscopic grain size (15).

In the high temperature region thoria appears to be relatively more effective as a strengthener than at intermediate temperatures. This is suggested by the ratios of the ultimate strength of the alloy to the ultimate strength of the high purity tungsten which increase at higher temperatures; Fig. 11. Grain boundary sliding, which becomes controlling at higher temperatures, is apparently decreased in the alloy because of the irregular boundaries which are directly the result of the thoria particles. The latter is indicated by the electron micrograph reproduced in Fig. 12, which shows a grain boundary held up by thoria particles. Also, the large elongated grains of W-1% ThO_2 are more desirable in terms of strengthening at temperatures above 0.5 T_m than the smaller equiaxed grains of the high purity tungsten, since the rate of grain boundary sliding is retarded by decreasing the total surface area (16). Void formation, which has been shown to be related to grain boundary sliding (5,6,7) is retarded in the alloy. The results tabulated in Table 3 suggest that at temperatures near 0.5 T_m , mechanisms which involve the condensation of vacancies from within the matrix may also contribute to void formation (8,9,10). The improved high temperature strength at faster strain rates is directly a consequence of the reduction in void formation. Taylor and Boone (11) attributed this strength improvement also to reduce void formation at faster rates. These authors claimed that a higher degree of strain induced grain boundary migration occurred at increasing strain rates and that the decrease in void formation resulted from the increase in grain boundary mobility. The results listed in Table 3 do not support this conclusion.

Apparent activation energies have been determined as a possible means of elucidating the deformation mechanism(s) involved. Plots of $\log \dot{\epsilon}$ for a given stress level vs $1/T$ are shown in Fig. 13 for high purity tungsten and in Fig. 14 for

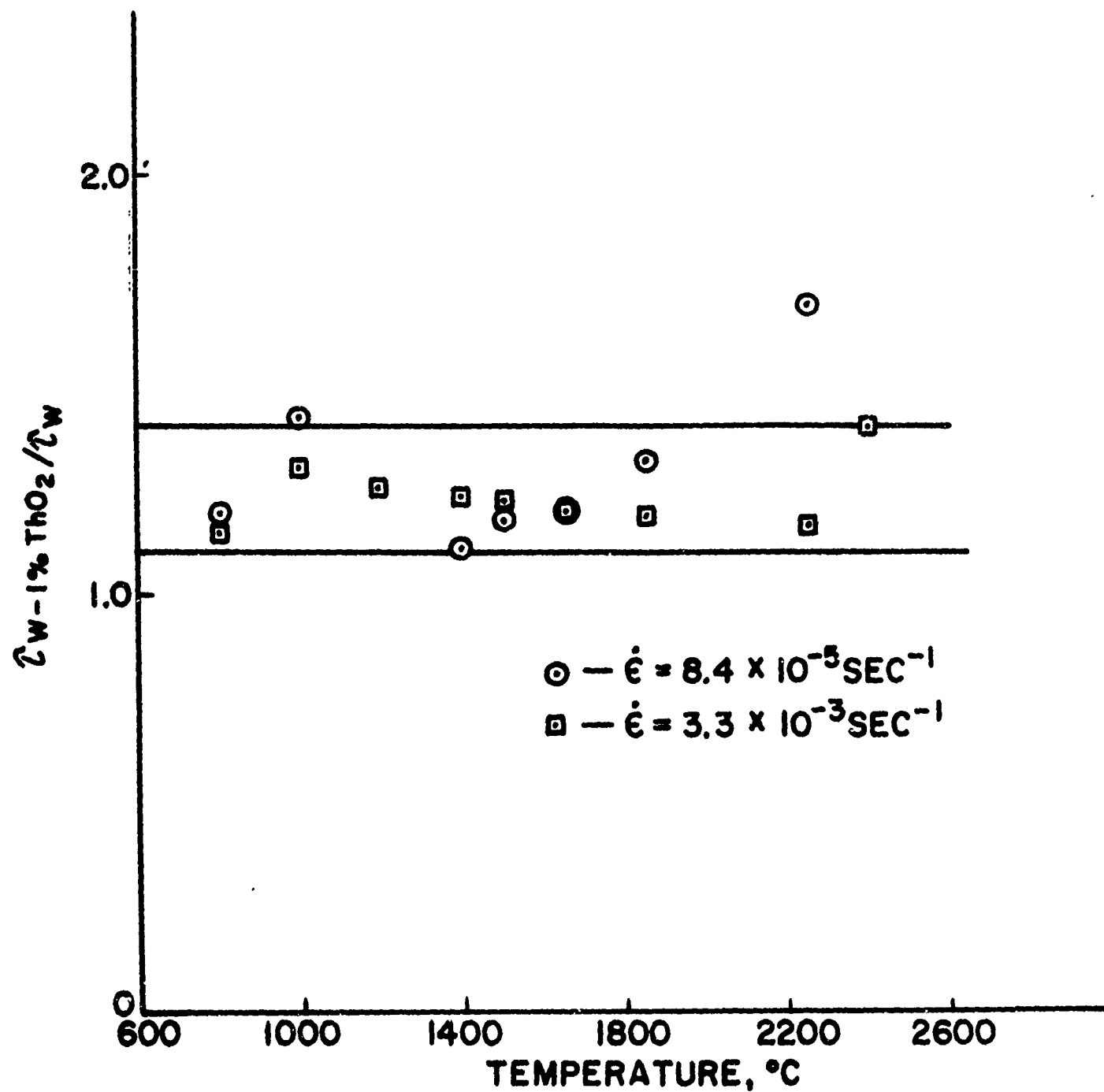


FIG. II RATIO OF THE ULTIMATE STRENGTHS OF W-1% ThO₂ AND PURE TUNGSTEN AS A FUNCTION OF TEMPERATURE AND STRAIN RATE.

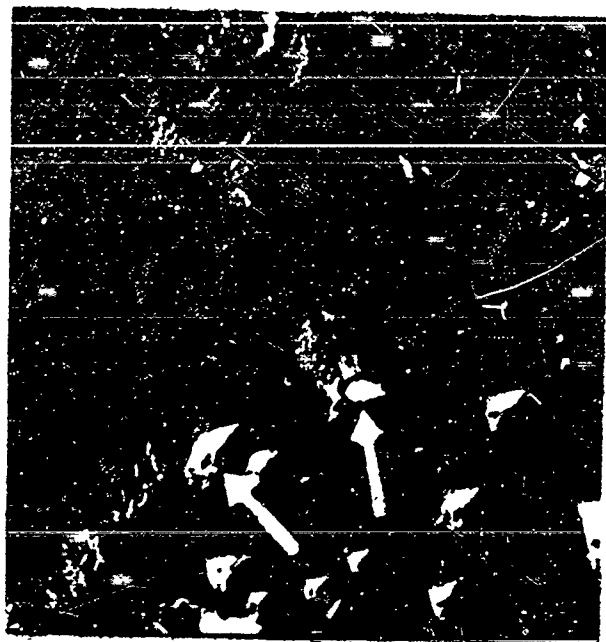


Fig. 12 GRAIN BOUNDARY (ROW OF ETCH PITS) HELD
UP BY THORIA PARTICLES INDICATED BY
ARROWS.

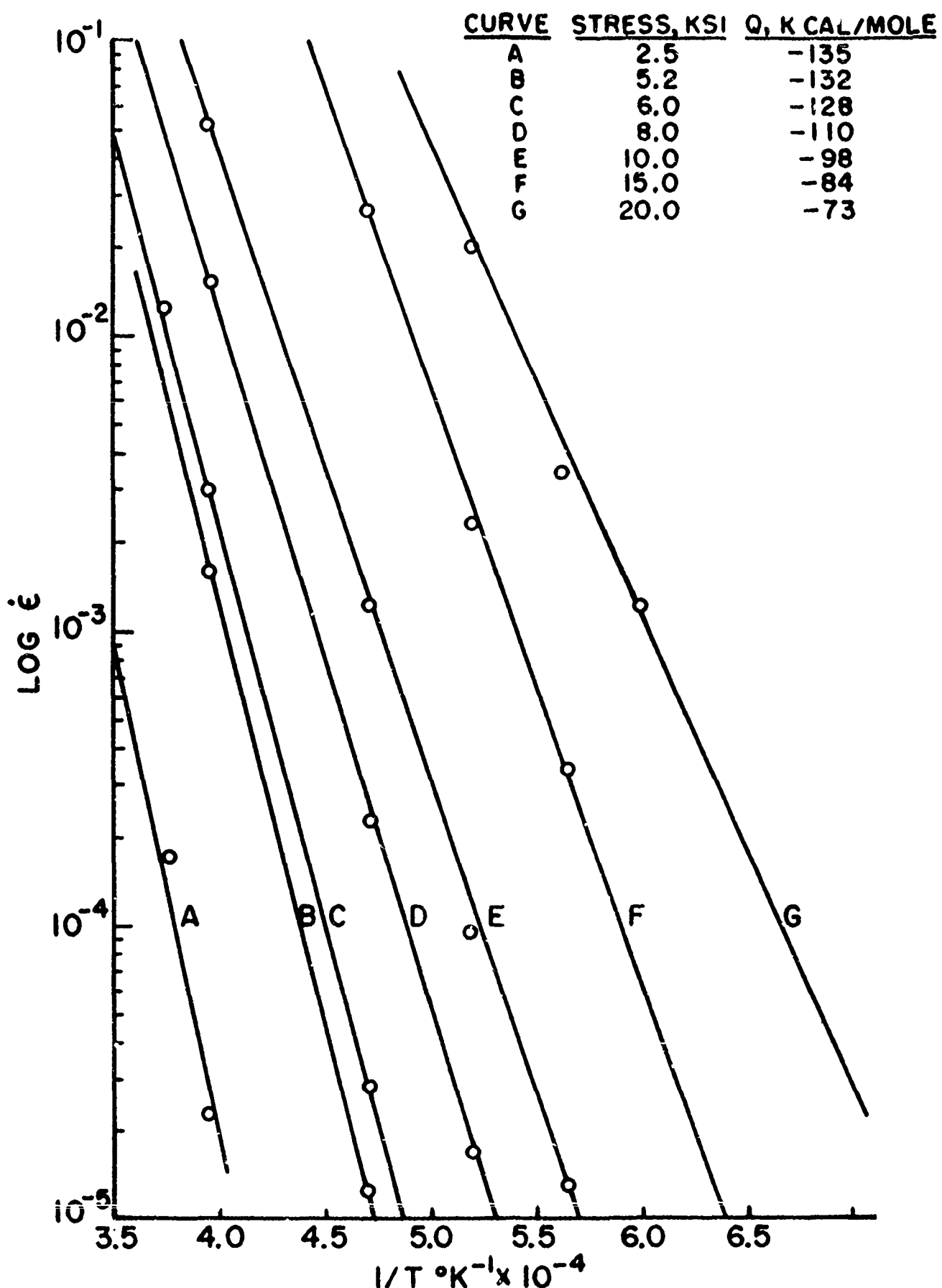


FIG. 13 LOG STRAIN RATE VERSUS $1/T$ OF HIGH PURITY TUNGSTEN AT VARIOUS STRESS LEVELS.

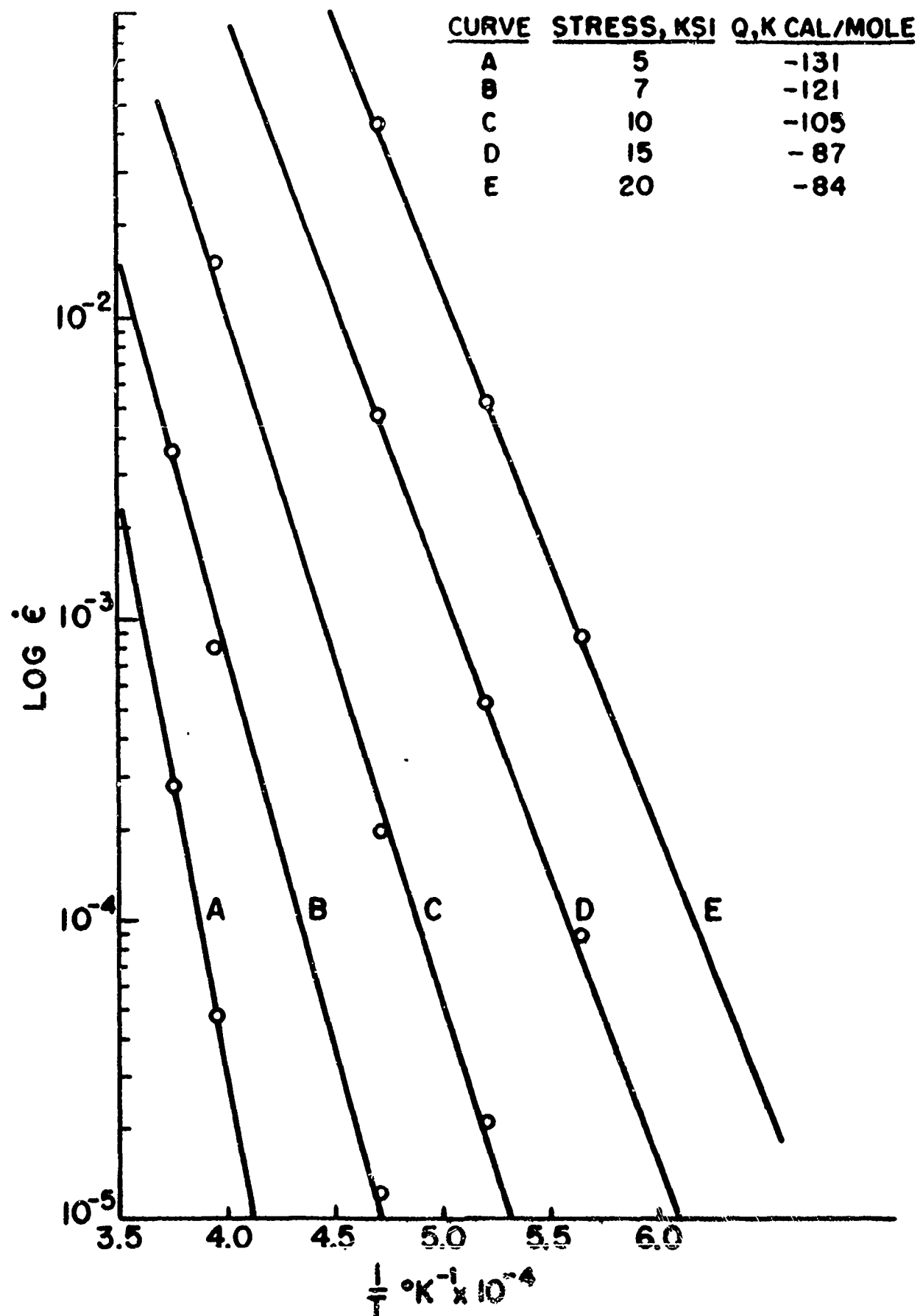


FIG. 14 LOG STRAIN RATE VERSUS 1/T FOR W-1% ThO₂ AT VARIOUS STRESS LEVELS.

W-1% ThO₂. The slopes of these plots (equal to Q/R) yield directly the apparent activation energies. Values of the apparent activation energies of high purity tungsten and of W-1% ThO₂, respectively, are plotted as a function of stress in Fig. 15. The values of Q vary from 140 KCal/mole at low stresses (high temperatures) to 72 KCal/mole at high stresses (low temperatures). The value of 140 KCal/mole is in good agreement with the activation energy for self-diffusion in tungsten reported elsewhere in the literature (18) and therewith the activation energy for grain boundary sliding which is approximately the same as that for self-diffusion. This result supports the metallographic observations which indicate that grain boundary sliding is more pronounced at the higher temperatures.

It is not possible to state unambiguously whether the spectrum of apparent activation energies calculated are the result of stress dependent mechanisms, rather than temperature dependent mechanisms. Several stress dependent mechanisms have been proposed for the deformation of metals at low temperatures (19, 20, 21). Although the results of this investigation differ in many respects with the details of these models, it is the opinion of the authors that the variation in the activation energies between 0.4 and 0.7 T_m reflect a stress dependent deformation mechanism.

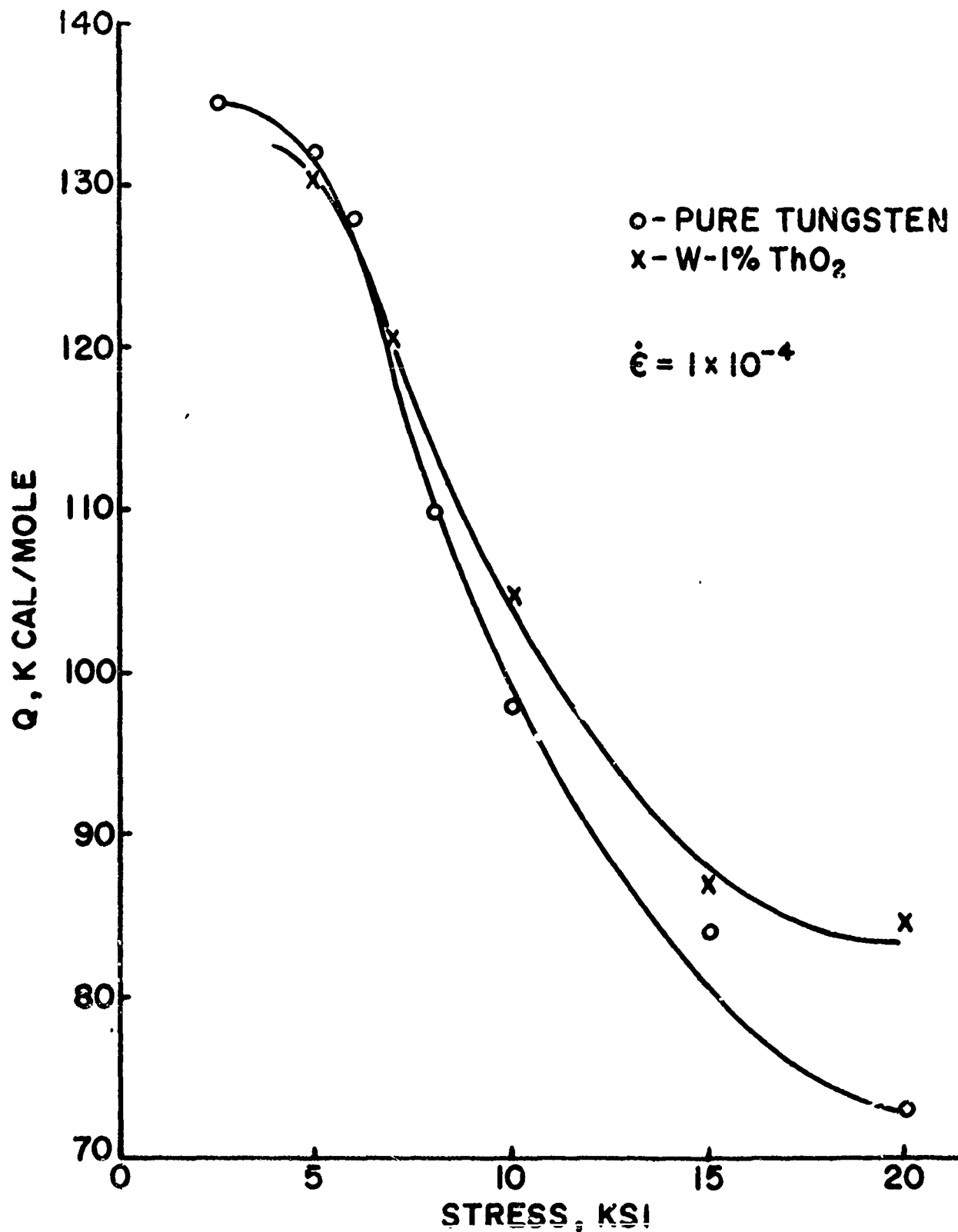


FIG. 15 APPARENT ACTIVATION ENERGY OF HIGH PURITY TUNGSTEN AND W-1% ThO_2 AS A FUNCTION OF STRESS.

III. EFFECT OF CARBON ON THE TENSILE PROPERTIES OF TUNGSTEN AND W-0.35%Ta

Previous investigations of both polycrystalline (22) and single crystal tungsten (3,4) have disclosed yield stress anomalies (peaks and valleys) in the temperature region from 300 to 800°C which have been attributed to interstitial impurities. Recently, internal friction and residual resistance ratio measurements (4) have revealed that carbide precipitation occurs within this temperature region. The objective of the work presented in this section was to investigate the effects of carbon on the tensile properties of both pure W and W-0.35%Ta single crystals, worked single crystals, and worked and recrystallized single crystals.

The alloy was chosen because preliminary high temperature tensile tests on alloys of W-Ta (1) and W-Nb(23) suggested these alloys as suitable high temperature - high strength materials.

A. Pure Tungsten and W-0.35%Ta Single Crystals

1. Preparation of Single Crystals and Test Procedure

The pure tungsten and the W-0.35%Ta single crystals were produced from wrought 0.250 inch diameter rod by the electron beam floating zone melting technique. Unless otherwise stated, these crystals were seeded to a [100] orientation. Tensile specimens having a 1 in. gauge length and a gauge diameter of 0.107 to 0.110 in. were ground from these crystals. The worked surface of the ground specimens was then removed by electropolishing about 0.010 in. from the gauge diameter.

Carbon dosing of specimens was carried out by the following method: A specimen, immersed in graphite powder which is contained in a graphite crucible, is inductively heated to 1800°C in vacuum and held at that temperature for 15 minutes. This results in the formation of a carbide case. Afterwards, the specimen is annealed in vacuum for two hours at 2200°C to diffuse carbon into the matrix. Finally, the residual carbon case is removed by electropolishing. Some specimens were slow cooled, others were quenched from high temperatures.

A vacuum furnace similar in design to that described by Taylor and Ryden (24) was used for quenching. The quenching procedure consisted of mounting a bundle of two to four specimens in the furnace, holding the bundle at temperature for the desired time, and then quenching the specimens into a bath of molten

indium at about 162°C. The quench was from 2200°C after a 15 minute hold at that temperature.

Photomicrographs of two carbon dosed W-0.35%Ta crystals showing typical carbide precipitate distributions in slowly cooled specimens resulting from this non-equilibrium treatment have been reproduced in Fig. 16. The carbide precipitate distribution in pure tungsten crystals is similar to those shown in Fig. 16.

Tensile tests were conducted in a vacuum furnace mounted to an Instron tensile machine. The strain rate was always 8.4×10^{-5} /sec. The time for the tensile specimens to reach test temperature and stabilize at that temperature was about 30 to 45 minutes. Temperatures below 1200°C were measured with a chromel-alumel thermocouple and above 1200°C with an optical pyrometer.

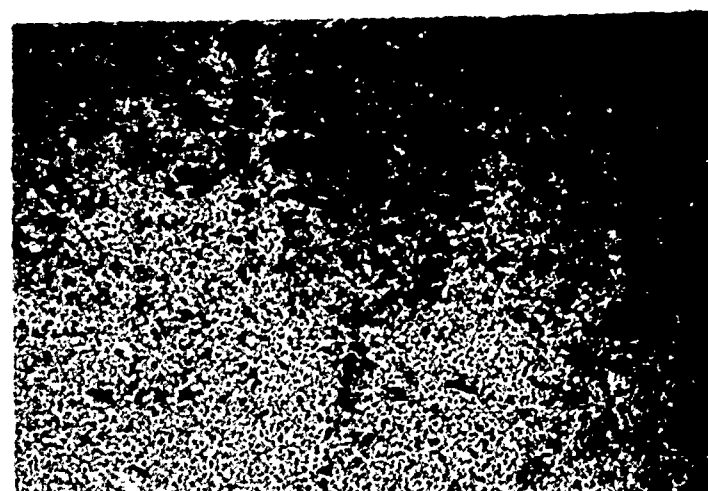
2. Impurity Analyses

Carbon, vacuum fusion, and quantitative spectrographic analysis of both pure W and the W-0.35%Ta single crystals are listed in Table 4. Tantalum concentrations were determined by neutron activation analyses developed by Gorth for tantalum in tungsten (25). The interstitial impurity values are average values of the number of analyses listed in the brackets. It can be noted that the carburizing procedure increased the carbon concentration by about 50 wgt.ppm.

Residual resistance ratio measurements reported previously (4) were also used to estimate the carbon concentration in solid solution. These measurements have been reproduced in Table 5. The residual resistance ratio of a carburized and quenched tungsten crystals was measured to be 39. Since pure tungsten has a resistivity of $5.5 \mu \Omega \text{ cm}$ at 293°K (26), a residual resistance ratio of 39 is equivalent to a resistivity of $1.4 \times 10^{-1} \mu \Omega \text{ cm}$ at 4.2°K. If one assumes that this residual electrical resistivity is caused entirely by carbon in solid solution and further, that one atomic percent of carbon in solid solution will increase the resistivity by $1 \mu \Omega \text{ cm}$ one estimates a carbon concentration of 91 ppm by weight for a ratio of 39. Taking into account the possible contributions of other interstitials to the residual resistance, the value of 91 ppm by weight is in reasonable agreement with the average value of 81 ppm by weight determined by the vacuum combustion technique (Table 4).

3. Tensile Test Results

Tensile properties were determined for the following condi-



CARBIDES ALONG SUBGRAIN
BOUNDARIES.
100X



CARBIDES WITHIN SUBGRAINS.
100X

Fig. 16 Carbide Precipitates in W-0.35% Ta After
Carburizing.

() = Number of analyses.

Quantitative Spectroscopic Analyses of W and $W=0.35\%Ta$ Single Crystal Alloys

Specimen	Al	Si	Ca	Fe	Al	Si	Ca	Fe	Al	Si	Ca	Fe
W-0.35%	5	3	-	10	-	5	-	10	14	6	-	17
Tungsten	11	5	-	10	14	6	-	10	14	6	-	17
Mean	11	5	-	10	14	6	-	10	14	6	-	17
SD	2.0	0.4	-	1.7	1.7	0.5	-	1.7	1.7	0.5	-	1.7

<u>Specimen</u>	<u>Carbon</u>	<u>Oxygen</u>	<u>Nitrogen</u>	<u>Hydrogen</u>	<u>Tantalum</u>
Virgin	29 \pm 12 (9)	20 \pm 10 (10)	4 \pm 3 (10)	2 \pm 1 (10)	3,520 \pm 304 (5)
Carburized	84 \pm 27 (17)	10 \pm 2 (5)	6 \pm 3 (5)	2 \pm 2 (5)	3,712 \pm 241 (5)

Average Carbon, Vacuum Fusion, and Tantalum Analyses of Fractioned W-0.35% Single Crystal Test Series - ppm by weight

Specimen	Carbon	Oxygen	Nitrogen	Hydrogen
Virgin	81 \pm 29 (6)	24 + 9 (8)	3 \pm 1 (4)	1 \pm 1 (4)
Carburized		18 + 9 (8)	4 + 1 (8)	1 + 2 (8)

Average Carbon and Vacuum Fusion Analyses of Fractured
Tungsten Single Crystal Textiles - ppm by weight

Table 4

tions: virgin (as grown), quenched, carburized, and carburized followed by a quench. The temperature dependence of the yield stress for the various conditions is plotted in Fig. 17 for tungsten single crystals and in Fig. 19 for W-0.35%Ta single crystals. The ductility as a function of temperature for the same specimens is plotted in Figs. 18 and 20, respectively. Discontinuous yield points or serrated stress-strain curves were occasionally observed and are indicated by the subscripts "y.p." or "s", respectively, in these figures. The tensile test results have been listed in Tables 6 and 7.

a) Tungsten Single Crystals

The temperature dependence of the yield stress of the virgin crystals and those virgin crystals which were quenched exhibited small yield stress anomalies (peaks and valleys) between 300 and 800°C. The quench did affect these anomalies somewhat. From 800 to 1200°C, a relatively constant yield stress of about 5,000 psi is measured in the virgin crystals. No measurements have been made above 800°C for the quenched virgin crystals. Carburizing the virgin crystals results in a pronounced increase in the yield stress between 300 and 1200°C (Fig. 17). Although the data of the carburized and quenched crystals show substantial scatter, a constant yield stress is suggested from 350 to 800°C. Two curves which possibly fit the data have therefore been drawn. Above 850°C the yield stress falls off rapidly from about 60,000 psi to about 20,000 psi at 1200°C.

The virgin and quenched virgin crystals also exhibit anomalies in the % R.A. and % elongation plots (Fig. 18) similar to those noted in the yield stress plots. The limited data for the carburized crystals indicate that carburizing per se does not affect the two ductility parameters. Quenching, on the other hand, has a pronounced effect on the % elongation values of carburized single crystals. Values of about 10% are measured from 300 to 800°C. The % R.A. curve shows a broad minimum from 500 to 900°C, but % R.A. values are still significantly large (approx. 30-60%).

b) W-0.35%Ta Single Crystals

The temperature dependence of the yield stress of the alloy (Fig. 19) is similar to that of the pure tungsten single crystals for the virgin condition and the carburized condition. Small anomalies are apparent in the carburized and quenched condition. The W-0.35%Ta single crystals disclose a strong peak in yield strength as a function of temperature, with a maximum of about 60,000 psi at 600°C. The maximum yield stress is about four times

Table 5

Residual Resistance Ratios ($R_{2980K}/R_{4.20K}$) of as Melted and Carburized Tungsten Single Crystals as a Function of Heat Treatment

<u>Specimen</u>	<u>Treatment</u>	<u>Residual Resistance Ratio</u>
W single crystal	"as melted"	12,320
" " "	quenched from 2200°C - after 15 min. hold	634
W single crystal	aged after quenching 700°C - 128 min.	2,742
W single crystal	aged after quenching 700°C - 512 min.	3,385
Carburized W single crystal	"as carburized"	930
" "	quenched from 2200 C - after 15 min. hold	39
" "	aged after quenching 700°C - 128 min.	190
" "	aged after quenching 700°C - 512 min.	223

Table 6

Tensile Properties of Tungsten Single Crystals

As Grown (Virgin)

<u>Test Temp.°C</u>	<u>0.2% Yield Stress (lb/in²)</u>	<u>Ult. Strength (lb/in²)</u>	<u>% Elong.</u>	<u>% R.A.</u>
100	46,200	53,000	0.7	0.0
200	44,000	53,500	23.8	89.0
300	22,800	43,500	21.5	86.0
400	12,200	32,000	108.0	82.0
500	7,150	27,200	80.0	80.0
600	4,900	24,800	114.0	81.0
700	6,500	24,000	124.0	100.0
800	5,000	18,700	75.0	100.0
1000	5,350	17,600	124.0	100.0
1200	5,300	17,000	128.0	100.0

As Grown (Quenched)

200	40,000	86,700	14.5	16.0
300	22,800	38,200	23.0	100.0
400	11,000	35,000	107.0	89.0
450	8,800	29,200	93.0	85.0
500	8,500	29,300	83.0	86.0
550	8,800	28,200	79.5	69.0
600	5,800	24,000	68.0	89.0
704	8,200	24,500	128.0	90.0
806	5,250	18,600	73.0	100.0

Carburized

400	11,000	38,000	57.7	100.0
600	9,700	32,000	71.3	100.0
800	9,800	25,400	92.6	100.0
1000	9,750	22,000	132.4	100.0

(cont'd.)

Table 6

Tensile Properties of Tungsten Single Crystals (cont'd.)

Carburized + Quenched
(2200°C)

<u>Test Temp.°C</u>	<u>0.2% Yield Stress</u> (lb/in ²)	<u>Ult. Strength</u> (lb/in ²)	<u>% Elong.</u>	<u>% R.A.</u>
300	65,000	74,000	9.5	63.0
146	66,000	72,500	9.0	72.0
500	70,000	72,000	7.6	63.0
600	57,600	63,500	5.1	42.0
788	66,000	72,000	5.2	30.0
800	57,600	59,100	9.6	63.0
1000	35,500	38,500	14.2	100.0
1200	20,000	21,800	22.0	100.0

Carburized + Quenched
(2450°C)

300	28,500	42,000	22.0	67.0
300	35,300	56,200	18.0	65.0
500	55,000	55,000	11.3	60.0
600	57,000	57,000	10.0	78.0
700	48,500	50,100	14.1	100.0
800	24,600	28,000	38.0	100.0
1000	14,150	21,000	79.0	100.0

Table 7
Tensile Properties of W-0.35%Ta Single Crystals

As Grown (Virgin)

<u>Test Temp.°C</u>	<u>0.2% Yield Stress (lb/in²)</u>	<u>Ult. Strength (lb/in²)</u>	<u>% Elong.</u>	<u>% R.A.</u>
30	98,050	144,500	12.0	14.4
100	57,700	110,000	12.0	27.2
200	46,000	71,150	20.9	77.7
300	23,800	39,900	97.5	82.5
350	14,000	37,350	105.7	84.0
400	14,550	34,650	ND	68.4
450	8,450	32,550	103.1	77.5
500	13,250	32,750	93.5	68.0
550	5,750	27,550	95.5	66.0
600	15,650	30,850	108.4	52.5
700	17,050	27,750	93.1	66.7
800	8,050	24,350	76.6	69.7
1000	5,700	23,400	66.4	ND
1200	7,000	20,000	49.0	ND
1200	7,600	17,000	33.0	ND
1400	5,700	10,700	70.0	ND
1600	2,900	6,100	64.0	ND

As Grown (Quenched)

RT	88,000	89,000	0.6	0.0
200	46,500	98,800	26.8	100.0
400	13,000	31,200	49.0	100.0
610	23,100	36,400	54.0	100.0

Carburized

RT	70,150	96,950	4.3	2.5
100	53,250	116,900	10.3	16.9
200	42,450	72,200	16.6	29.9
300	23,200	48,000	42.1	81.3
400	19,900	36,100	56.9	70.1
500	11,500	34,200	67.5	63.5
550	15,200	32,000	59.0	59.7
600	16,350	31,200	58.0	64.0
700	16,750	32,000	68.6	70.1
800	6,100	26,100	70.3	66.2
1000	9,400	24,000	62.4	ND
1200	8,700	24,300	45.9	ND
1200	9,400	20,000	50.0	ND
1400	8,100	14,000	63.0	ND
1600	5,350	8,350	63.0	ND

ND - not determined

(continued)

Table 7
Tensile Properties of W-0.35%Ta Single Crystals (Cont'd.)

Carburized + Quenched
(2200°C)

<u>Test Temp.°C</u>	<u>0.2% Yield Stress</u> (lb/in ²)	<u>Ult. Strength</u> (lb/in ²)	<u>% Elong.</u>	<u>% R.A.</u>
RT	74,000	76,500	6.0	7.5
200	43,000	60,500	28.0	100.0
300	16,500	42,500	88.0	79.0
300	23,100	ND	ND	ND
400	44,500	55,500	38.4	70.0
500	54,000	60,200	18.0	48.0
600	63,500	67,500	12.4	41.0
700	52,000	57,500	33.3	82.0
820	38,000	48,500	54.0	64.0
1030	11,600	30,000	85.8	100.0

Carburized + Quenched
(2450°C)

300	82,500	85,500	18.9	70.0
300	92,500	94,000	21.0	60.0
400	62,000	62,000	13.8	61.0
500	49,000	50,000	9.2	50.0
600	55,000	57,000	12.0	56.0
700	56,000	63,000	10.7	53.0
1000	27,200	31,500	84.7	100.0

ND - not determined

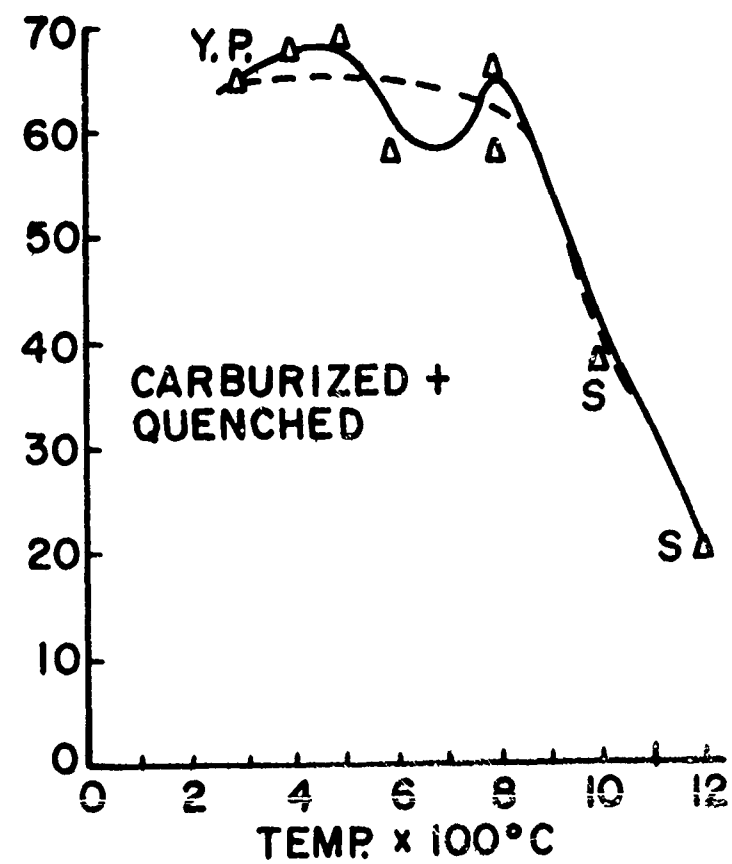
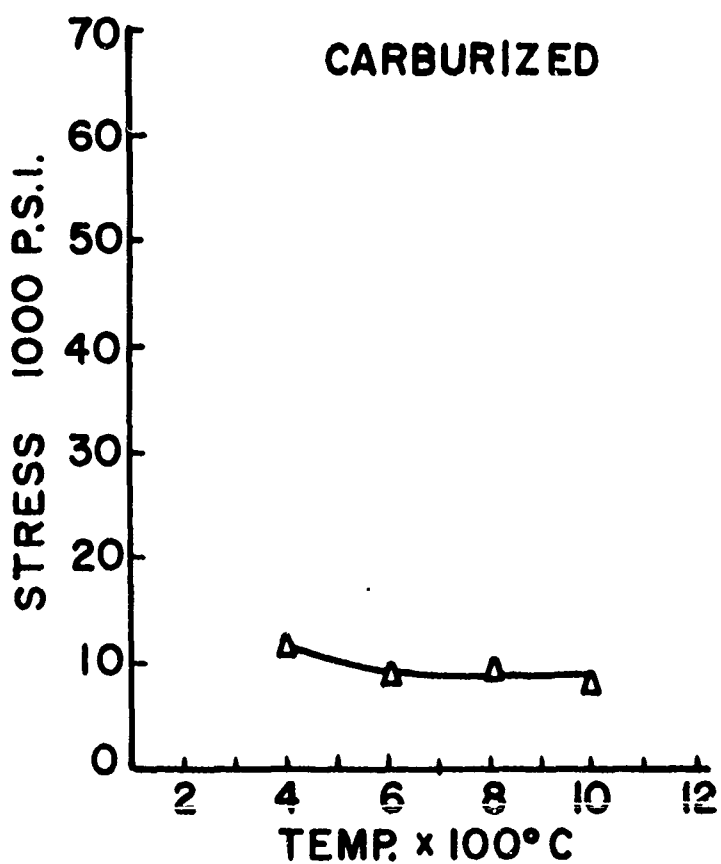
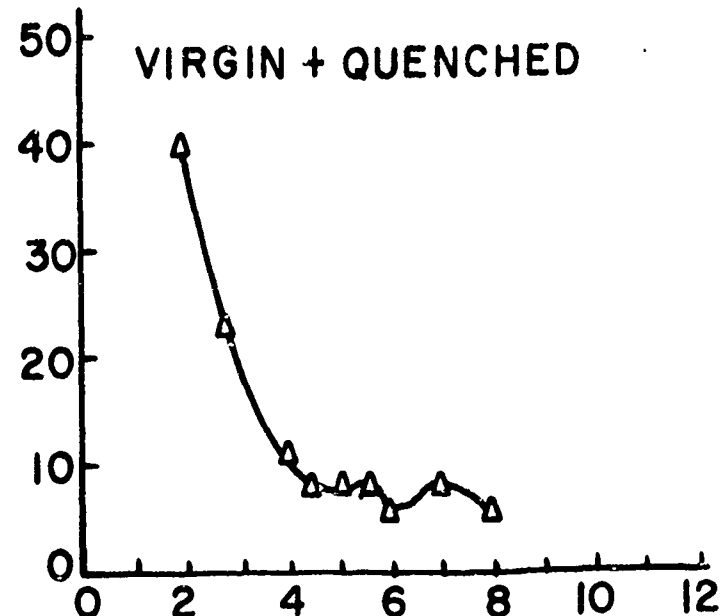
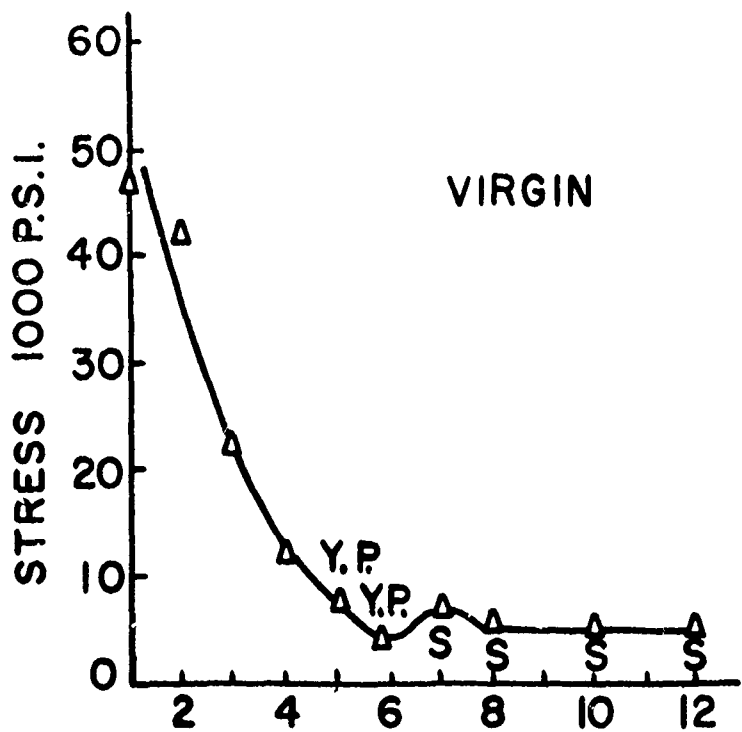


FIG. 17 0.2% YIELD STRESS OF VARIOUSLY TREATED TUNGSTEN SINGLE CRYSTALS.

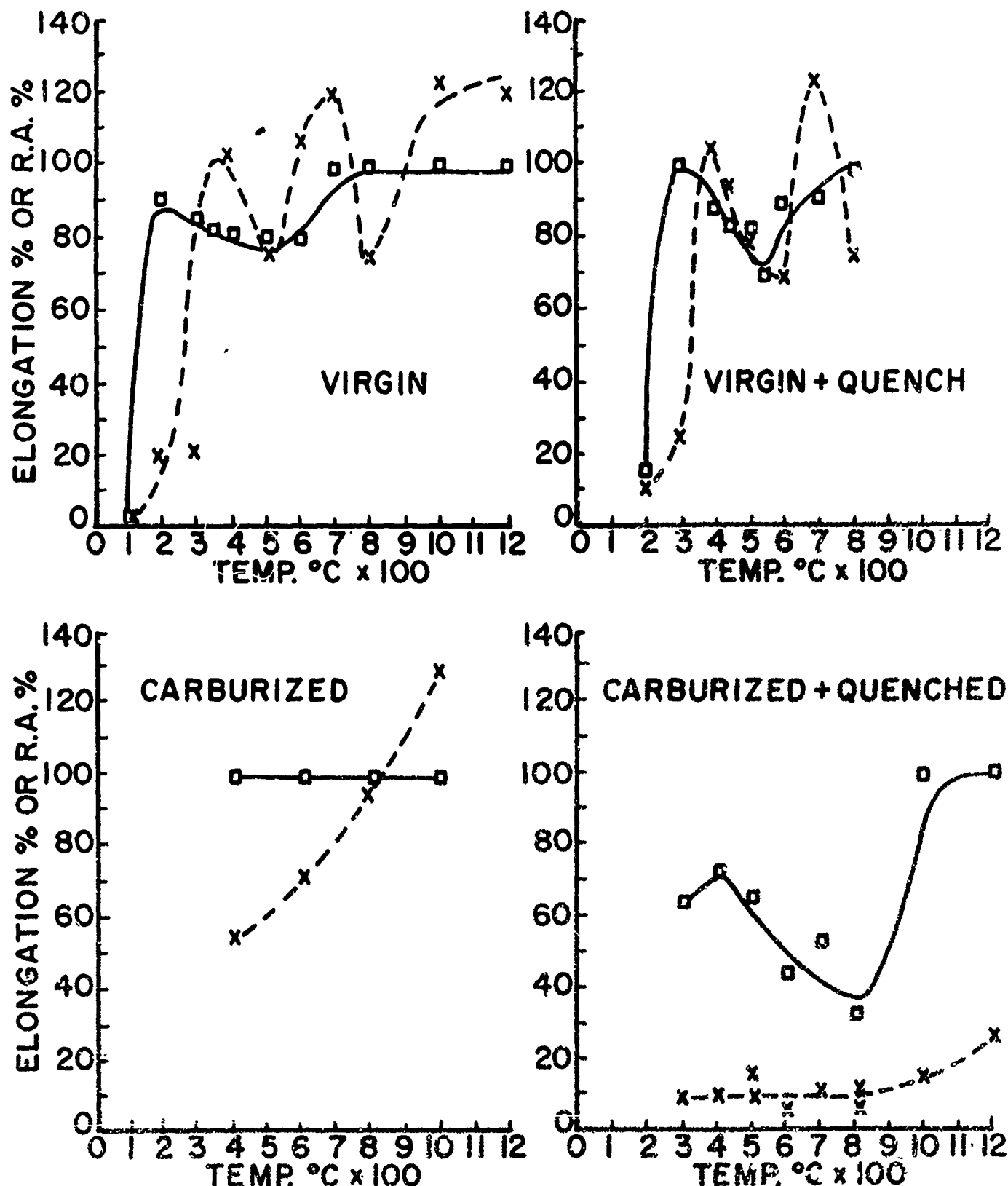


FIG. 18 DUCTILITY OF PURE SINGLE CRYSTAL TUNGSTEN
FOR VARIOUS CONDITIONS, (x---x ELONG., o—o % R.A.)

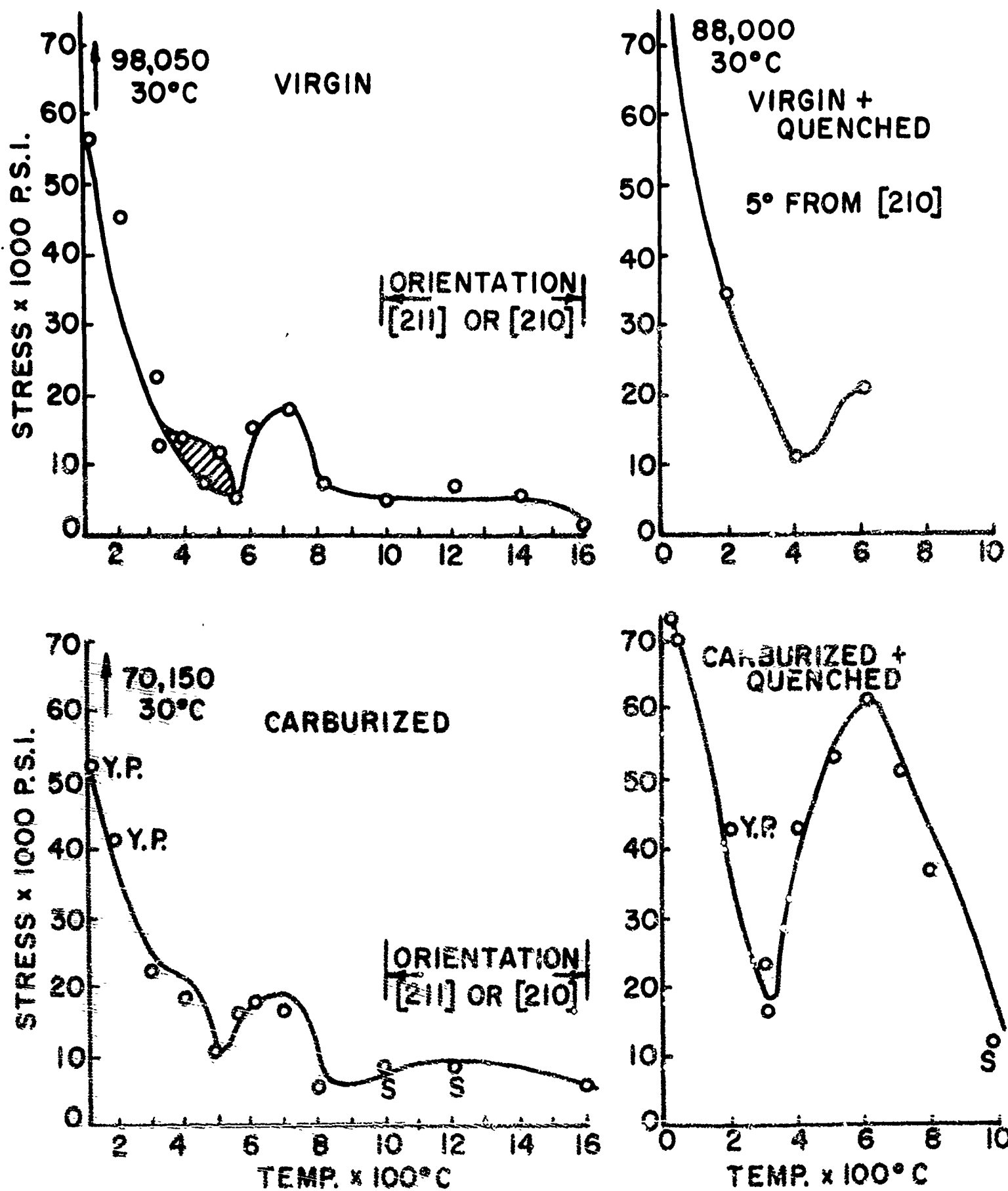


FIG. 19 0.2% YIELD STRESS OF VARIOUSLY TREATED W-0.35% Ta SINGLE CRYSTALS.

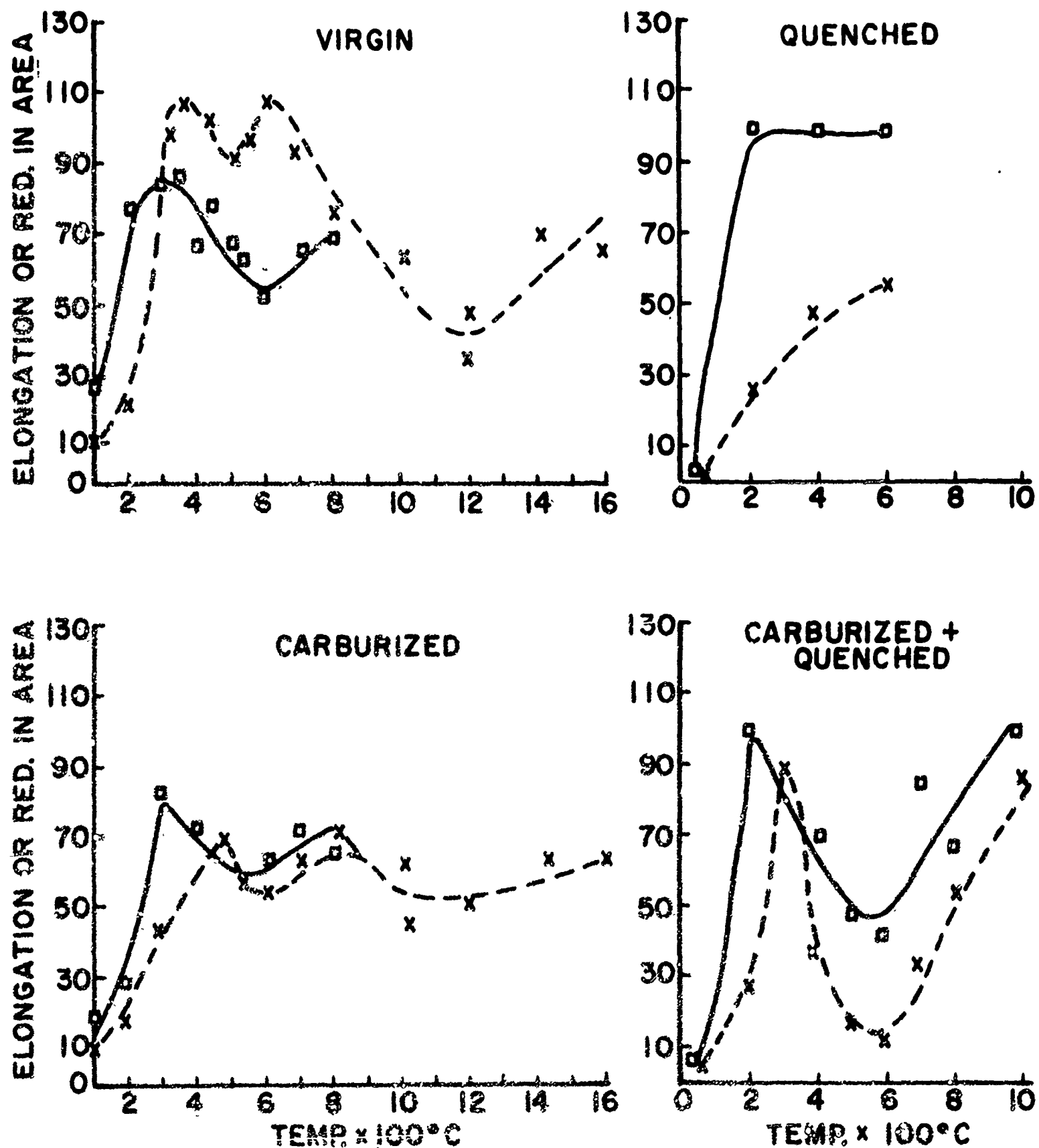


FIG. 20 DUCTILITY OF THE VARIOUSLY TREATED W-0.35% Ta SINGLE CRYSTALS. (x---x % ELONG.; □—□ % R.A.)

that of the virgin or carburized virgin alloy crystals.

Anomalies (peaks and valleys) are also apparent in both the %R.A. and % elongation curves of the virgin and the carburized virgin crystals, respectively (Fig. 20). The data for the quenched virgin condition are too few to give a definite pattern. A pronounced broad minimum in both ductility parameters is noted for the carburized and quenched condition corresponding with the strong yield stress peak.

c) Effect of Quenching Temperature

The different temperature dependencies of the yield stress of the carburized and quenched tungsten and W-0.35%Ta single crystals led to an investigation of the effect of quenching temperature on tensile properties. A constant yield stress from 300 to 600°C is evident for the carburized tungsten after a 2200°C quench (Fig. 17), while a yield stress peak is apparent for the carburized alloy single crystals (Fig. 19). To better understand this difference in behavior, crystals were quenched from 2450°C after a 30 minute hold at quenching temperature. The effect of this quench on the tensile properties of the materials is shown in Fig. 21. A yield stress peak with a maximum at 600°C rather than a plateau is now evident in pure tungsten. On the other hand, the yield stress of the alloy is greatly increased in the temperature region from 300 to 500°C, but the temperature dependence of the yield stress above 500°C is practically unaltered. The minimum in yield stress which occurred at 300°C after the 2200°C quench is now observed at 500°C.

A comparison of the magnitude of the yield stress from 300 to 1000°C of carburized pure W single crystals quenched from 2450°C with carburized W-0.35%Ta single crystals quenched from 2200°C is made in Fig. 22. A close similarity is seen between the data.

A well defined minimum in the % elongation curve is noted. Overall, this material exhibits greater ductility after the 2450°C quench than after the 2200°C quench. The ductility of the W-0.35%Ta is not as much affected. A strong decrease in both % R.A. and % elongation is noted only at 300°C.

d) Aging Effects in W-0.35%Ta Single Crystal

Aging effects in tungsten single crystals were indicated by the residual resistance ratio measurements of quenched virgin crystals and quenched carburized crystals reported in Table 5. Aging effects in W-0.35%Ta single crystals were investigated by

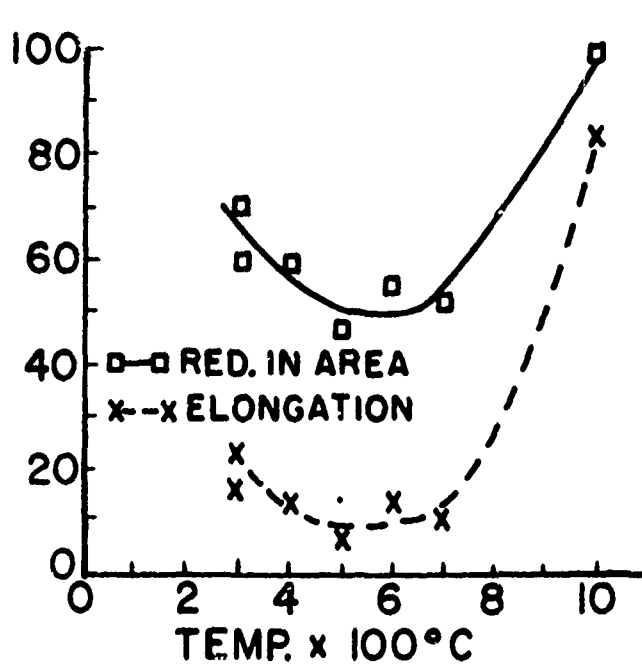
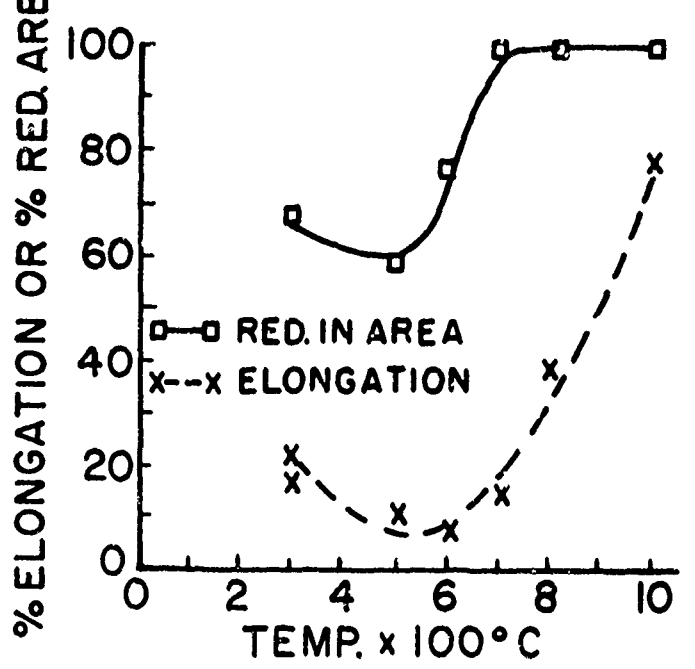
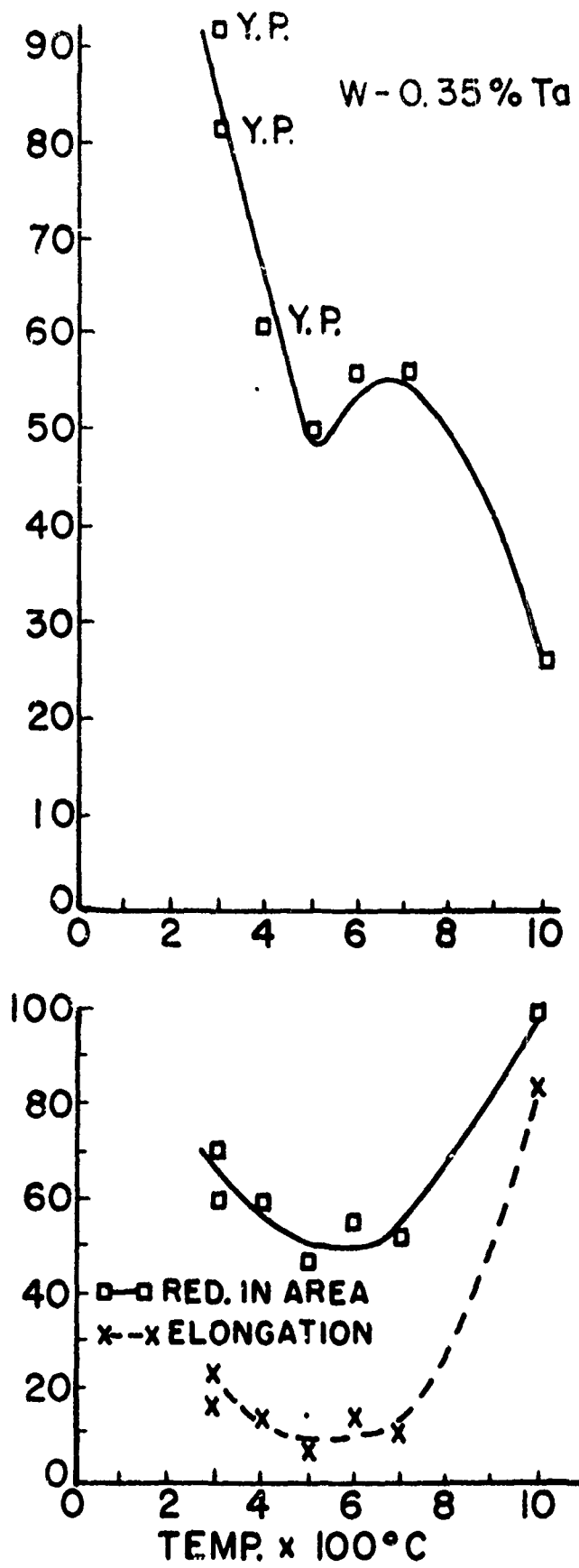
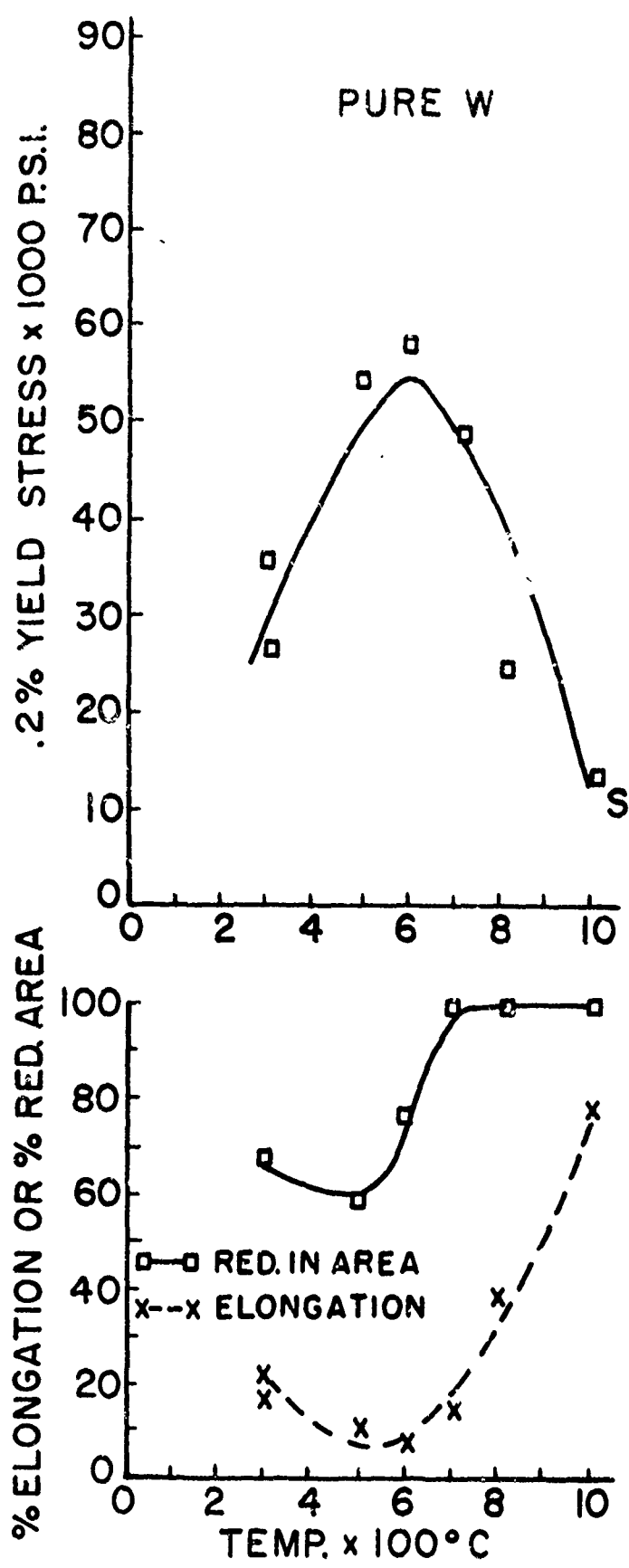


FIG. 21 EFFECT OF 2450°C QUENCH ON TENSILE PROPERTIES OF CARBURIZED SINGLE CRYSTALS OF PURE W AND W-0.35% Ta

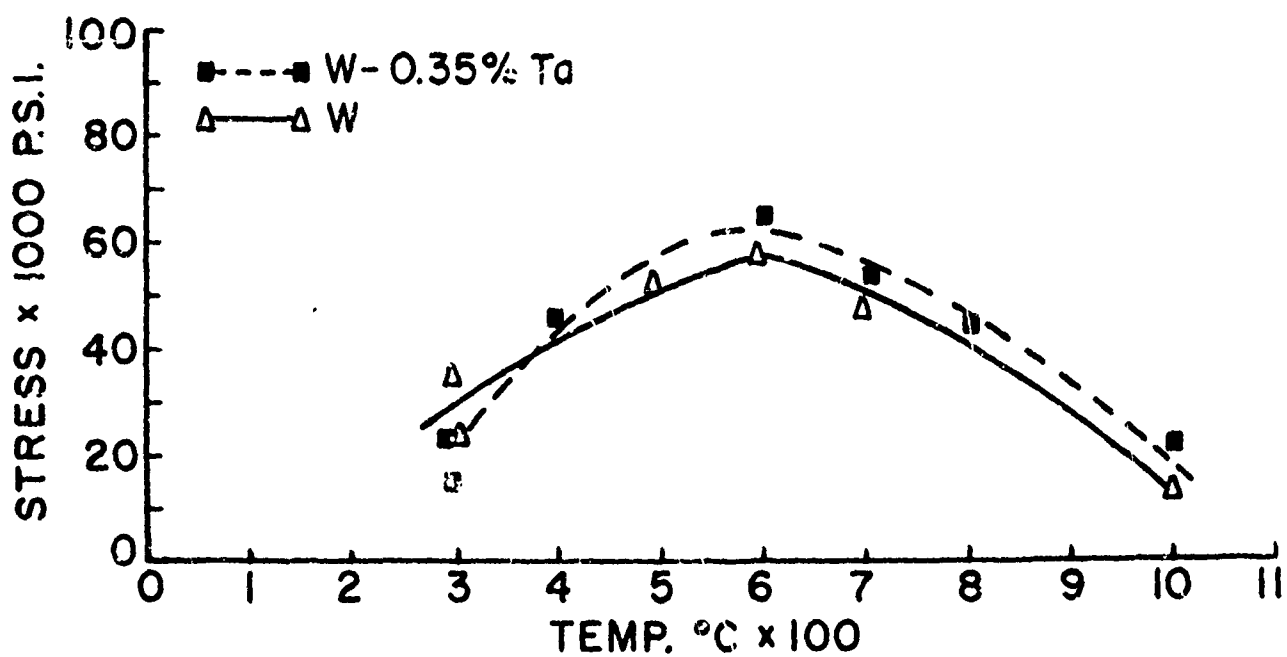


FIG. 22 COMPARISON OF THE 0.2% YIELD STRESS PEAK OF CARBURIZED AND QUENCHED SINGLE CRYSTALS OF TUNGSTEN QUENCHED FROM 2450°C AND W-0.35% Ta QUENCHED FROM 2200°C.

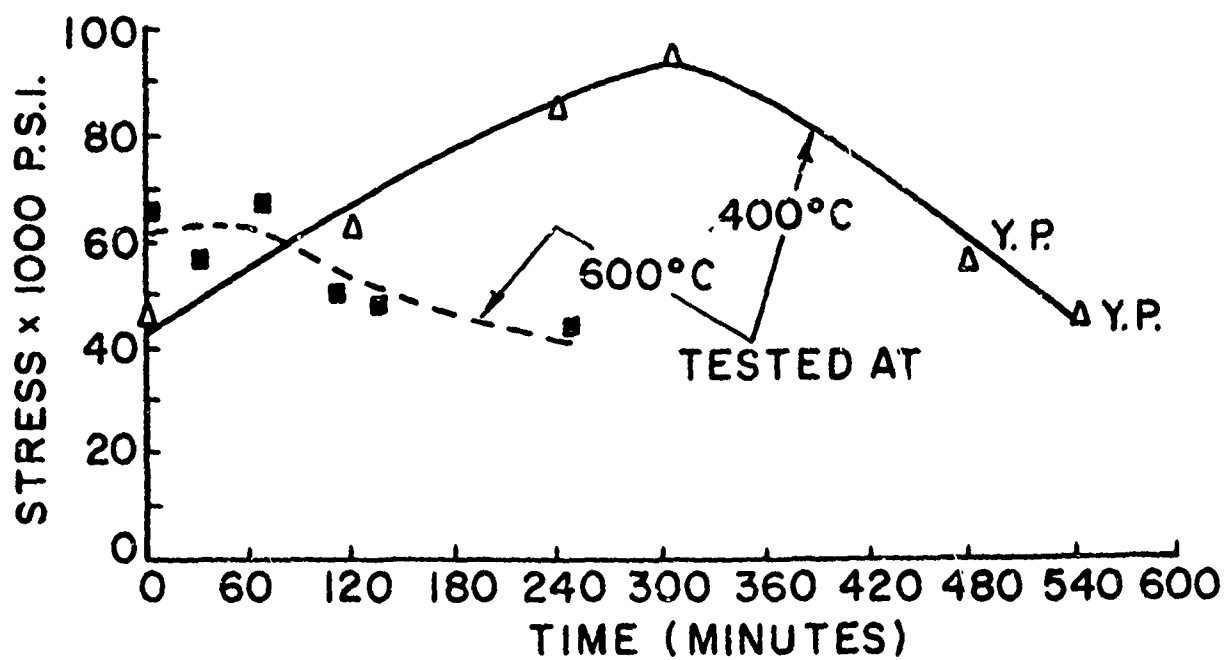


FIG. 23 EFFECT OF ISOTHERMAL ANNEALS ON THE YIELD STRESS OF CARBURIZED AND QUENCHED W-0.35% Ta SINGLE CRYSTALS.
 (Δ—Δ ANNEALED 400°C; ■—■ ANNEALED 700°C)

yield stress measurements on carburized and quenched crystals, rather than by residual resistance ratio measurements, since large residual resistance ratios cannot be realized in the alloy crystals because of the 0.35%Ta addition. Carburized and quenched crystals were annealed at 400°C and 700°C, respectively, for different aging times. Tensiles annealed at 400°C were tested at 400°C and tensiles annealed at 700°C were tested at 600°C. The results are shown in Fig. 23. As is evident from this figure, a maximum of about 95,000 psi occurs after 320 minutes for the 400°C anneal. The maximum yield strength of specimens annealed at 700°C is somewhat lower (about 60,000 psi) than for the 400°C anneal (95,000 psi) and occurs practically within the time required to bring the specimens to annealing temperature (~ 30 min).

e) Strain Aging Effects in W-0.35%Ta Single Crystals

The effect of aging on prestrained (1%) W-0.35%Ta single crystals was investigated for all but the quenched virgin condition. The effect of aging on the stress-strain curves of the various specimens have been summarized in Fig. 24. Specimens were tested at 300°C. The difference between the proportional limit and the terminal flow stress of the preceding test was used as a measure of the strain aging effect. This strain aging parameter is designated $\Delta \delta$ in Fig. 25, and the magnitude of the yield drop as Δy and is also plotted in Fig. 25.

As is evident from Fig. 24, no strain aging occurred in any of the crystals tested after an 80 min. anneal at 300°C. Annealing at 600°C resulted in a discontinuous yield point in all crystals tested. The magnitude of the yield drop is 2500-4500 psi. The strain aging parameter $\Delta \delta$ is about the same for both the virgin and the carburized virgin condition. An increase of about 35,000 psi for $\Delta \delta$ was obtained for the carburized and quenched condition.

The yield point return in carburized and quenched crystals after various isochronal anneals (80 minutes) was further studied. For this purpose, two additional prestrained (1%) carburized and quenched specimens were annealed at 400 and 500°C, respectively, and then tested at 300°C. An indication of a yield point was observed at 400°C and a pronounced yield point occurred after the 500°C anneal; Fig. 25. The specimens annealed at 600°C and tested at 300°C were reannealed at 600°C and then tested at 600°C. Serrations were now evident in the carburized and quenched specimen, but were not observed in the as grown specimen and the carburized specimen.

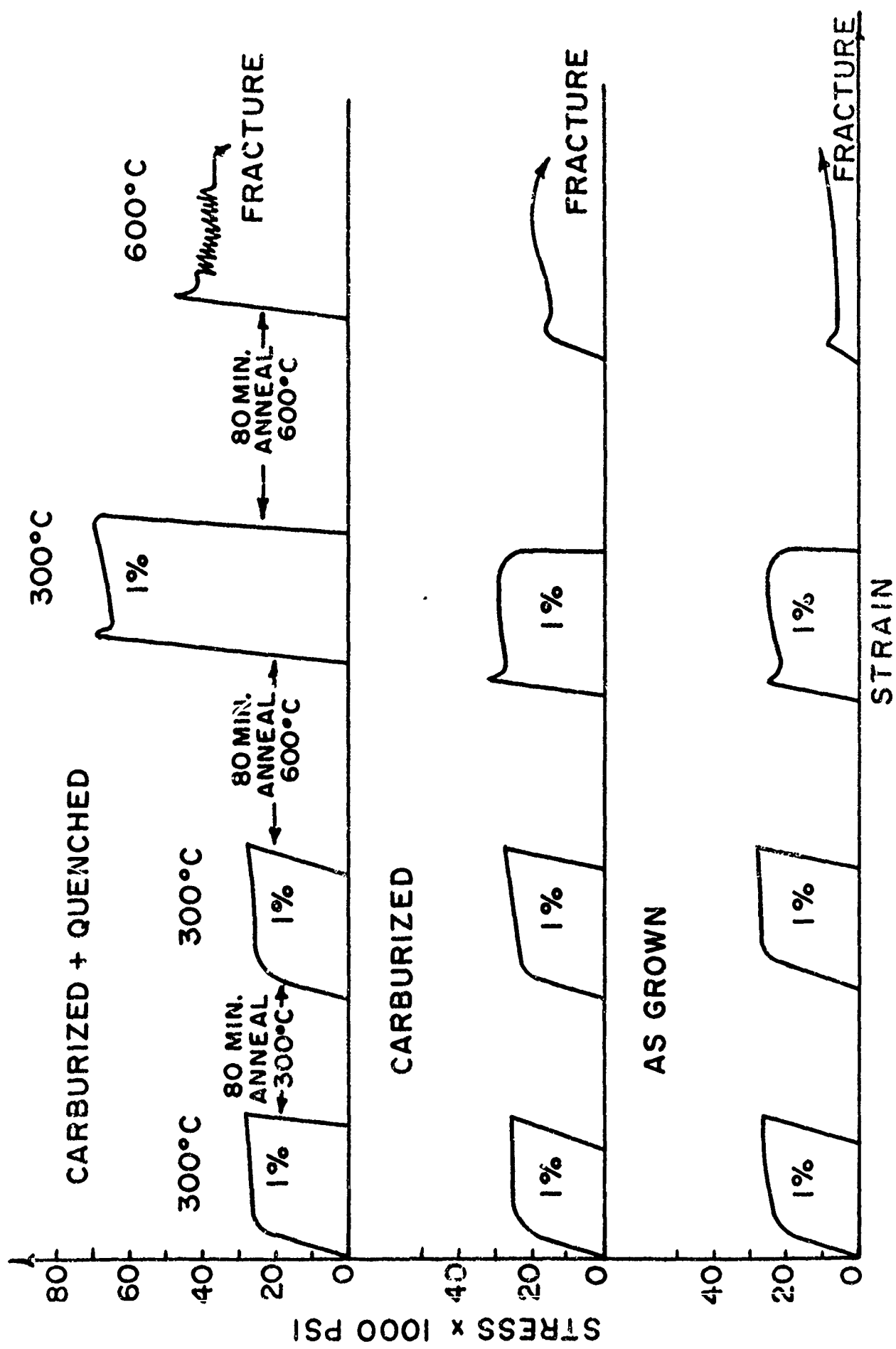


FIG. 24 STRAIN AGING EFFECTS IN VARIOUSLY TREATED W-0.23% Ta SINGLE CRYSTALS TESTED AT 300°C AND 600°C.

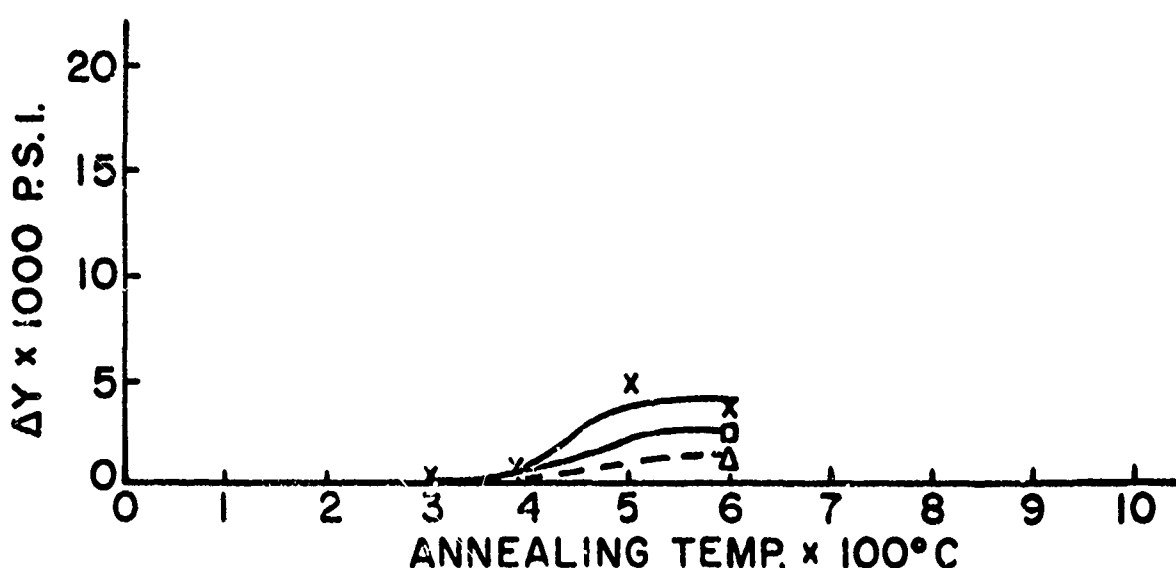
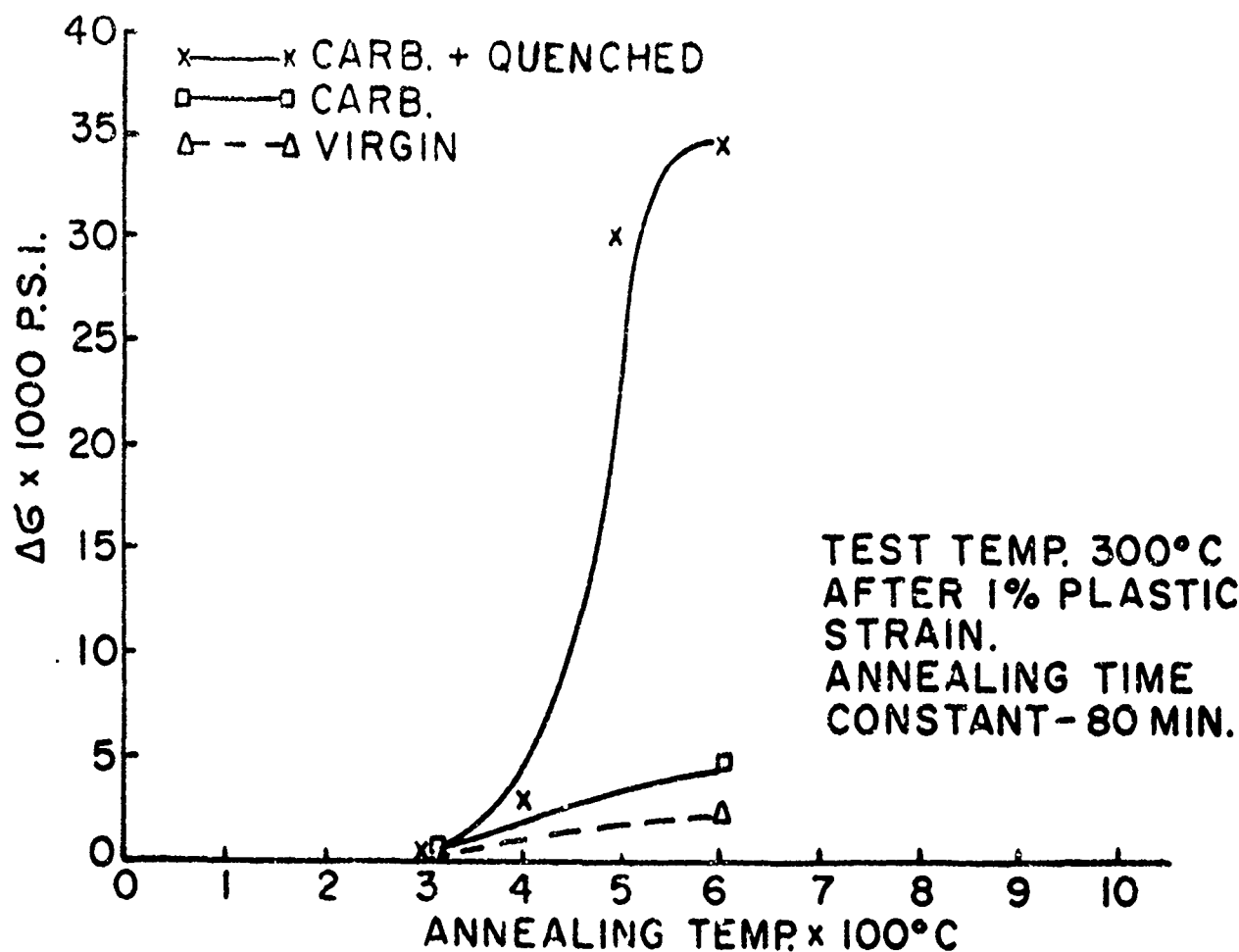


FIG. 25 EFFECT OF ISOCRONAL ANNEALING (80 MIN.)
ON ΔY AND ΔG OF PRESTRAINED (1%) W-0.35%
Ta SINGLE CRYSTALS IN VARIOUS CONDITIONS
AND TESTED AT 300°C.

4. Optical and Electron Metallography

Since carbide precipitation was clearly indicated in the quenched and aged crystals, fractured tensile specimens of the two materials were constantly examined by optical microscopy for the appearance of precipitates. Precipitates in carburized and quenched specimens were evident in low concentrations only in tensiles tested at 1000°C and high temperatures. Such precipitates in pure W and W-0.35%Ta are shown in Figs. 26A and B, respectively.

Transmission electromicrographs of carburized tungsten and W-0.35%Ta single crystals are shown in Figs. 27A and B, respectively. The occurrence of carbide precipitation on dislocations is inferred from the variation in contrast.

B. Worked and Recrystallized Pure Tungsten and W-0.35%Ta Single Crystals

In a previous investigation (4) the following results were obtained:

1. A dilute (0.35%) substitutional alloying addition of Ta increases the yield stress of tungsten single crystal by about 2000-3000 psi in the temperature range 600-1200°C.
2. The addition of 0.35% Ta increased the recrystallization temperature of heavily worked single crystals by approximately 400°C (from 1200°C to 1600°C).
3. Recrystallization of heavily worked tungsten single crystals resulted in a material with a large grain size (0.55 mm avg.) which had a yield stress similar to that of the single crystals.
4. Recrystallization of heavily worked W-0.35%Ta single crystals, likewise resulted in a material with a large grain diameter (0.12 mm avg.) which had a substantially higher yield stress (approx. 10,000 psi) than the recrystallized tungsten single crystals.

In the light of the large effect of carburizing and quenching on the mechanical properties of single crystals it was important to extend this investigation to evaluate also the effect of carbon on recrystallization temperature and the tensile properties of the worked and recrystallized crystals.

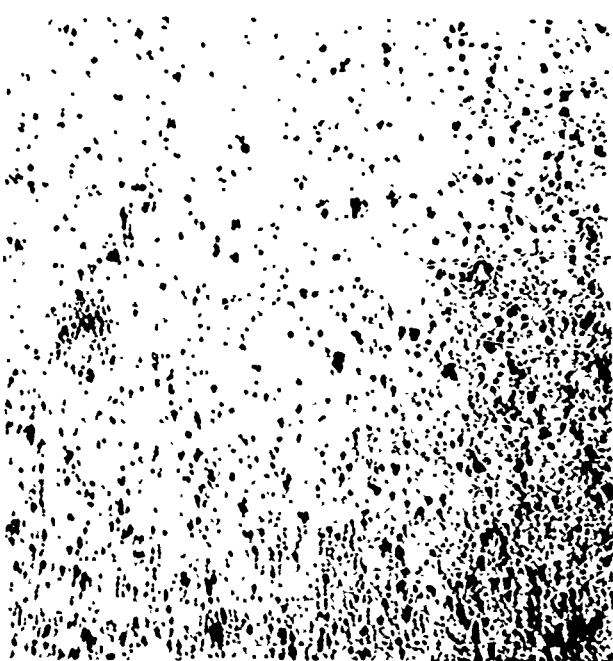


Fig. 26A - Carburized Plus
Quenched Pure W Single Crystal,
Tested 1200°C - 500X



Fig. 26B - Carburized Plus
Quenched W-0.35% Ta Single
Crystal Tested 1000°C - 500X



Fig. 27A - Transmission Elec-
tron Micrograph of a Carbu-
rized Single Crystal Tungsten
21,000X



Fig. 27B - Transmission Elec-
tron Micrograph of a Carbu-
rized W-0.25% Ta Single
Crystal - 20,000X

1. Preparation of Specimens and Test Procedure

Sections (2 to 3 in. long) of single crystals were carburized by the method described earlier. Some of the carburized sections were quenched prior to working to study the effects of dynamic age hardening during working. Other sections were quenched after working (recrystallized during quenching) to study the effect of grain boundaries. The working procedure consisted of encasing these crystal sections in stainless steel tubing prior to rolling (approximately 50% R.A.).

Preheat temperatures were 700°C and 1300°C, respectively. The stainless steel cladding was removed after rolling by dissolving in aqua regia, after which test specimens were fabricated by grinding. Finally, about 0.010 to 0.020 inch of the diameter of the ground specimens was removed by electropolishing.

2. Recrystallization Temperature of W-0.35%Ta

Two conditions were evaluated: (1) As carburized and (2) carburized and quenched. The recrystallization response was followed by metallographic techniques and by hardness measurements. Specimens were annealed for 30 minutes in vacuum. The results are presented in Fig. 28. Recrystallization was 100% complete in all cases after annealing at 1600°C.

It is also apparent from the data in Fig. 28 that quenching the carburized crystals prior to rolling resulted in an age hardening effect during annealing, but there is no significant increase in the recrystallization temperature beyond that obtained by a 0.35%Ta addition. The data in Fig. 28 were obtained for a crystal carburized to a carbon level of approximately 80 ppm by weight.

3. Tensile Test Results

a) As Worked Crystals

Tensile data were obtained on pure W and W-0.35%Ta single crystals which had been carburized and quenched first and then rolled (approx. 50% R.A.) at 700°C and 900°C, respectively. The results are presented in tables 8 and 9 and plotted in Fig. 29 which also includes earlier data (4) on worked (from 1100°C) pure W and W-0.35%Ta single crystals. It is apparent that a significant increase in yield strength has been achieved at the expense of ductility, by carburizing and then quenching prior to working.

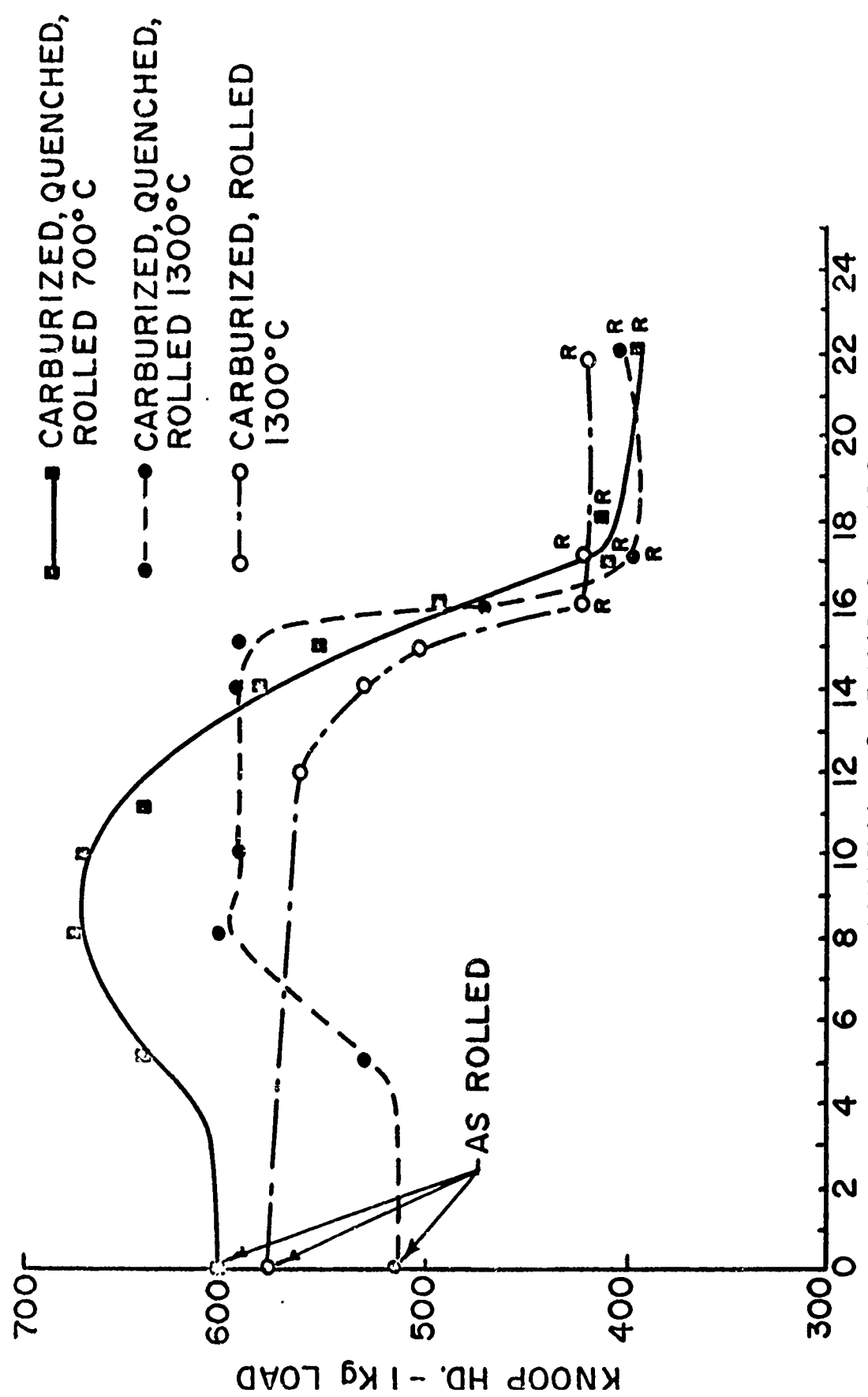


FIG. 28 RECRYSTALLIZATION RESPONSE OF ROLLED W-0.35% Ta ALLOY SINGLE CRYSTALS (~50% R.A.).

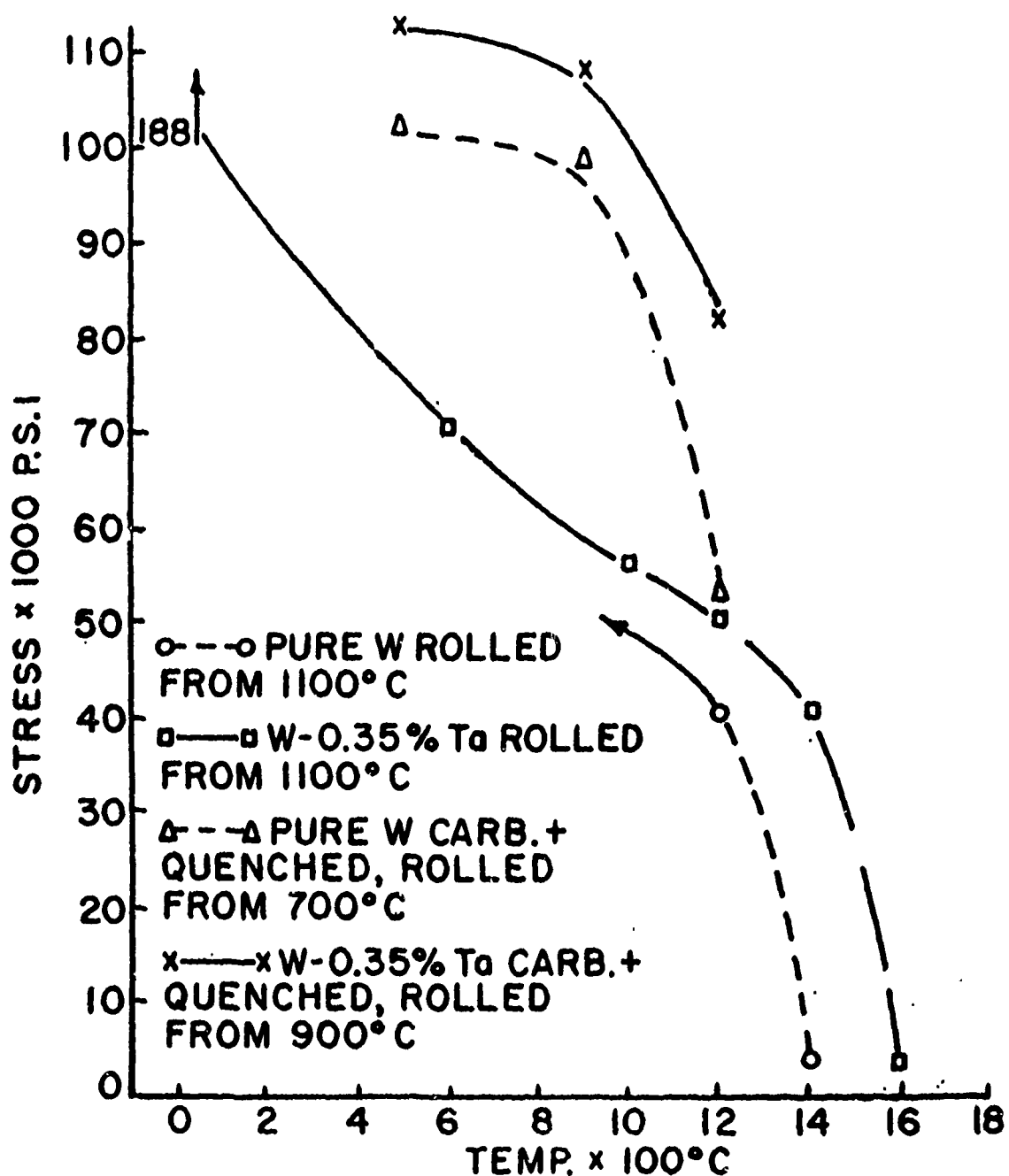


FIG. 29 EFFECT OF CARBURIZING AND QUENCHING ON THE 0.2% YIELD STRESS OF ROD ROLLED (~50% R.A.) TUNGSTEN AND W-0.35% Ta SINGLE CRYSTALS.

Table 8

Tensile Properties of Carburized and Quenched
Single Crystal Tungsten, Rolled at 700°C to 50% R.A.

<u>Test Temp. °C</u>	<u>0.2% Yield Stress, psi</u>	<u>Ult. Strength, psi</u>	<u>% Elong.</u>
600	103,000	105,000	1.0
900	98,000	99,000	7.0
1200	53,000	54,500	20.3

Table 9

Tensile Properties of Carburized and Quenched W-0.35%Ta
Rolled at 900°C to 50% R.A.

<u>Test Temp. C</u>	<u>0.2% Yield Stress, psi</u>	<u>Ult. Strength, psi</u>	<u>% Elong.</u>
600	114,000	115,000	0.0
900	109,000	110,000	7.0
1200	83,500	85,000	7.0

b) Worked and Recrystallized Crystals

Polycrystalline specimens were produced from the pure W, the pure alloy and the carburized alloy single crystals by annealing at 1600°C or quenching from 2200°C after rod rolling to a 50% R.A. from preheat temperatures of 1100°C. The grain sizes obtained in the various crystals by the heat treatments are listed below in Table 10.

Table 10

Grain Size of Carburized and Quenched W and W-0.35%Ta
Rolled to 50% R.A. and Recrystallized

<u>Material</u>	<u>Heat Treatment</u>	<u>Mean Grain Size, mm</u>
Carburized Tungsten	Quenched, 2200°C	0.25
W-0.35%Ta	Annealed, 1600°C	0.12
W-0.35%Ta	Quenched, 2200°C	0.55
Carburized, W-0.35%Ta	Quenched, 2200°C	0.35

A comparison of the tensile properties of pure carburized and quenched single crystal tungsten with the carburized worked and recrystallized tungsten crystal, respectively, is shown in Fig. 30; Table 11. It is apparent that the yield strength (over the temperature range compared) of the two materials is similar except for a somewhat greater peak in yield strength at about 600°C in the recrystallized crystals. The ductility of the polycrystalline material is lower in the temperature region below 700°C, Fig. 30.

Table 11

Tensile Properties of Carburized Polycrystalline Tungsten
Made from Single Crystal (quenched after rolling)

Test Temp. °C	0.2% Yield Stress, psi	Ult. Strength, psi	Elong.	R.A.	%	%
400	70,000	77,000	3.0	20		
500	68,000	74,500	2.5	0		
600	74,500	76,600	1.0	0		
700	70,500	78,500	4.0	12		
1000	36,800	38,200	24.0	100		
1200	23,000	23,500	36.0	100		

The yield strength of the alloy crystals is shown in Fig. 31. It is seen that the recrystallized W-0.35%Ta, having an average grain size of 0.12 mm, has greater strength than the pure single crystal alloy. However, the yield strength of quenched (Table 12) alloy crystals with the larger grain size (0.55 mm) below 700°C is similar to that of the single crystal material and more like the smaller grain size (0.12 mm) W-0.35%Ta above 700°C.

Table 12

Tensile Properties of Polycrystalline W-0.35%Ta made from
Single Crystal (quenched after rolling)

Test Temp. °C	0.2% Yield Strength, psi	Ult. Strength, psi	Elong.	R.A.	%	%
200	34,000	58,000	8.0	12.0		
300	19,600	43,500	25.0	39.0		
400	12,000	36,500	21.0	71.0		
550	19,000	27,000	13.0	90.0		
600	21,000	23,200	22.0	100.0		
700	16,500	23,000	25.0	100.0		
800	15,300	28,000	25.0	100.0		
1000	14,600	30,100	25.0	100.0		

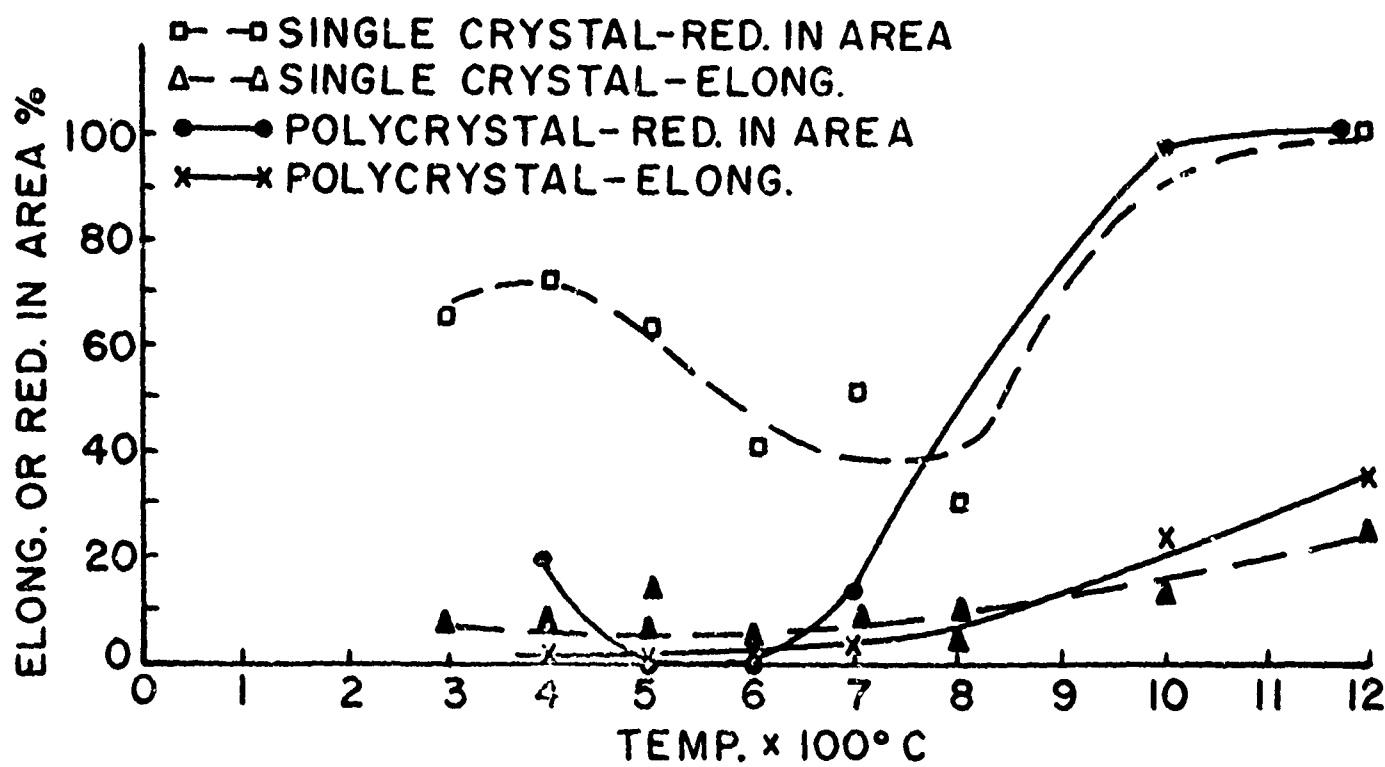
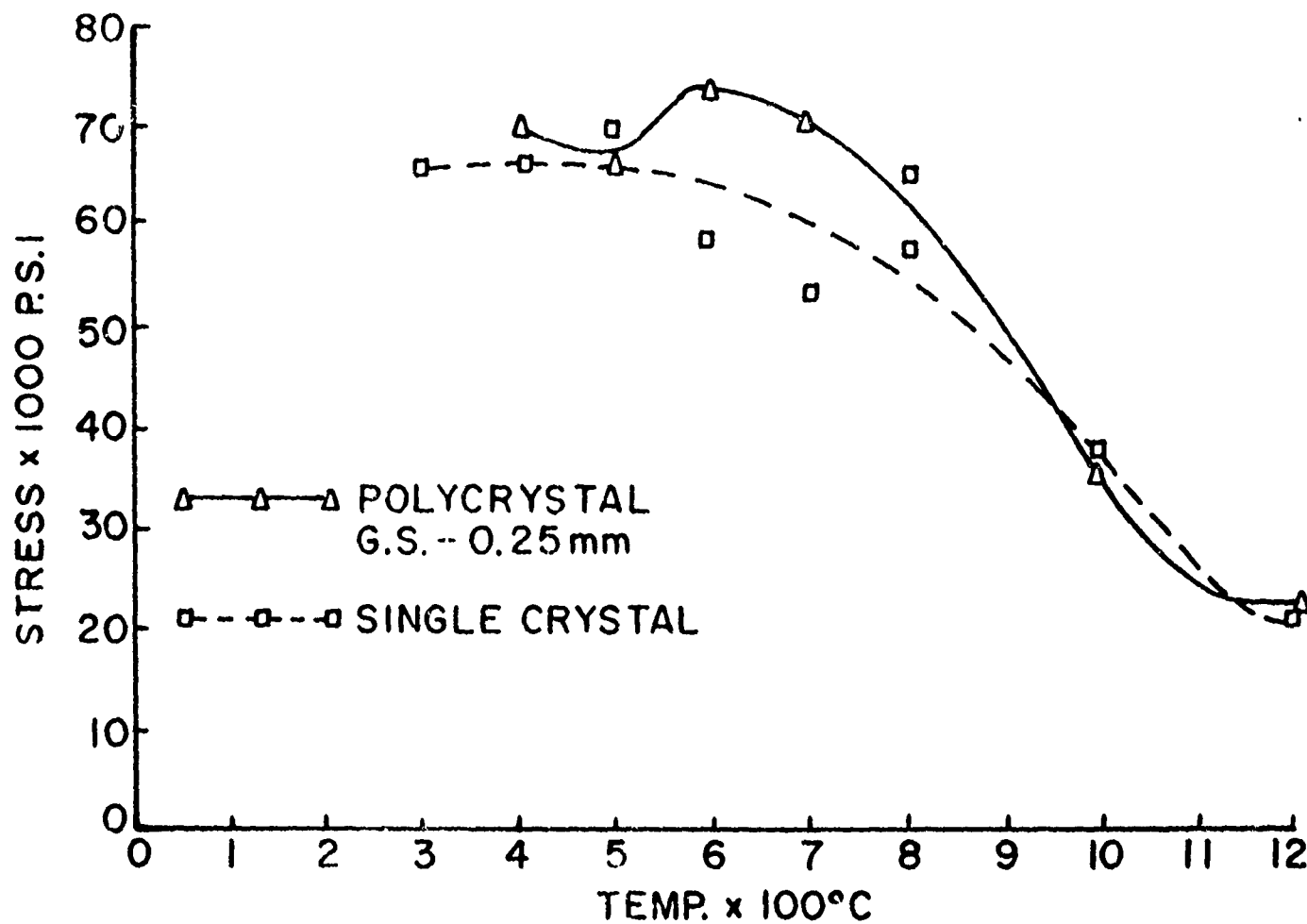


FIG. 30 COMPARISON OF A 2200°C QUENCH ON THE TENSILE PROPERTIES OF SINGLE CRYSTAL AND POLYCRYSTALLINE TUNGSTEN.

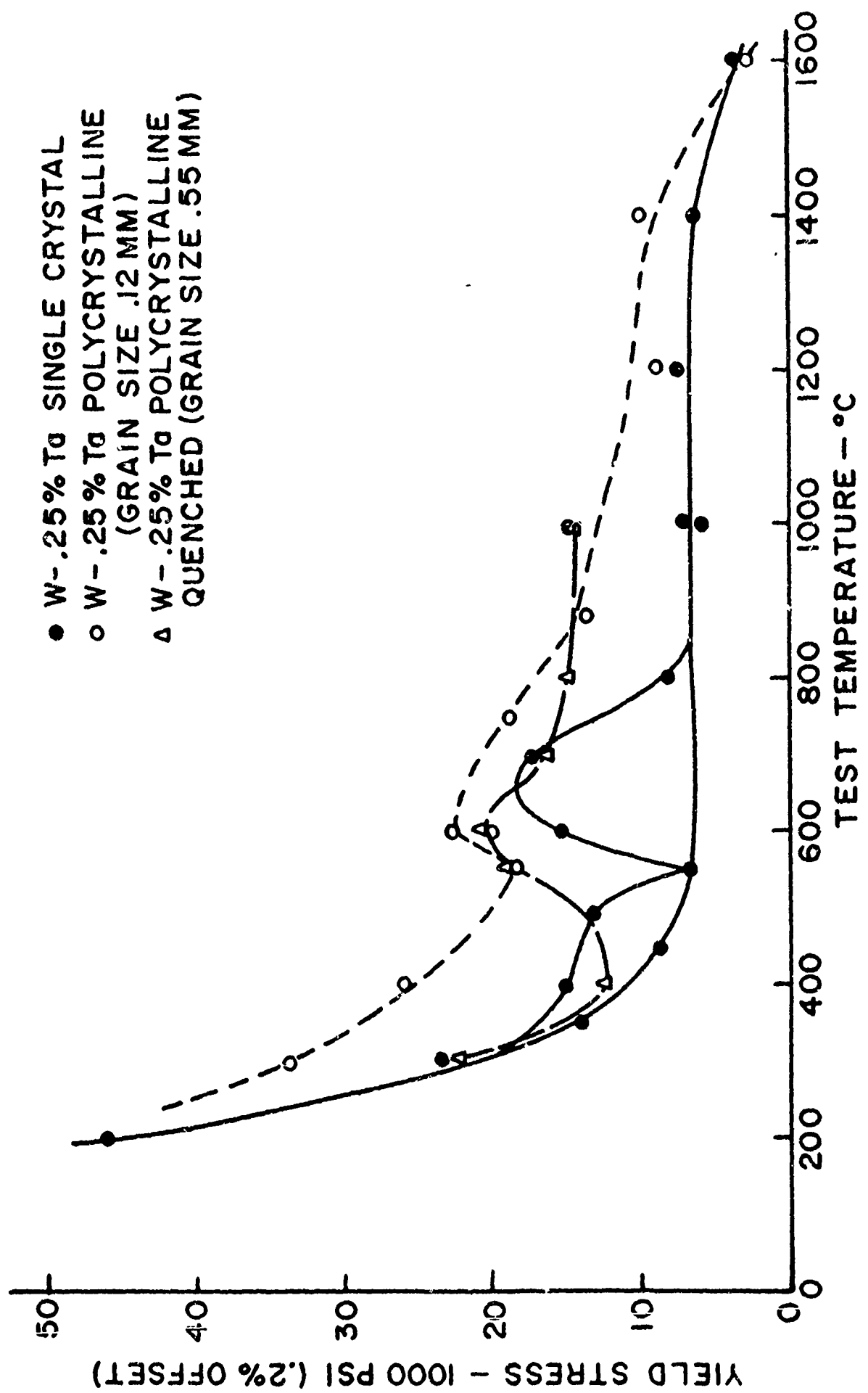


FIG. 31 2% YIELD STRESS OF ALLOY SINGLE CRYSTAL AND POLYCRYSTALLINE ALLOY.

The tensile data for carburized and quenched single and polycrystalline (0.36 mm avg. g.s.) alloy crystals is plotted in Fig. 32; Table 13. The results show that the carburized and quenched polycrystalline alloy crystals have a higher yield strength than the carburized and quenched single crystals over the entire test temperature region. As discussed previously, carburizing and quenching improves the yield strength of the single crystals.

Table 13

Tensile Properties of Carburized Polycrystalline W-0.35%Ta
made from Single Crystal (quenched after rolling)

Test Temp. °C	0.2% Yield Stress, psi	Ult. Strength, psi	Elong. %	R.A. %
250	82,000	84,500	3.0	4.0
300	76,000	76,500	16.5	21.0
400	79,000	91,000	2.0	5.0
600	79,000	89,000	4.0	5.0
800	67,500	76,500	2.0	3.0
1200	20,600	28,300	27.0	100.0

The ductility of the alloy crystals is also summarized in Fig. 32. Generally, it can be said that the ductility of the larger grain carburized and quenched polycrystalline alloy (0.36 mm dia.) is considerably lower than that of the carburized and quenched alloy single crystals. Again, it is evident from the microstructures of carburized single and polycrystalline tensile specimens (Fig. 33) that carbide precipitation is responsible for the large increase in yield strength.

C. Discussion

This investigation has disclosed that quench-aging of a carburized pure or alloy tungsten single crystal is an effective means of greatly improving strength properties over the temperature region of 300-1000°C. In the following some effects caused by quench-aging are briefly discussed.

1. Strengthening Mechanism

The limited solubility of carbon in tungsten (27) is in itself sufficient reason to consider carbide precipitation as a means of strengthening tungsten. The following results can be interpreted in terms of carbide precipitation or the interaction of dislocations with precipitates.

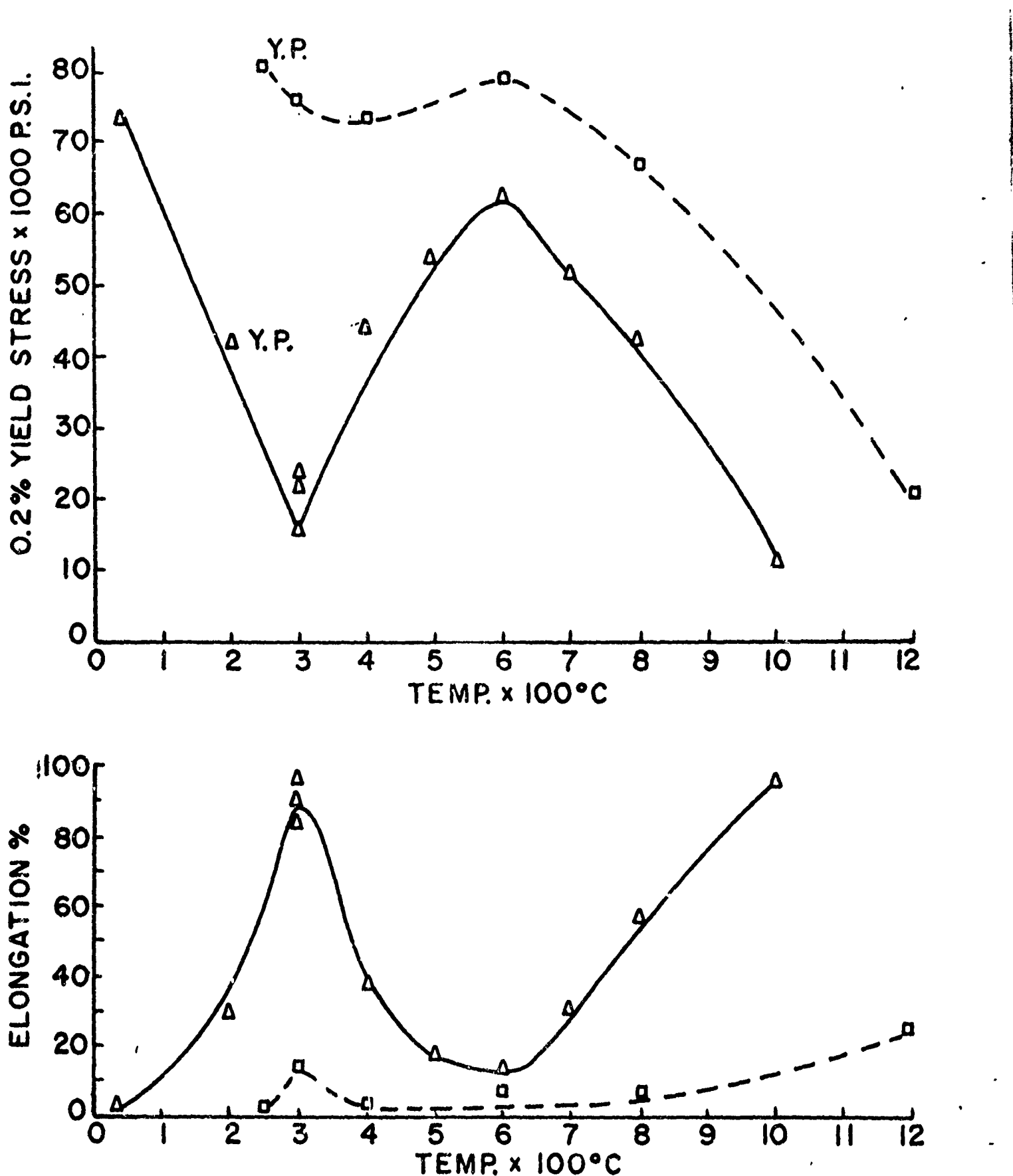


FIG. 32 COMPARISON OF 0.2% YIELD STRESS AND % ELONGATION OF CARBURIZED AND QUENCHED POLYCRYSTALLINE (G.S.- 0.36mm) AND SINGLE CRYSTAL W-0.35% Ta.
 (▲—▲ SINGLE CRYSTAL; □—□ POLYCRYSTAL)

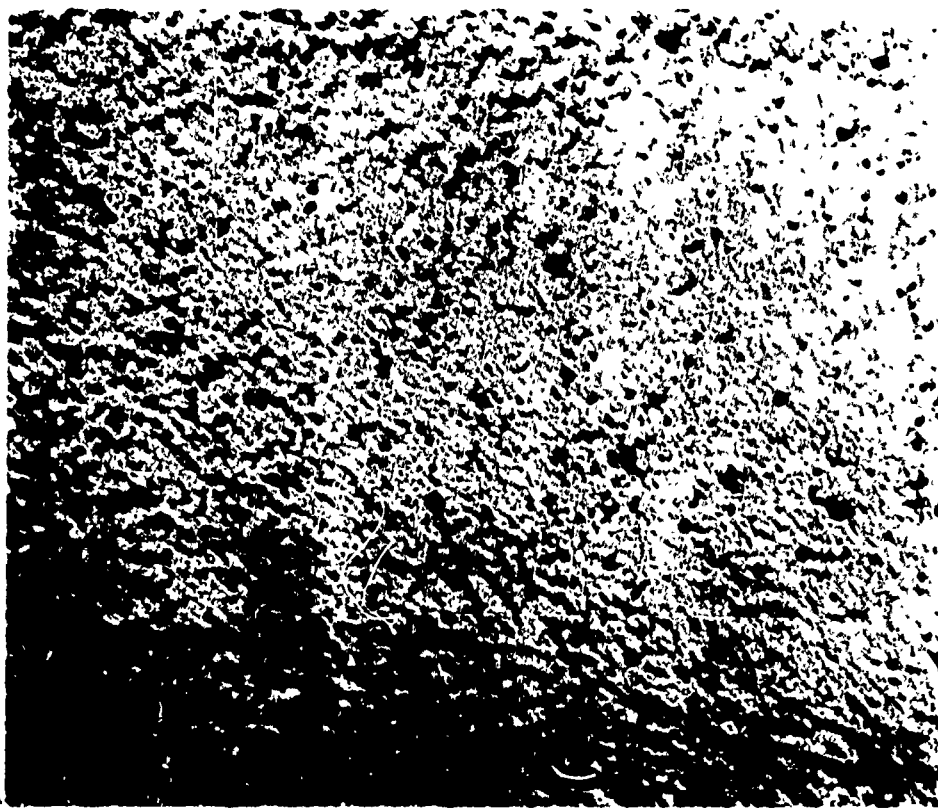


Fig. 33A Precipitates in a Carburized Worked and
Quenched W-0.35% Ta Tensile Specimen
Tested at 1200°C 500X

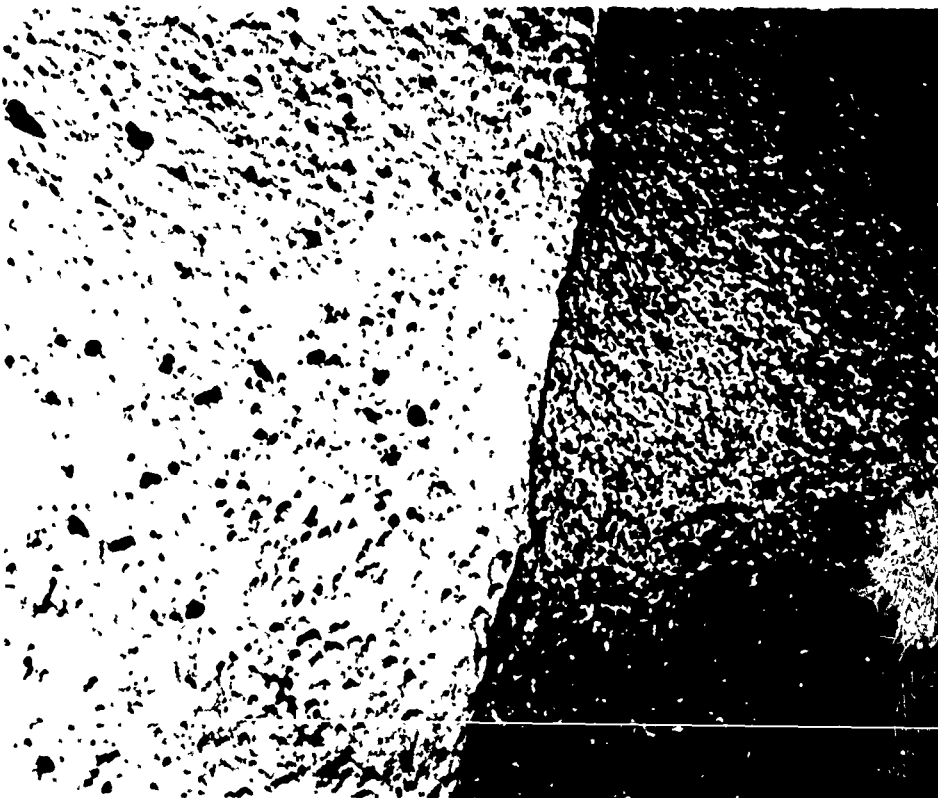


Fig. 33B Precipitates in a Carburized Worked and
Quenched W-0.35% Ta Tensile Specimen
Tested at 800°C 500X

- a) The increase in the residual resistance ratio after annealing at 700°C (Table 4).
- b) The great instability of the Snoek internal friction peaks (3).
- c) The maximum in the yield stress which occurs after short anneals at 700°C, or after longer anneals at 400°C (Fig. 23).
- d) The large increase in the yield strength of the carburized, quenched, and strain-aged alloy crystals (Fig. 25).

Overall, these results leave little doubt that the large increase in yield stress in the temperature region in question is caused by precipitation hardening.

The possibility of strengthening by the Schoeck and Seeger mechanism (28) (Snoek ordering) is not controlling because strengthening by this mechanism should be proportional to the concentration of solute carbon in tungsten and should be independent of test temperatures. The observed yield stress peak at 600°C is, therefore, inconsistent with the Schoeck-Seeger mechanism.

2. Yield Points and Serrations

Discontinuous yield points were noted only below 600°C and repeated yielding (serrations) from 600-1200°C. Discontinuous yield points can be caused by either Cottrell atmospheres or precipitation. Repeated yielding, however, has been solely attributed to dislocation - interstitial interactions (28,29). The latter requires the diffusion of interstitial impurities for which an activation energy can be deduced from Cottrell's equation $D = 10^{-9} \xi^2 (30)$ where $D = D_0 \exp(Q/RT)$. Taking for the temperature the temperature at which the first indication of serrations in the W-0.35%Ta crystals were noted (600°C), and D_0 as 0.01, one calculates an activation energy of 45,000 cal/mole. This activation energy is close to the activation energy for the diffusion of carbon in tungsten, as determined by internal friction measurements (18) and indicates that the diffusing species are carbon atoms. If one assumes a dislocation density of about 10^7 cm^{-2} and that one interstitial carbon atom per plan along a dislocation will cause locking, one finds that the carbon concentration required for complete locking is about 1×10^{-3} wgt. ppm. It is therefore surprising that serrations are not observed in all conditions, even in quenched virgin tungsten single crystal.

3. The Effect of Quenching Temperature

A different temperature dependence of the yield stress has

been found for carburized single crystals of W and W-0.35% Ta quenched from 2200°C after a 15 minute hold at quenching temperature (Figs. 17 and 19). The pronounced yield stress peak of the W-0.35% Ta crystals is explained in terms of an aging effect; i.e. strengthening is realized once carbon precipitates from supersaturated solid solution. Carbon in solution, even in supersaturated solution, does not seem to contribute to strengthening. This assumption finds evidence in the low yield stress value of the alloy at 300°C. How can one then explain the high yield stress value of pure carburized and quenched tungsten at 300°C and the plateau which extends from 300-600°C?

The tungsten-carbon phase diagram (27) discloses that carbon has a solubility of about 60 to 80 wgt. ppm at 2200°C and about 150 wgt. ppm at the eutectic temperature. Since the carburized tungsten crystals contain, on the average, 81 wgt. ppm of carbon and possibly greater concentrations, it can be assumed that not all carbides were dissolved during the 2200°C quench. Consequently, nuclei or embryo are probably present at 2200°C which, upon quenching, cause accelerated precipitation and hence the high yield stress in the temperature region between 300 and 600°C. This conclusion draws support from the fact that these crystals, when quenched from the eutectic temperature (about 2450°C), exhibit a yield stress peak at 600°C (Fig. 21) and the yield stress at 300°C has dropped to much lower values.

In a similar manner, the temperature dependence of the yield stress of the alloy crystals, when quenched from 2450°C, reflects the effects of accelerated aging. It is not known at present whether the carbides precipitated in a W-Ta alloy are mainly tantalum carbides, tungsten carbides, or complex tungsten-tantalum carbides. In any case, the level of strengthening obtainable in the carburized W-0.35% Ta alloy single crystals, under appropriate conditions, is about the same as obtainable in the carburized tungsten single crystals.

4. The Effect of Carbon in Recrystallized Tungsten and W-0.35% Ta Crystals

Work hardening will, of course, greatly increase the strength of pure or alloy tungsten single crystals. If the crystals are carburized and quenched prior to warm working (700-1100°C), dynamic strain-aging will occur during working, resulting in a higher level of strength.

Upon annealing, the worked carburized tungsten single crystals recrystallize at about the same temperature as the uncarburized tungsten single crystals (1200°C). The addition of 0.35% Ta, however, increases the recrystallization temperature of

tungsten by about 400°C (1200-1600°C). Carburizing the alloy single crystals has no further effect on the recrystallization temperature.

Recrystallization results in a large grain polycrystalline aggregate (Table 10). The range of grain sizes developed is too small to evaluate quantitatively the contribution of the grain boundaries to the tensile properties.

The effects of alloying by Ta and/or C and the effects of various treatments on the yield stress of pure W single crystals is shown schematically in Fig. 34. Data on commercial powder metallurgy tungsten and polycrystalline W produced from single crystals have been included in Fig. 34 for comparison.

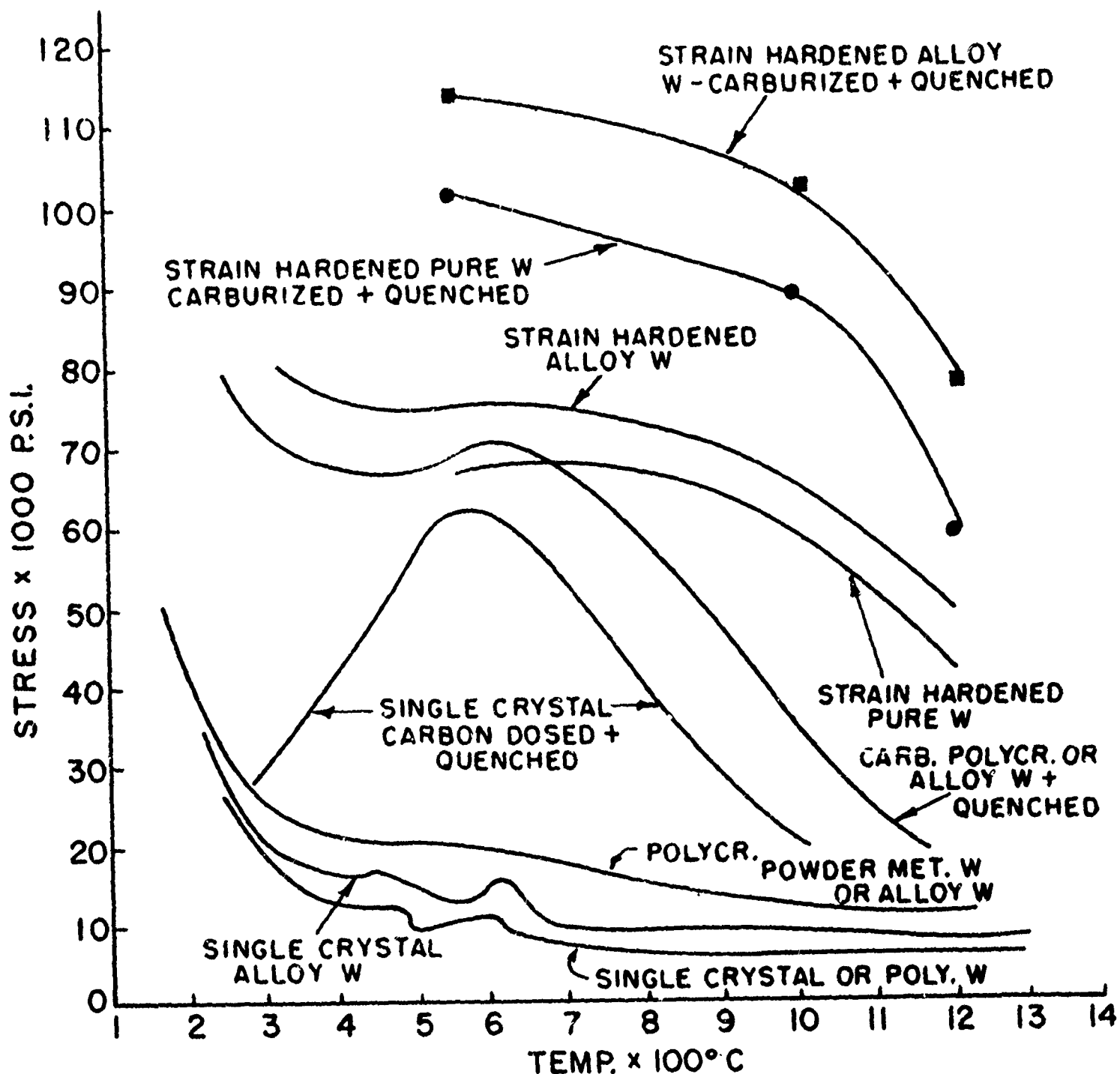


FIG. 34 SCHEMATIC OF THE VARIOUS APPROXIMATE STRENGTHENING CONTRIBUTIONS TO THE YIELD STRESS OF TUNGSTEN.

IV. SCREENING ALLOYS

The results of the investigation on the W-1%ThO₂ alloy and the observed effects of carbide precipitation on the mechanical properties of pure tungsten and W-0.35%Ta single crystals and worked single crystals, respectively, raised many questions primarily with respect to the effects of the size, distribution, composition and chemical stability of dispersed second phase particles on strength properties. No attempt, other than those reported in preceding chapters, have been made to investigate these variables. A new contract (31) is to be initiated shortly which will deal with these variables in great detail.

Under the screening program two solid solution alloys with a dispersed second phase present were chosen to be evaluated on a screening basis for the purpose of answering two questions: (1) How effective as a strengthening agent is a stable dispersed second phase of thoria or HfN in the solid solution alloy W-25%Re, and (2) how does a greater concentration of a solid solution alloying addition of Ta affect the high temperature tensile properties of precipitation hardening (carbon dosed and heat treated) W-Ta alloy single crystals?

A. The Effect of 1%ThO₂ or 1%HfN on the High Temperature Tensile Properties of W-25%Re

Alloys of the composition W-25%Re, W-25%Re-1%ThO₂ and W-25%Re-1%HfN were produced by a standard powder metallurgy technique. Ingots 24 inches long x 3/8 inch square cross section were compacted from sieved powder blends, sintered in hydrogen to approximately 91% density, and swaged to about 48% R.A. from preheat temperatures of approximately 1700°C. Button head tensile specimens were machined by grinding from the swaged rods.

Metallographic observation of the swaged rods revealed that a high degree of dynamic recovery occurred during swaging. All tensile specimens were annealed for 1/2 hour at 2400°C before testing. As shown in Fig. 35, this treatment resulted in an equiaxed fine grain structure. The dispersoids which were added as submicron size particles in the case of thoria, and of micron size in the case of hafnium nitride, were present in the annealed specimens in the form of large particles ($> 1\mu$).

1. Tensile Test Results

Tensile tests were made at temperatures varying from 1500-2400°C for two strain rates, 8.4×10^{-5} sec⁻¹ and 3.3×10^{-2} sec⁻¹. The tensile data have been tabulated in Table 14 and plotted in

Table 14

Tensile Properties of W-25%Re, W-25%Re-1%Th0₂
and W-25%Re-1%HfN

Alloy	Temp. °C	sec ⁻¹	Yield Str. psi	Ult. Str. psi	% Tot. Elong.	% R.A.
W-25Re	1500	3.3x10 ⁻²	39,800	58,200	77	74
	1650	"	38,500	48,000	61	71
	1850	"	29,000	34,800	84	50
	2250	"	14,700	14,700	*124	64
	2400	"	10,000	10,000	80	83
	2400	8.4x10 ⁻⁵	5,050	5,800	32	20
W-25Re-1Th0 ₂	1650	3.3x10 ⁻²	54,200	56,300	18	22
	1850	"	35,500	35,500	9	15
	1850	"	34,100	34,900	12	12
	2250	"	17,000	17,000	12	21
	1850	8.4x10 ⁻⁵	11,300	12,600	5	9
	2250	"	2,350	3,200	8	9
W-25Re-1HfN	1500	3.3x10	56,900	64,200	28	38
	1650	"	42,700	49,800	18	24
	1850	"	31,200	32,700	20	24
	2250	"	16,300	16,300	28	23
	2250	"	16,700	16,700	31	20
	2400	"	12,300	12,300	27	29
	1850	8.4x10	9,800	10,400	20	19
	2250	"	2,100	3,000	8	11
	2400	"	1,400	1,600	23	20

* - Did not fracture at end of crosshead travel.

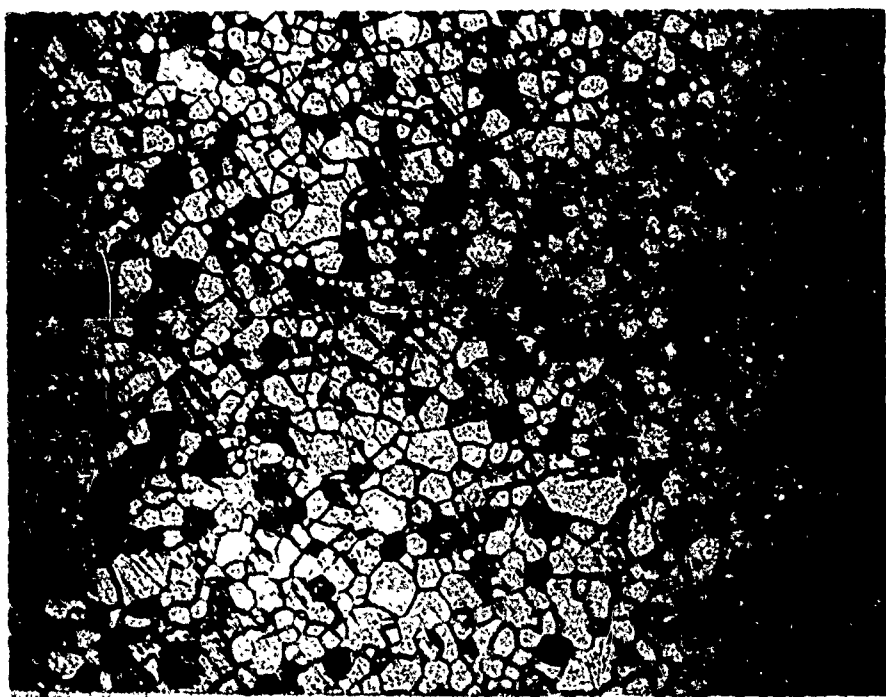


Fig. 35 Microstructure of Recrystallized
(1/2 Hr.; 2400°C) W-25% Re. 50X

Fig. 36. The tensile data obtained on pure W under this contract as well as other data reported in the literature for pure tungsten (10,11) and a W-20%Re (32) have been included in Fig. 36 for comparison. It is seen that the W-25%Re alloy has superior tensile properties to unalloyed tungsten at temperatures below 2400°C. At or above 2200°C, the tensile properties of the alloy are only slightly better except for ductility than that of the high purity tungsten. The addition of 1%ThO₂ or 1% HfN to the W-25%Re solid solution alloy has no further benefit on strength properties and causes a loss of ductility.

2. Discussion of Results

The tensile data of the tungsten rhenium alloys, in agreement with results previously reported by Pugh (32), show that the solid solution alloying addition of 25% Re is quite effective as a strengthener in the temperature region to approximately 2400°C. The addition of a coarse dispersion of 1%ThO₂ or 1%HfN has no further benefit on strength.

The improved high temperature strength of the W-Re alloys is, no doubt, related in part to the effect of the alloy addition on void formation during testing. In all of the three W-Re alloys investigated, void formation has been found to be greatly reduced during tensile testing at high temperatures. The result is apparently not simply one involving structure, as indicated for the W-1%ThO₂ alloy previously discussed, since the recrystallized structures of the W-Re alloys are very similar to recrystallized high purity tungsten. Wedge shaped voids were formed at 2250°C or above; however, the small spherical type of voids at transverse or parallel boundaries which were prominent in high purity tungsten and W-1%ThO₂ were virtually absent. This observation suggests that only Zener (33) type voids were formed as the result of sliding. It is in regard to repression of grain boundary sliding that a finely dispersed stable second phase may provide the improvement needed to retain the benefits provided by the substitutional alloying addition.

B. The Effect of Carbon Precipitates on the High Temperature Strength Properties of W-3.5%Ta Single Crystals

One single crystal of [100] orientation was produced by electron beam floating zone melting of a powder compact of W-5%Ta. The tantalum concentration of the "as grown" rod is estimated to be 3.5%. This estimate is based on previous experience with the same material identically produced (3).

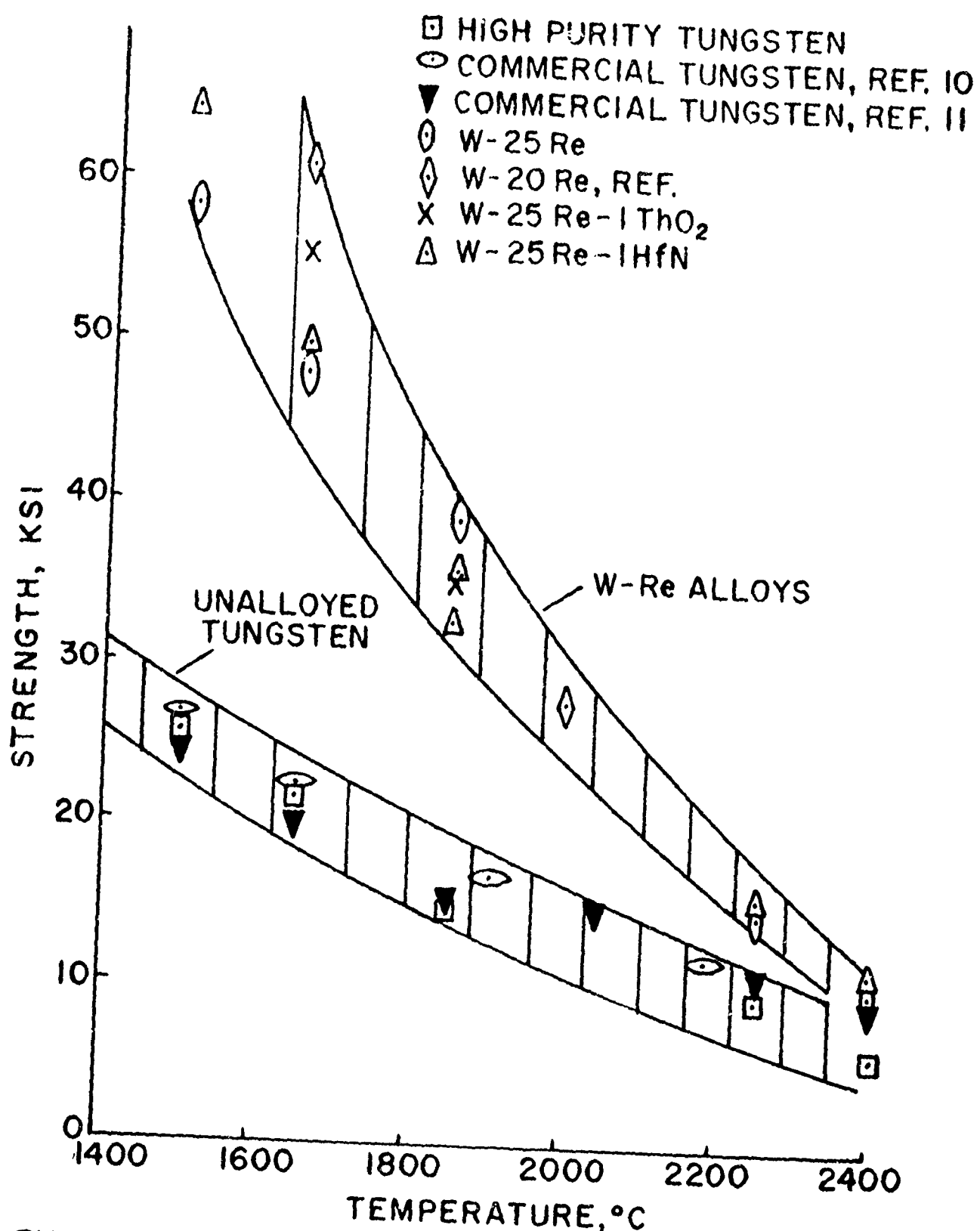


FIG. 36 ULTIMATE TENSILE STRENGTH OF PURE AND COMMERCIAL TUNGSTEN, AND SEVERAL TUNGSTEN RHENIUM ALLOYS.

Four sections of the W-3.5%Ta single crystal were carburized by the technique used for the W-0.35%Ta single crystals. To insure the formation of a greater amount of a second phase, the temperature of the high temperature vacuum anneal in the carburizing procedure was increased from 2200°C to 2400°C and the time at temperature extended from 2 to 4 hours. Three of the four specimens were quenched from 2450°C after a 15 minute hold at temperature.

1. Tensile Test Results

Tensile tests were carried out at 1600°C and 2250°C at a strain rate of $0.4 \times 10^{-3} \text{ sec}^{-1}$. The results of the four tests have been summarized in Table 15. The remaining two carburized and quenched specimens were tested at 2250°C.

Table 15

Tensile Properties of Carburized and Quenched W-3.5%Ta Single Crystals

<u>Test Temp.</u>	<u>Condition</u>	<u>0.2% Yield Stress</u>	<u>Ultimate Stress</u>	<u>%Elong.</u>
1600°C	carb.	29,500	46,000	12
1600°C	carb.+quench	47,000	51,000	12
2250°C	carb.+quench	4,800	5,000	33
2250°C	carb.+quench	3,700	3,900	51

At 1600°C the carburized alloy single crystal has a yield strength about 4 times that of pure tungsten. Upon quenching, the yield stress at 1600°C is raised from 29,500 to 47,000 (i.e. increased by about 60%), but the ultimate strength is essentially unaffected. At 2250°C the yield stress has dropped to a value of about twice that of pure tungsten. Typical microstructures of the fractured specimens are shown in Fig. 37A, B and C. A profusion of precipitates are present in the specimens tested at 1600°C, but are absent in the specimen tested at 2250°C.

2. Discussion of Results

The strength increase which has been realized at 1600°C in the as carburized W-3.5% Ta alloy single crystal must be attributed in part to solid solution hardening. This follows from the fact that carburizing and quenching W-0.35%Ta single crystals has little effect on the yield strength at 1200°C. The further increase in strength of the carburized W-3.5% Ta alloy upon quenching is obviously caused by precipitation hardening. Like in all precipitation hardened alloys, strength is lost once overaging occurs.



Fig. 37A Photomicrograph of Carburized and Quenched Single Crystal, Tested 1600°C 500X



Fig. 37B Carbon Replica of W-3.5% Ta Carburized Plus Quenched Single Crystal, Tested 1600°C 5000X

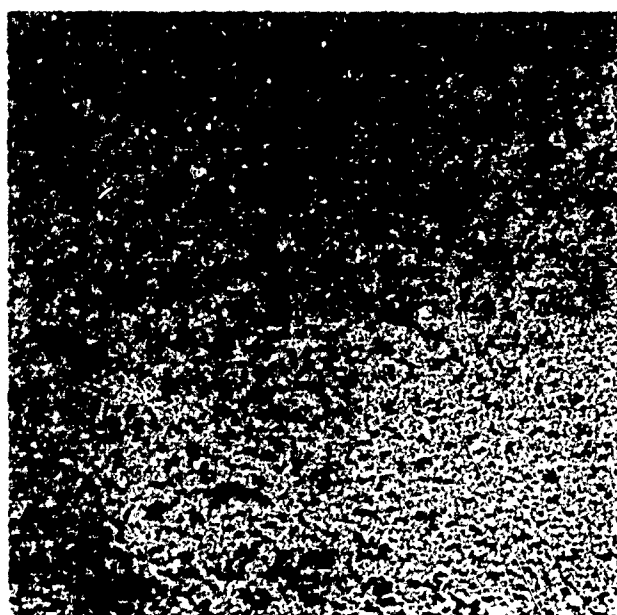


Fig. 37C Photomicrograph of W-3.5% Ta Single Crystal Carburized and Quenched, Tested at 2250°C 500X

At temperatures below about 1800°C, good creep properties can be expected. Higher concentrations of Ta and C hold promise of additional strength improvements over those already obtained.

V. THERMOCHEMISTRY OF DISPERSED SECOND PHASE IN TUNGSTEN

Studies on the decarburization of TaC, and the behavior of ThO₂ in the presence of W and some other refractory materials when heated in vacuum were completed. A sufficient number of melting point determinations were made on various W-Ta-C compositions so that the liquidus surface for this system could be visualized; and models and diagrams defining the approximate W-Ta-C liquidus surface were constructed. The bulk of the experimental work was centered around a modified electron beam furnace and a thermogravimetric vacuum balance. Samples were monitored and analyzed primarily by spectrographic and X-ray diffraction analysis.

1. Automatic Recording Balance

Equipment was assembled which permits the thermogravimetric analysis (TGA) and differential thermal analysis (DTA) of samples to approximately 2500°C in vacuum or inert atmospheres. The general assembly is shown in Fig. 38. The furnace (R.D. Brew and Co., Model 1030) has a stainless steel vacuum chamber. In the view shown in the photograph, the door swings open toward the instrument panels. The tantalum heating element is of the "clam shell" type to facilitate sample handling. The sample crucible is suspended by means of a hang-down extending from the balance beam through a connecting pyr. tube and into the furnace hot zone. Temperature control and measurements are affected by means of W-W/26%Re thermocouples.

The balance (see Fig. 39 also) is a UGINE-EYRAUD, Model B-60. The balance operates by the interaction of an optical and solenoid-magnet system. A weight change causes a change in the angle of the balance beam and this deflection activates a photocell. The cell, in turn, causes a current variation and creates a counter-balancing action which restores the beam. Weight change is thus measured (and recorded) as current intensity. The general arrangement of the solenoid coil, optical system ("black box" in the illustration), and the balance beam can be seen in Fig. 39.

The control and recording instruments (Honeywell), D, E and F of Fig. 38, are more or less standard and, therefore, will not be discussed in any detail here. The following comments might be



Fig. 38 Automatic Recording Balance Assembly. (A, vacuum pump unit; B, furnace; C, balance; D, program controller; E, Temperature and DTA recorder; F, TGA recorder)

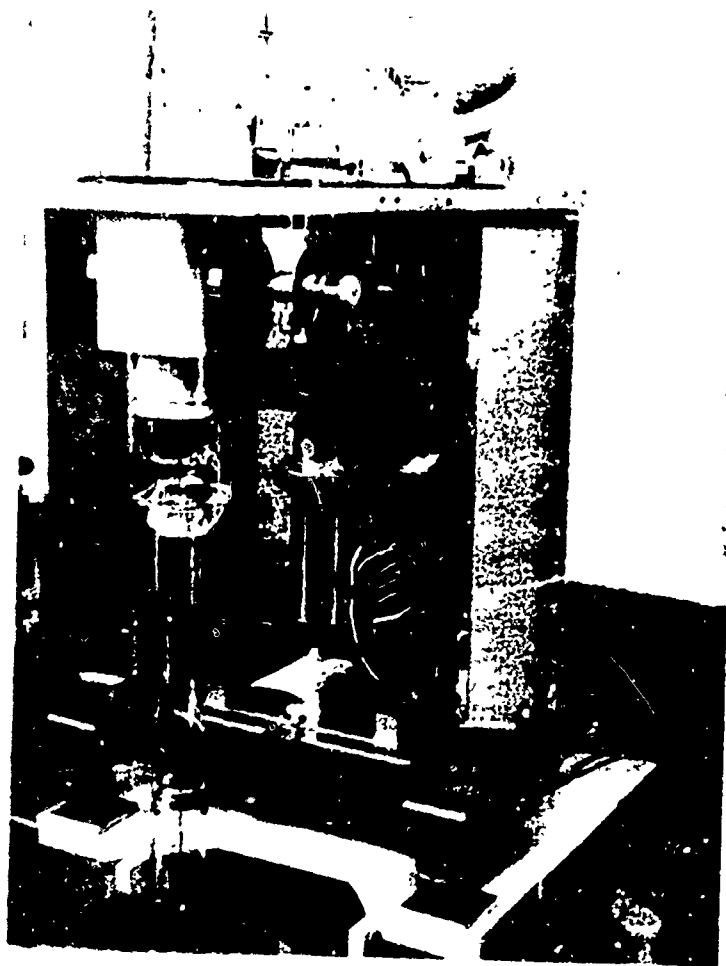


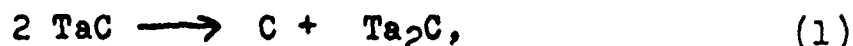
Fig. 39 Continuous Recording Balance
With Vacuum Housing Raised
and Case Open

pertinent, however. When on automatic control, the furnace may be either heated or cooled at any desired rate up to a maximum speed of $25^{\circ}\text{C}/\text{min.}$, and when heated at constant temperature, the temperature can be maintained to within $\pm 5^{\circ}\text{C}$. Weight loss (or gain) recordings can be made that are accurate to within $\pm 0.1 \text{ mg.}$

Fig. 40 is a view of the furnace elements and shielding. The movable electrode has been swung out on its hinge in order to show the heat shields and general structure. Two crucibles can be seen here. The upper crucible is suspended from the hang-down wire for TGA; the lower one is supported on a rod and will be used for DTA. Thermocouples pierce the furnace tank wall by means of vacuum tight conax fittings. The outer shield as well as the heavy copper block electrodes are water cooled. Note the vacuum exhaust port in the rear wall of the tank.

2. Decarburization of TaC

Fine Fansteel TaC ($3\text{ }\mu$, total C=6.34%) and coarse material from Gallard and Schlesinger ($45\text{ }\mu$, total C=6.07%) was mixed and pressed into compacts. Loose powders and pellets were also fired. Measurements with the vacuum balance indicated that very slow initial decarburization may start as low as 1250°C . At high temperatures (2000°C or higher) decarburization is rapid. Fig. 41 shows a polished section from a TaC compact fired in the EB furnace for 20 minutes at 3325°C . X-ray diffraction measurements made on the outer surface of the decarburized section showed that it was composed of Ta_2C . Thus, decarburization proceeds according to the reaction



which is in agreement with the literature (34).

Hardness measurements (Knoop) made on the decarburized edge and the compacted center of this compact gave average values of 1535 and 560, respectively. A compact fired for approximately the same length of time but at 2950°C gave an edge value of 665, and a third compact fired at 2725°C gave an edge value of 375. The Knoop hardness for TaC crystals (Gallard and Schlesinger) was found to be about 3180. The hardness measurements suggest that consolidation of the decarburized material continues as the temperature is increased. It also appears that TaC is considerably harder than Ta_2C .

3. The W-Ta-C Liquidus Surface

Forty compacts varying in composition so as to follow the two join lines shown in Fig. 42 were prepared from W, Ta, TaC and WC components. Their approximate melting temperatures were deter-

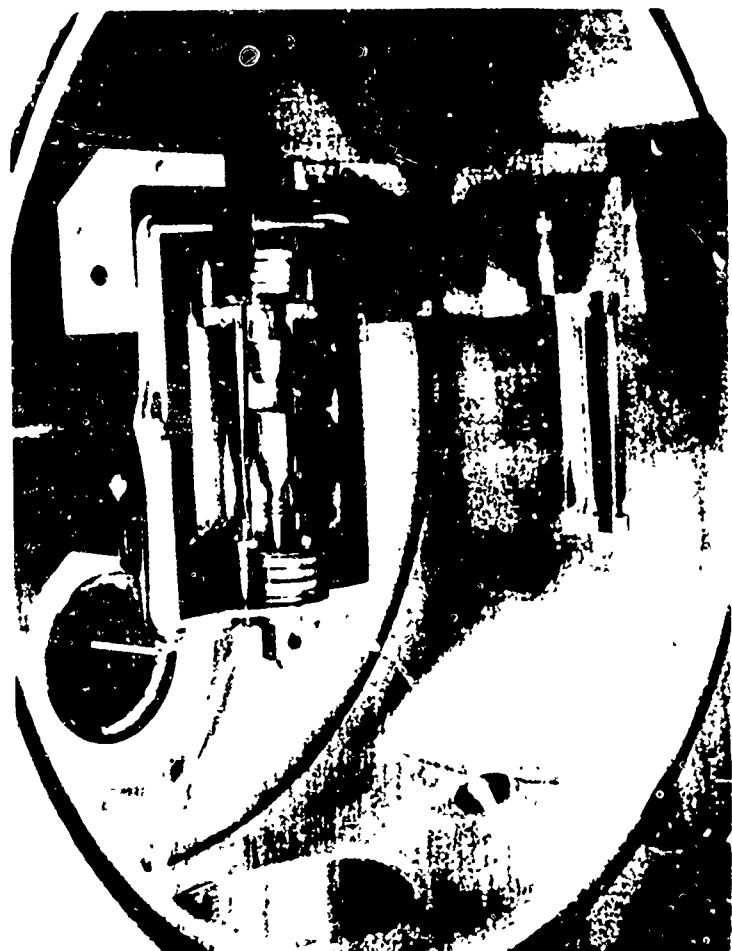


Fig. 40 View of Vacuum Furnace With Element Opened For Loading.

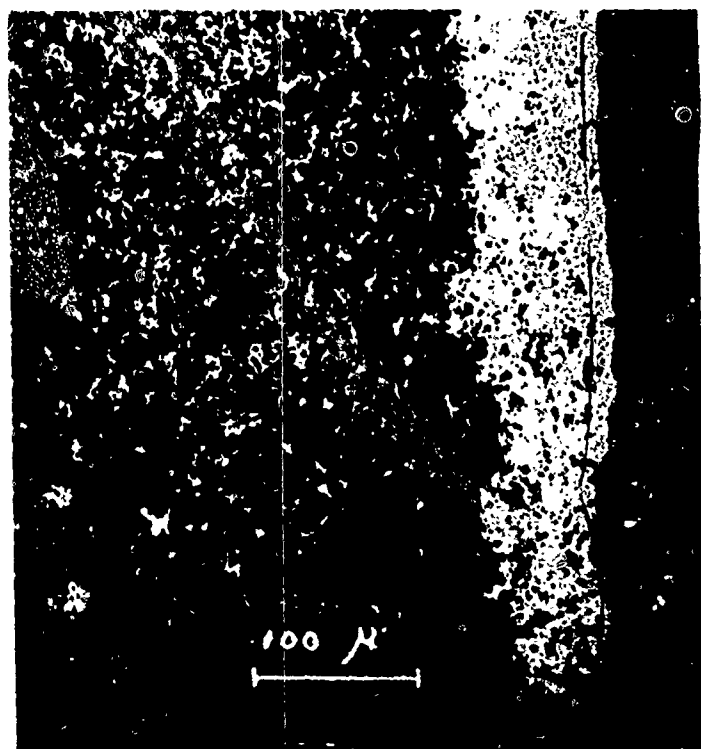


Fig. 41 Polished Section of a TaC Compact Fired at 3325°C for 20 Min. in the EB Furnace. Decarburized Skin is Light Section at the Right.

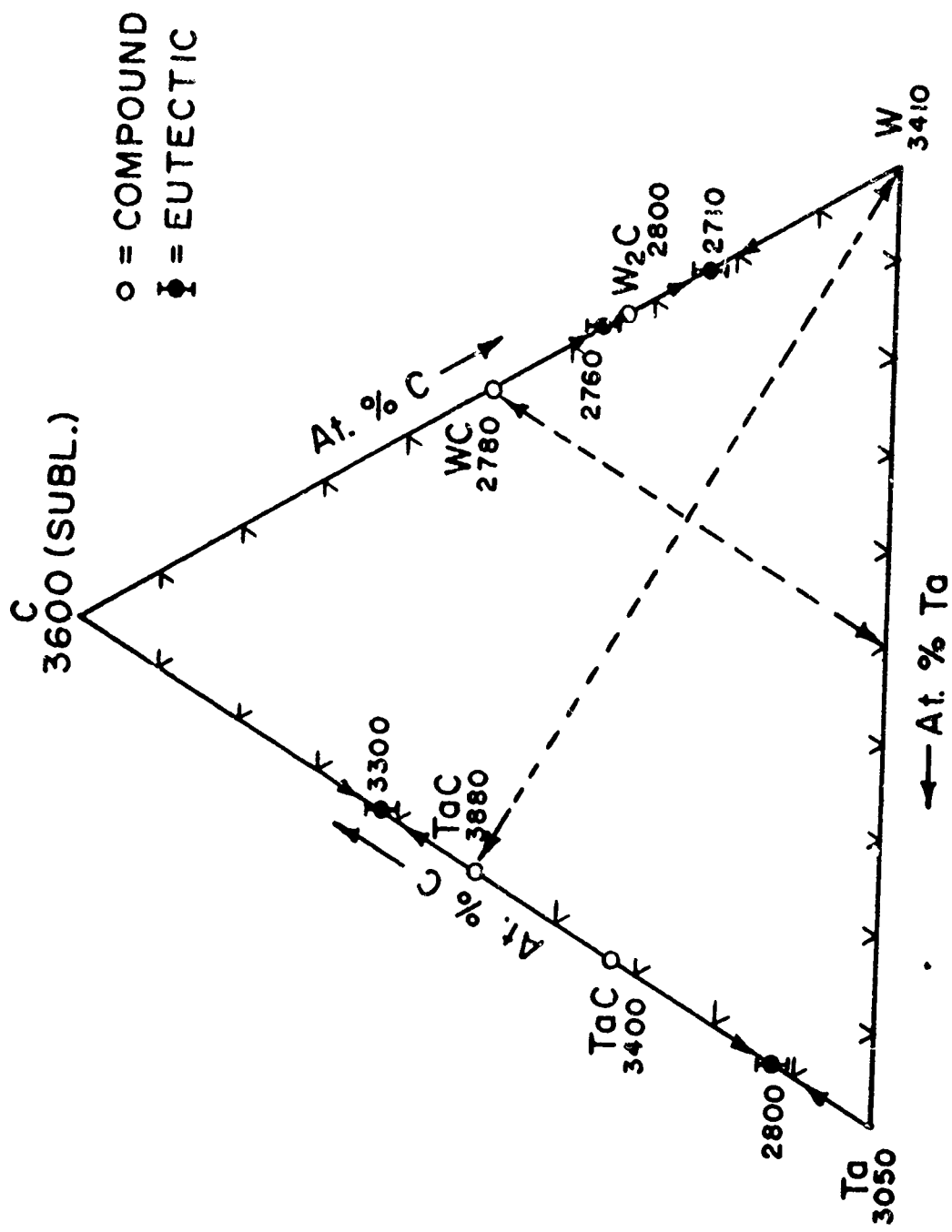


FIG. 42 JOINS ALONG WHICH MELTING POINT DETERMINATIONS WERE MADE (DASHED LINES) IN THE W-Ta-C SYSTEM.

mined by heating in the EB furnace. Temperatures were corrected for emissivity and optical absorption by the bell jar, and the melting temperature accuracies were estimated to be within $\pm 25^{\circ}\text{C}$. A preliminary Plexiglas model was made defining the periphery of the W-Ta-C ternary based on binary data given by Goldschmidt and Brandt (27), and English (35). This model is shown in Fig. 43. By combining the binary data with the ternary melting point determinations, it was possible to map the approximate liquidus surface for the W-Ta-C system. The result is shown in Fig. 44 in which arrows are drawn on the heavy lines separating the primary phase fields. The arrows point toward regions of lower temperature and converge at two eutectics having the approximate compositions 50W-30Ta-20C and 50W-15Ta-35C. A maximum is indicated in the region corresponding to the empirical composition $W_2(\text{TaC})$. Approximate melting points of these three points were found to be 2700° , 2600° , and 2850°C , in the order given. A clay model was constructed in order to illustrate the salient features of the liquidus surface and this is shown in Fig. 45.

Three metallographic sections were taken along the Ta-C-W join near the tungsten-rich corner of the W-Ta-C system. These have the approximate compositions shown by a, b, and c on the diagram of Fig. 44 and the structures obtained are illustrated in Fig. 46. Section (a) resembles the pearlitic-type structure obtain by Lally and Hiltz (36) upon firing TaC-coated tungsten rods for two minutes at 6000°F . X-ray diffraction patterns were taken, but the results were inconclusive. All three sections gave patterns corresponding to W, (W,Ta)C, and $W_2(\text{TaC})$ with (b) and (c) showing the higher concentrations of the two solid-solution carbides. A more specific analysis would require more carefully controlled firing conditions than those used in these melting experiments.

4. ThO_2 Reactions with W and Some Other Refractory Materials

Thoria is of considerable interest as a dispersoid in tungsten; and although it has been a constituent in tungsten alloys for many years, its behavior in this matrix has not been clearly defined. Some thermogravimetric experiments supplemented by X-ray diffraction analyses were performed in the hope that they would throw some light on this problem. Experiments with mixtures of thoria with some refractory carbides were also run in order to determine the compatibility of thoria with these materials.

a) Thoria + Tungsten Reaction

Samples of tungsten, thoria, and a thoria + tungsten mixture were fired in the vacuum thermobalance to approximately 2250°C . The results are summarized in Fig. 47, where it can be seen that

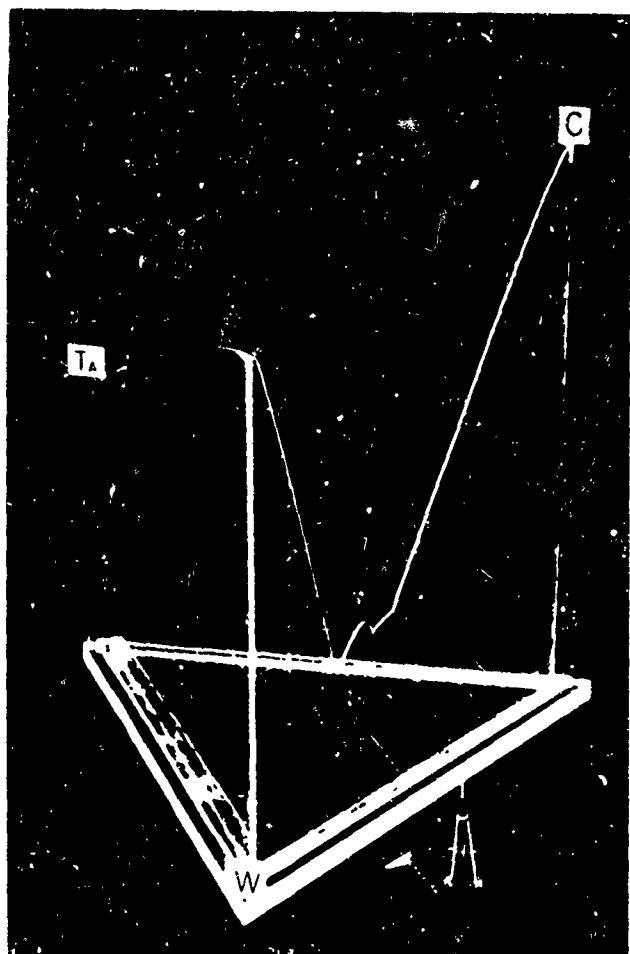


Fig. 43 An Early Stage in the Construction of a Plexiglas Model of the W-Ta-C Liquidus Surface. Grid Spacing Equals 100°C, and the Base of the Model Represents 2400°C.

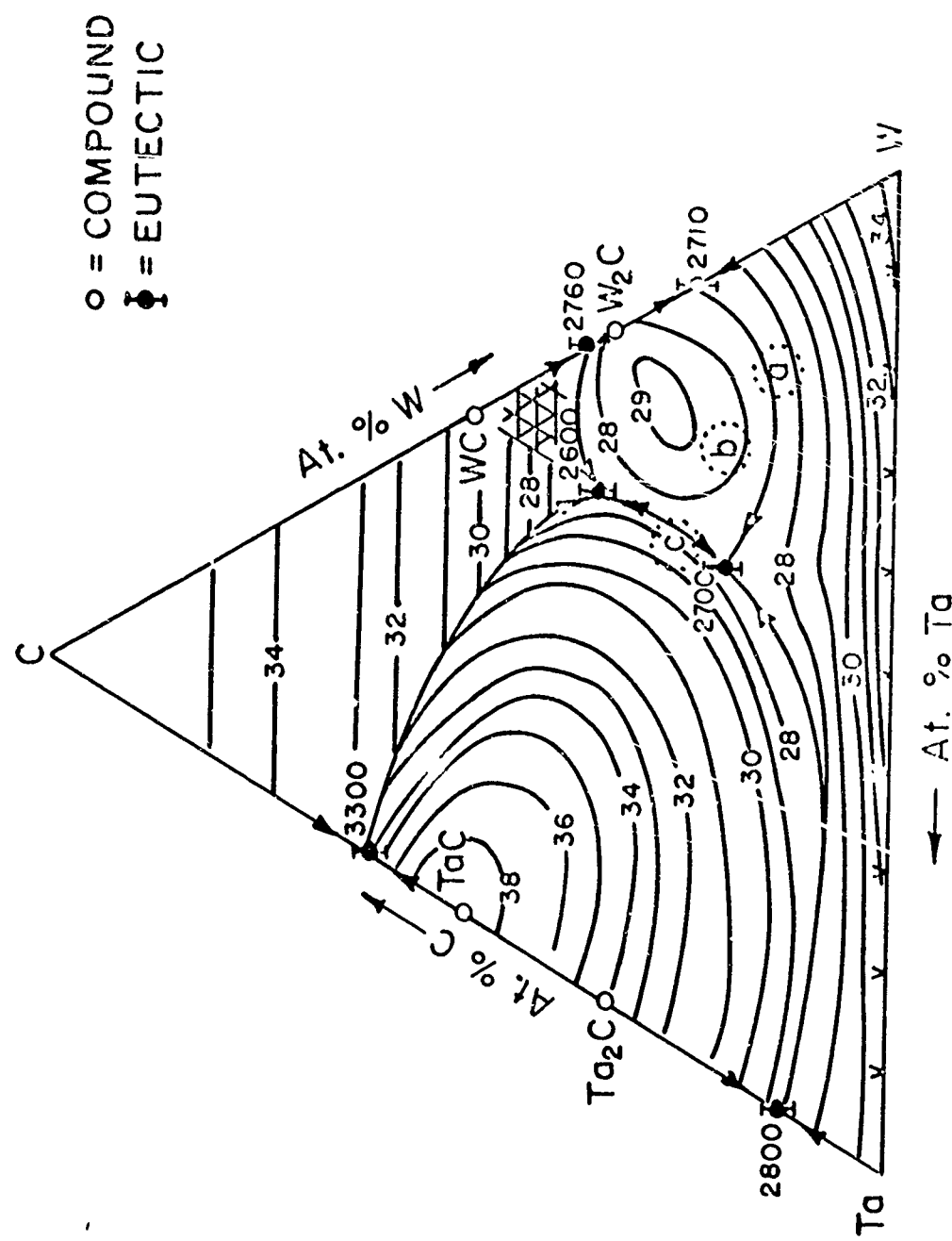
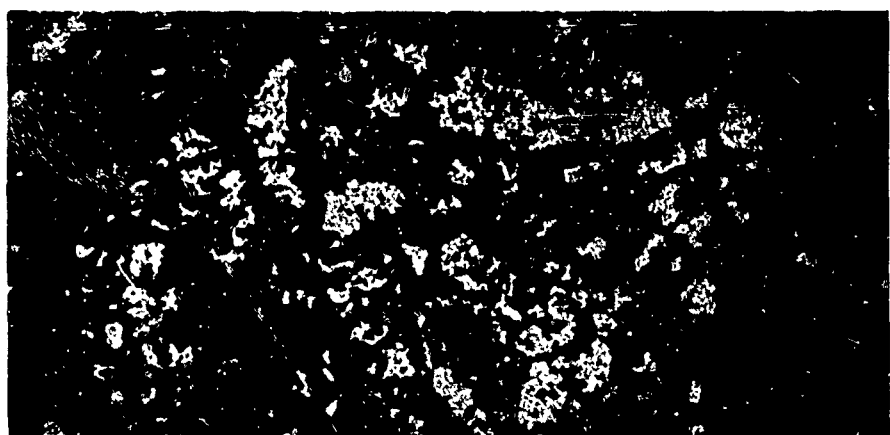


FIG. 44 CONTOUR ISOTHERMS OF THE LIQUIDUS SURFACE
SUGGESTED FOR THE $W-Ta-C$ SYSTEM.

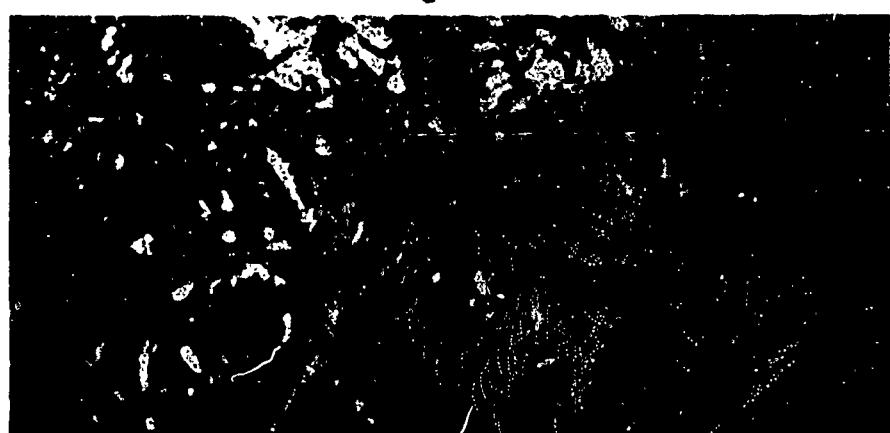


Fig. 45 Clay Model of W-Ta-C
Liquidus Surface. "Peak"
in Background is TaC.



A

100 μ



B

100 μ



C

Fig. 46 Metallographic Sections Taken Near the W-Rich Corner of the W-Ta-C System. 100μ

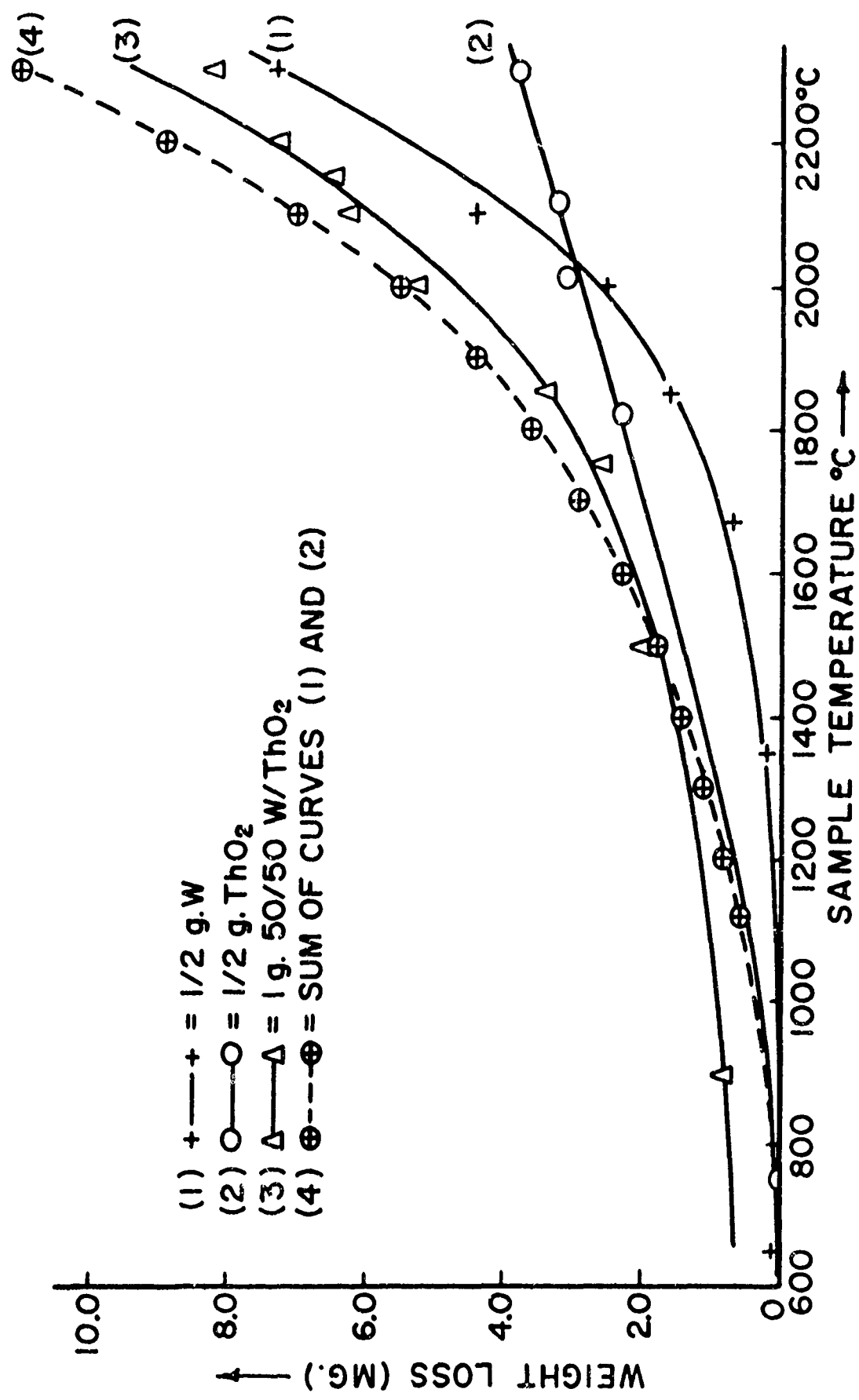
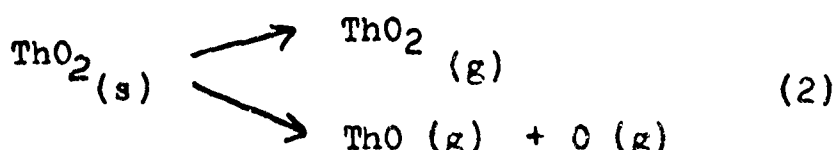
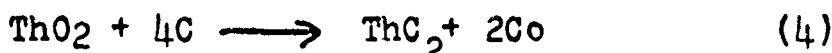
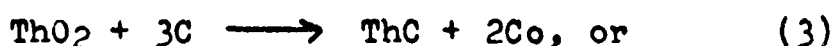


FIG. 47 WEIGHT LOSS OF W, ThO₂, AND A W + ThO₂ MIXTURE.

there is no evidence for weight loss of a $\text{ThO}_2 + \text{W}$ mixture due to chemical reaction. Within experimental error, the sum of the thoria and tungsten curves is equal to the curve produced by the mixture. An even closer match would be expected if certain bulk geometry corrections had been incorporated in the data. X-ray diffraction data taken both on fired and unfired mixtures gave patterns for W and ThO_2 only. The results are in agreement with Ackermann et. al (37), who suggest that there is no chemical reaction between W and ThO_2 but that thoria may volatalize from the mixture via two possible paths: i.e.,



The authors also state that any thoria loss involving the formation of free Th metal would require the presence of a reducing agent such as carbon. A number of $\text{ThO}_2 + \text{C}$ mixtures were fired in the vacuum thermobalance and the results are summarized in Figs. 48 and 49. It was observed that reaction starts at about 1400°C , which is in good agreement with Kroll and Schlechter's (38) observation of 1380°C . Either the monocarbide or dicarbide is produced via the reactions



ThC was found to be cubic with $a_0 \approx 5.30$, and was formed preferentially when ThO_2 was present in excess. ThC_2 is pseudo-tetragonal or mono-clinic. It was formed rather than (or from) the monocarbide when C was present in excess. This behavior of ThO in the presence of C is well-substantiated by earlier workers (39,40,41,42,43). The statement made by Ackermann, et al (37), that carbon present as an impurity in thoriated tungsten will produce thorium metal at about 2000°K via the reaction



is incorrect. This reaction does not occur, even though it may be thermodynamically feasible. Both ThC and ThC_2 are quite stable in this temperature region as can be seen from Fig. 48, so these compounds do not appear to be likely sources of free Th. Another important observation to be made from Figs. 48 and 49 is that when

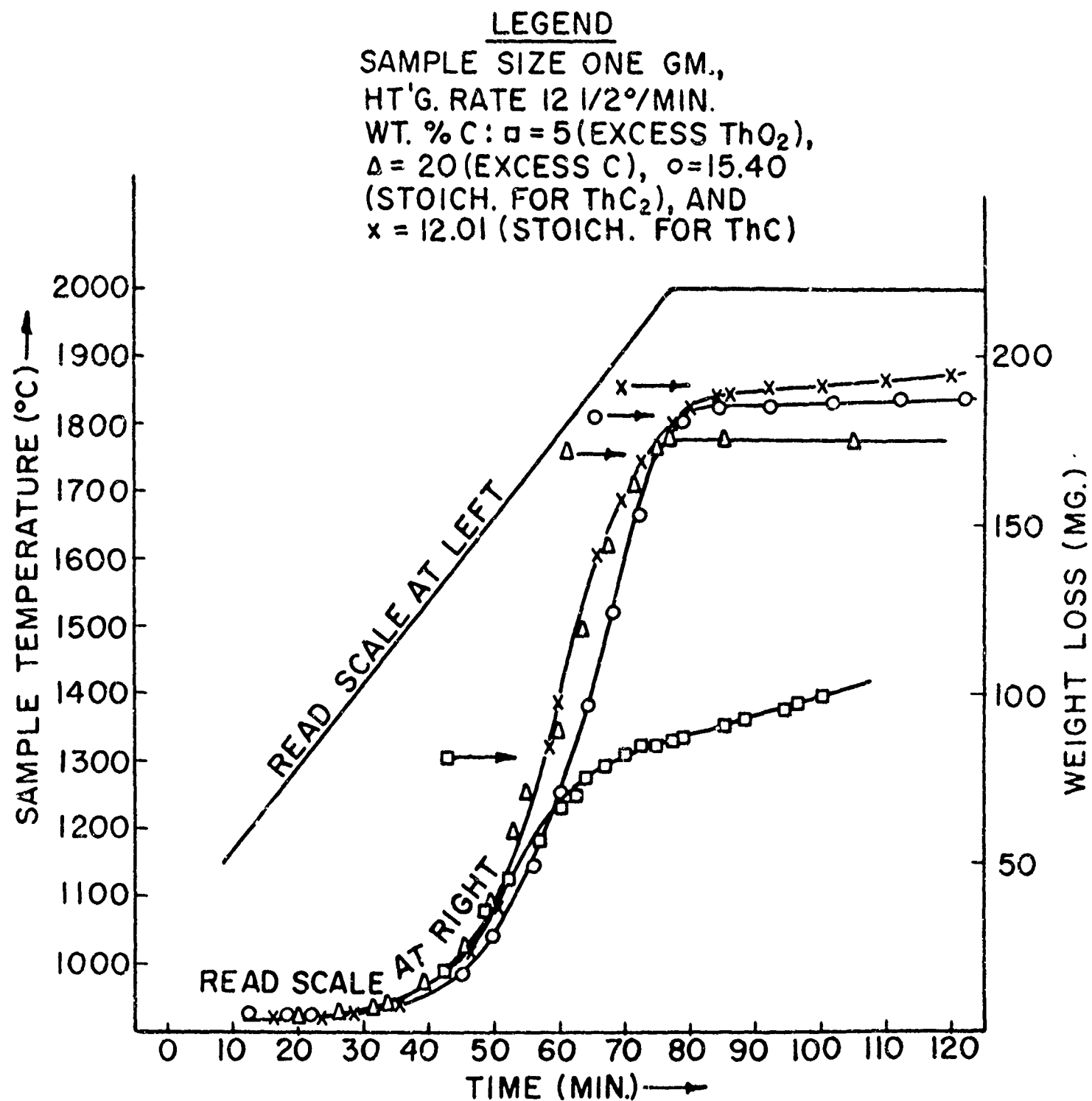


FIG. 48 WEIGHT LOSS OF $\text{ThO}_2 + \text{C}$ MIXTURES HEATED TO 2000°C. (ARROWS INDICATE THEORETICAL LOSS EXPECTED.)

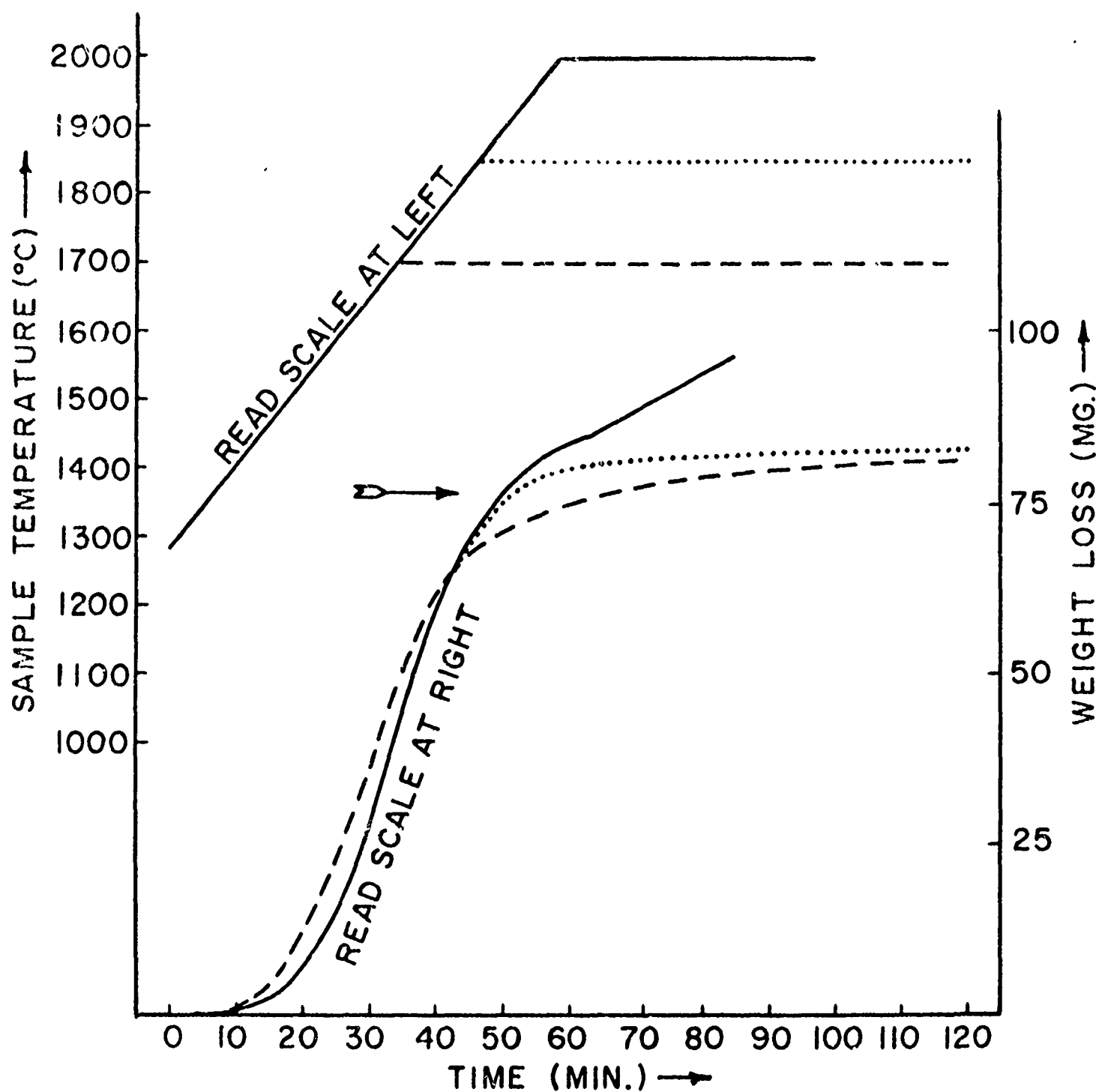


FIG. 49 WEIGHT LOSS OF $\text{ThO}_2 + 5\% \text{ C}$ MIXTURES
HEATED TO 1700° , 1850° , AND 2000°C . (ARROW
INDICATES THEORETICAL LOSS EXPECTED.)

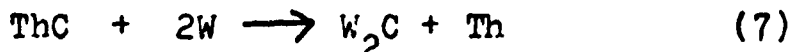
ThO_2 is present in excess, it gradually volatilizes. It can be seen that this volatilization starts somewhere between 1850°C and 2000°C . Very likely it is defined by equation (2), or some modification of this reaction. The fact that thoria volatilization starts at about the same temperature that Schneider (44) first finds free Th in thoriated tungsten filaments is of considerable interest since it suggests the possibility that the Th may form via some reaction in which one of the gaseous phases of thorium oxide plays an important role.

b) Thoria + WC Reaction

Thoria mixtures containing various amounts of WC were fired to 2000°C in the vacuum thermobalance. The results are illustrated in Fig. 50. Reaction begins at 1500°C to 1700°C , and according to X-ray analyses and stoichiometry is defined by the following equation:



Unlike its reaction with carbon, thoria does not produce thorium dicarbide when reacted with tungsten carbide. Instead this work indicates that the monocarbide produced via equation (6) reacts with additional tungsten in the 1900°C to 2000°C region, probably as follows:



Thorium has not as yet been identified here as a reaction product, but W_2C has. Note that equations (6) and (7) offer a possible mechanism for the depletion of thoria from tungsten via the formation of thorium, with a carbon contaminant (WC) as a reducing agent.

c) Reactions of Thoria and Some Other Carbides

Mixtures of thoria with W_2C , NbC , or TaC were fired in the vacuum thermobalance. The first of these was taken to 2000°C , the other mixtures to 2250°C . The results are shown in Fig. 51. There is little evidence of chemical reaction with W_2C , which is in line with observations made in the previous section. An X-ray diffraction pattern indicated that the original W_2C material (a sub-micron product from Ciba) contained a fairly high concentration of free W. X-ray patterns of fired and unfired mixtures of $\text{ThO}_2 + \text{W}_2\text{C}$ were about the same. In the $\text{NbC} + \text{ThO}_2$ mixtures, the fired mix with the higher thoria concentration showed NbC plus an unidentified compound (weak indication); the low thoria concentration mixture showed only NbC by X-ray analysis. Analysis of the $\text{TaC} + \text{ThO}_2$

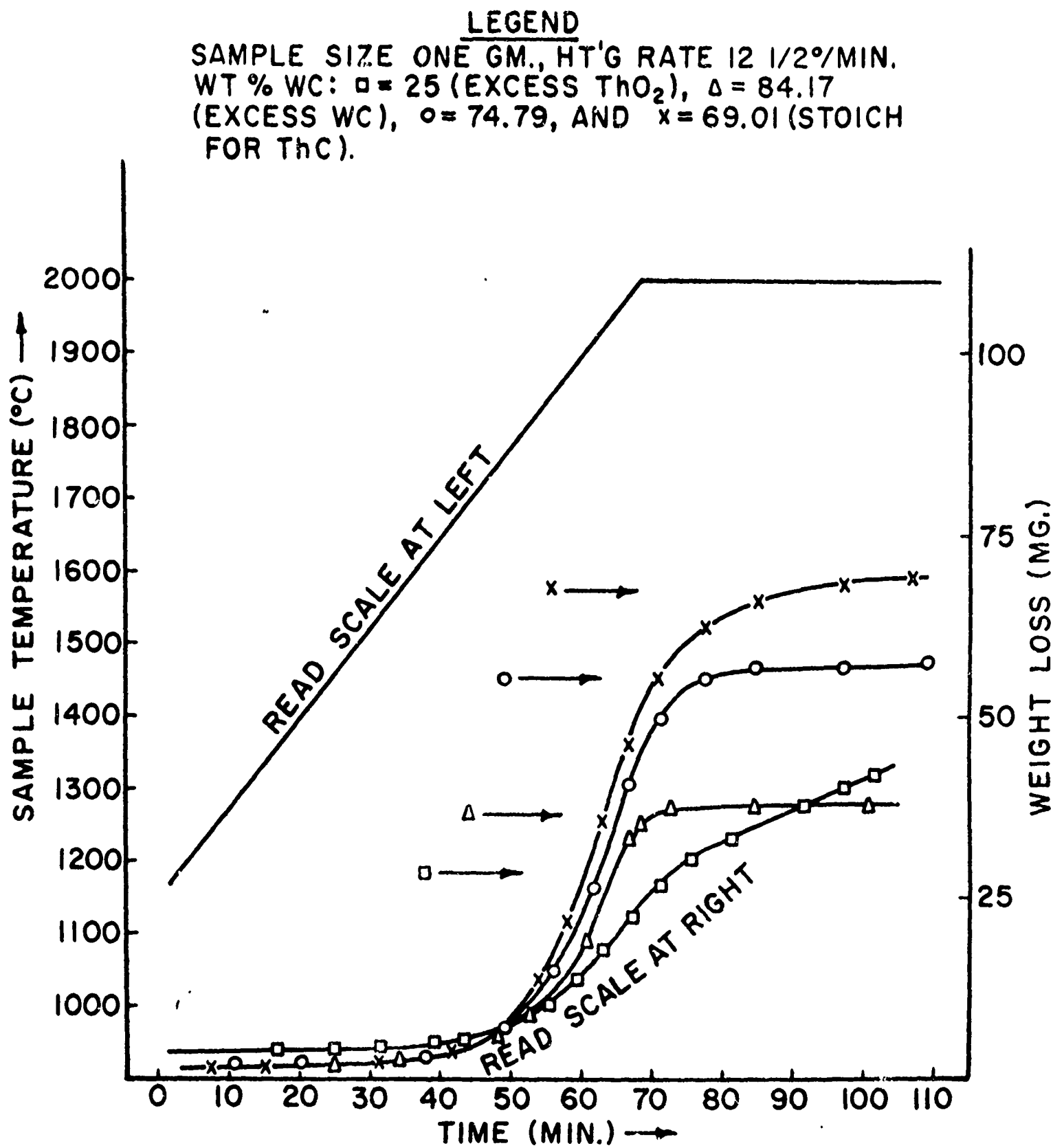


FIG. 50 WEIGHT LOSS OF ThO₂ + WC MIXTURES HEATED TO 2000°C. (ARROWS INDICATE THEORETICAL LOSS EXPECTED.)

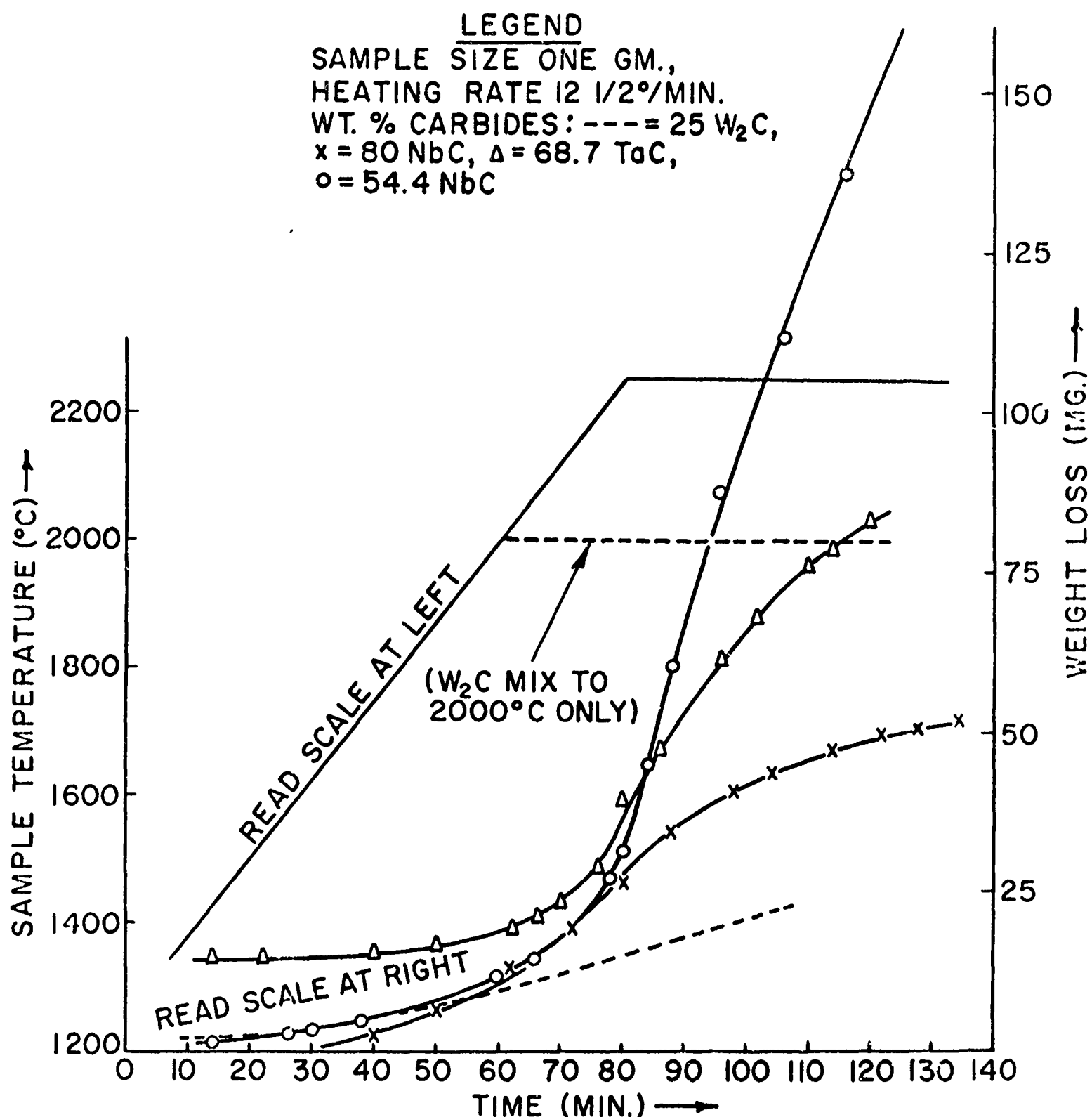


FIG. 51 WEIGHT LOSS OF VARIOUS ThO₂ + CARBIDE MIXTURES.

fired mixture showed the presence of ThO_2 , TaC , and a third compound tentatively identified as Ta_2C . The weight loss curves seem to bear out the conclusion that there is little or no chemical reaction between the carbides of Nb or Ta with ThO_2 . The reaction appears to be primarily physical; i.e., the volatilization of the ThO_2 as one or more of the gaseous thorium oxide species.

VI. SUMMARY

This investigation has brought forth significant results which allow one to assess the potential for the successful development of a high temperature strengthened alloy of tungsten on a considerably more refined basis. The results especially lend weight to the theoretical prediction that this alloy will be a dispersion strengthened alloy and not a precipitation hardened alloy. Major problems in the development of this alloy have become apparent.

The area which deserves the greatest immediate attention is the processing area. All theories of dispersion strengthening require a fine particle dispersion but in none of the alloys investigated under this contract was such a dispersion achieved. The processing methods employed included high temperature sintering for the consolidation of the alloys which resulted in either decomposition or agglomeration of the dispersoids. An advancement of the art of compact consolidation is one of the more urgent requirements.

None the less, the modest increase in strength achieved in the dispersion hardened alloys revealed valuable information which will be of much benefit for future developments of high temperature, high strength alloys. The 1% thoria addition had a large effect on the structure of tungsten, which in turn influenced the high temperature tensile properties. The results indicate that the structure factor was primarily responsible for a large reduction in void formation during tensile testing. A significant result of the work under this contract is the qualitative correlation between void volume formed during tensile deformation and tensile strength: The lower the void volume, the higher is the strength. At present, there is little known about the void formation process. Strain rate greatly affects the process of void formation. Faster strain rates cause less void formation and higher tensile strength and vice versa. Thus alloying for creep resistance will, no doubt, be the major difficulty in a high temperature alloy.

Grain boundary sliding is an important factor in high temperature creep. As stated above, the results showed that the coarse thoria dispersion greatly affected grain growth during and after recrystallization. This result offers the hope that a fine dispersion will also aid high temperature creep resistance.

It is, however, apparent that purity plays an important role in void formation. The largest void volume was found in pure tungsten. The void volume was somewhat reduced in W-1% ThO₂ and greatly suppressed in the W-25%-Re alloys tested at the same temperatures.

The large increments in strength which were obtained in the carbon dosed, heat treated and aged single crystal of W, W-0.35%Ta and W-3.5% Ta have clearly demonstrated that a fine dispersion of submicron size particles can be very effective in strengthening tungsten. While overaging limits the usefulness of those alloys, a fine dispersion of chemically stable particles in tungsten and more so in W-Re or W-Re-Ta alloys would extend the temperature range of their usefulness.

VI. REFERENCES

1. Atkinson, R.H. and Staff, "Physical Metallurgy of Tungsten and Tungsten Base Alloys", WADD T.R. 60-37, March 1960.
2. Sell, H.G., Keith, G.H., Koo, R.C., Schnitzel, R.H., Corth, R., "Physical Metallurgy of Tungsten and Tungsten Base Alloys", WADD T.R. 60-37, Part II, May 1961.
3. Sell, H.G., Keith, G.H., Koo, R.C., Schnitzel, R.H., Corth, R., "Physical Metallurgy of Tungsten and Tungsten Base Alloys", WADD T.R. 60-37, Part III, November 1962.
4. Sell, H.G., Keith, G.H., Schnitzel, R.H., Cerulli, N.F., "Physical Metallurgy of Tungsten and Tungsten Base alloys", WADD T.R. 60-37, Part IV, May 1963.
5. McLean, D., "Grain Boundaries in Metals", Oxford Univ. Press, Oxford (1957).
6. Gifkins, R.C., Acta Met., 4, 98 (1956).
7. Chen, C.W., and Machlin, E.S., Acta Met., 4, 655 (1956).
8. Greenwood, J.N., Miller, R.D., and Suiter, J.W., Acta Met., 2, 250 (1954).
9. Machlin, E.S., Journal of Met., 8, No. 2, 106 (1956).
10. Sikora, P.F., and Hall, R.W., NASA TN D79, Lewis Research Center, Cleveland, Ohio (1961).
11. Taylor, J.L., and Boone, D.H., Trans. ASM 56, No. 3, 643 (1963).
12. Koo, R.C., J. Less-Common Metals, 3, 412 (1961).
13. Orowan, E., Inst. of Metals, "Symposium on Internal Stresses in Metals and Alloys", Monograph and Report Series No. 5, (1948).
14. Fisher, J.C., Hart, E.W., Pry, R.H., Acta Met., 1, 336 (1953).
15. Ball, C.J., J. Iron and Steel Inst., 191, 232 (1959).
16. McLean, D., J. Inst. Metals, 80, 507 (1951-1952).
17. Balluffi, R.W., and Seigle, L.L., Acta Met., 5, 449 (1957).
18. Schnitzel, R.H., J. Appl. Phys., 30, 2011 (1959).
19. Conrad, H. Wiedersich, H., Acta Met., 8, 128 (1960).

20. Thorton, P.R., Hirsch, P.B., Phil. Mag., 3, 738 (1958).
21. Gregory, D.P., and Rowe, G.H., "Columbium Metallurgy", Interscience Publishers, New York, 309 (1960).
22. Bechtold, J.H., Shewmon, P., Trans. ASM, 46, 397 (1954).
23. Depierre, V., Saul, G., ASD-TDR 63-782 (1963).
24. Taylor, A., Ryden, H.B., J. Less Common Metals, 4, 451 (1962).
25. Corth, R., Analytical Chem., 34, 1607 (1962).
26. Handbook of Chemistry and Physics, 42nd Edition, Chemical Rubber Publishing Co., 2595 (1960-1961).
27. Goldschmidt, H.J., Brandt, J.A., J. Less Common Metals, 5, No. 2 (1963).
28. Schoeck, G. Seeger, A., Acta Met., 7, 469 (1959).
29. Cottrell, A.H., Bilby, B.A., Proc. Phys. Soc. (London) A62, 49 (1949).
30. Cottrell, A.H., Phil. Mag., 44, 829 (1953).
31. Sell, H.G., King, G.W., Morcom, W.R., Cerulli, N.F., "Development of a Wrought Tungsten Base Alloy", AF33(615)-1698, in progress.
32. Pugh, J.W., Amra, L.H., and Hurd, D.T., Trans. ASM, 55, 451 (1962).
33. Zener, C., "Elasticity and Anelasticity", Univ. of Chi. Press, Chicago, 1948.
34. Eckstein, B.H., and Forman, R., J. Appl. Phys. 33, 82 (1962).
35. English, J.J., DMIC Report No. 152, 59 (1961).
36. Lally, F.J., and Hiltz, R.H., J. of Metals 14, 424 (1962).
37. Ackermann, R.J., Rank, E.G., Thorn, R.J., and Cannon, M.C., J. Phys. Chem., 67, 762 (1963).
38. Kroll, W.J., and Schlechter, A.W., J. Electrochem. Society 93, 1948.
39. Komarek, K.L., Coucoulas, A., and Klinger, N., Electrochem. Soc. 110, 783 (1963).

40. Wilhelm, H.A., Chiotti, P., Snow, A.I. and Daane, A.H., J. Chem. Soc. S318 (1949).
41. Hunt, E.B., and Rundle, R.E., J. Am. Chem. Soc. 73, 4777 (1951).
42. Street, R.S., and Waters, T.N., United Kingdom AERE, Memo. 1114, (1962).
43. Greger, H.H., U.S. Pat. #2, 799,912 (1957).
44. Schneider, P., J. Chem. Phys. 28, 675 (1958).